

STAIRWAYS TO HEAVEN:
ORIGINS AND DEVELOPMENT OF CRYOPLANATION TERRACES

By

Kelsey Elizabeth Nyland

A DISSERTATION

Submitted to
Michigan State University
in partial fulfillment of the requirements
for the degree of

Geography—Doctor of Philosophy

2019

ABSTRACT

STAIRWAYS TO HEAVEN: ORIGINS AND DEVELOPMENT OF CRYOPLANATION TERRACES

By

Kelsey Elizabeth Nyland

Cryoplanation Terraces (CTs) are erosional landforms reminiscent of giant staircases, with alternating shallow sloping treads and steep scarps leading to extensive flat summits. CTs are associated with periglacial (cold and unglaciated) environments and are typically found in elevated positions on ridges and hillslopes. Despite identification and discussion in geomorphic literature as early as the 1890s in the Urals, and the early 1900s in Alaska and the Yukon Territory, a consensus still has not been reached on the processes involved in CT formation. Two hypotheses continue to receive support from different factions of periglacial geomorphologists: (1) CTs are controlled primarily by geologic structure; and (2) CTs are dominantly controlled by climate through nivation – the erosion process suite associated with late-lying snowbanks.

This dissertation addresses some of the long-standing questions surrounding CT formation related to the time-transgressive nature of terrace treads, CT exposure ages, and long-term erosion rates associated with nivation processes. Explicit field testing was conducted on CTs throughout eastern Beringia, including the Seward Peninsula and the Yukon-Tanana Upland. Many prominent researchers have noted the proliferation of well-developed, relict CTs in unglaciated Beringia, which has experienced periglacial conditions throughout most of the Quaternary Period.

Research questions are addressed in four interrelated, but self-contained chapters. Chapter 2 is a detailed review of CT terminology, formation hypotheses, and global distribution. A bibliometric analysis shows that no particular papers or authors have played “gatekeeping” functions that could explain the lack of explicit field testing over the last 50 years. Chapter 3 uses

spatial statistics to examine differences in relative weathering indices and finds that treads at Skookum Pass, Eagle Summit, and Mt. Fairplay likely formed through scarp retreat. Chapter 4 is a geochronology study using ^{10}Be and ^{36}Cl terrestrial cosmogenic nuclides to determine exposure ages across treads near Eagle Summit and on Mt. Fairplay and to estimate erosion rates. Boulder exposure ages across these surfaces are synchronous with cold-climate intervals, suggesting climatic influence. Chapter 5 describes an unmanned aerial vehicle (UAV) survey conducted in an active nivation environment of northwestern British Columbia. In this “naturally controlled field experiment,” long-term denudation rates for nivation since the Last Glacial Maximum on Frost Ridge were calculated from incipient terraces nearing the size and morphology of CTs in unglaciated Beringia.

Chapter 2 effectively summarizes the history and current state of research on CTs, including an inventory of existing evidence for strong climatic influences on CT formation. Previous research has documented CT treads cutting across geologic structures, statistically preferred poleward orientations of scarps, and subcontinental-scale elevation trends closely match the position of paleosnowlines. Results from field investigations on relict CTs and in an active nivation environment, conducted as part of this dissertation, lend additional support to the proposition that climate controls CT formation through the mass balance of late-lying snowbanks. New data presented here, utilizing contemporary technologies, indicate that (1) CT treads are likely time-transgressive features, forming under scarp retreat; (2) boulder exposure is synchronous with local glaciations; and (3) long-term operation of nivation processes can produce landforms approaching the typical size of CTs.

Copyright by
KELSEY ELIZABETH NYLAND
2019

This thesis is dedicated to Fritz.

ACKNOWLEDGMENTS

First, I want to acknowledge the Michigan State University (MSU) Distinguished University Fellowship that funded my degree. Next, I thank my guidance committee members, Drs. Ashton Shortridge, David Lusch, Grahame Larson, and co-chairs, Drs. Frederick Nelson and Randall Schaetzl. This thesis project involved three summers of remote field work in Alaska and Canada and I want to thank the many people who assisted me, including Anna Abramova, Forrest Melvin, Chris Cialek, Nina Feldman, Olivia Napper, Vasily Tolmanov, and John Nyland, but especially Clayton Queen and Raven Mitchell, who assisted me for multiple months.

Several individuals and funding agencies were instrumental in research and analysis conducted for specific chapters. MSU librarians, Devin Higgins and Scout Calvert, with the Digital Scholarship Lab contributed to the bibliometric analysis in Chapter 1. Dr. Richard Reger reviewed a draft of this chapter and Jerry Brown helped to find obscure literature and provided photos by Dr. Troy Péwé. Fieldwork for Chapter 2 was funded by MSU Graduate Office and College of Social Science summer research fellowships. The lab component of Chapter 3 was funded by US National Science Foundation Award No. 1817665 and was conducted at the University of Cincinnati geochronology laboratories with assistance from Sarah Hammer, and Drs. Lewis Owen and Paula Marques Figueiredo. Fieldwork for Chapter 4 was done in collaboration with the Juneau Icefield Research Program and was funded by the Geological Society of America's Graduate Student Research Grant, the Arctic Institute of North America's Grants-in-Aid program, and MSU's College of Social Science summer research fellowships. I am grateful to Norm Graham (Discovery Helicopters Ltd.), and Fionnuala Devine (Merlin Geosciences Inc.) for helicopter and drone piloting and photogrammetry post-processing.

TABLE OF CONTENTS

LIST OF TABLES	ix
LIST OF FIGURES	x
CHAPTER 1. INTRODUCTION	1
Research Context	1
Dissertation Focus and Organization	4
CHAPTER 2. HISTORY OF A GEOMORPHIC ENIGMA: REVIEW OF CRYOPLANATION AND ASSOCIATED HYPOTHESES	9
Introduction.....	9
A Diverse Lexicon	12
Global Distribution	16
A Century of Competing Hypotheses	19
Davisian Erosion.....	21
Scarp Retreat.....	22
Altiplanation	23
Geologic Structure	25
Mass Movement.....	25
Polygonal Cracking.....	26
Surface Lowering.....	27
Bibliometric Assessment of Contemporary Cryoplanation Literature	28
Co-Citation Analysis.....	30
Results and Interpretation	31
Discussion.....	35
Conclusions.....	36
CHAPTER 3. SCARP RETREAT ON CRYOPLANATION TERRACES IN EASTERN BERINGIA: STATISTICAL ANALYSIS OF RELATIVE WEATHERING INDICES	39
Introduction.....	39
Study Areas.....	41
Methodology	43
Clast Fracture Counts.....	45
Clast Shape.....	46
Rebound	47
Weathering Rind Thickness (WRT)	47
Results.....	48
Chi-Square Analysis of Fracture Counts	48
ANOVA Results: Shape, Rebound, and Weathering Rind Thickness.....	50
Discussion	56
Conclusions.....	60

CHAPTER 4. COSMOGENIC ^{10}Be AND ^{36}Cl GEOCHRONOLOGY OF CRYOPLANATION TERRACES IN THE YUKON-TANANA UPLAND, ALASKA	62
Introduction.....	62
Study Areas.....	65
Methodology.....	68
Results.....	70
Discussion.....	76
Conclusions.....	78
 CHAPTER 5. LONG-TERM EROSION RATES BY NIVATION, CATHEDRAL MASSIF, BRITISH COLUMBIA.....	80
Introduction.....	80
Study Area and Geomorphic Evolution.....	81
Methodology.....	85
Nivation Observations	85
Volumetric Comparison of Marginal Drainage and Incipient Terraces	86
Calculation of Nivation-Driven Denudation Rates.....	87
Results.....	87
Active Nivation Processes on Frost Ridge.....	87
Volumetric Comparison of Landforms	89
Nivation-Driven Denudation Rates.....	91
Discussion.....	92
Conclusions.....	93
 CHAPTER 6. CONCLUSIONS	95
Summary of Results.....	95
Recommendations for Future Research	96
Broader Impacts	97
 APPENDICES	99
APPENDIX A: Chapter 2 Supplementary Materials.....	100
APPENDIX B: Chapter 3 Supplementary Materials	110
APPENDIX C: Chapter 4 Supplementary Materials	117
APPENDIX D: Chapter 5 Supplementary Materials.....	133
 BIBLIOGRAPHY.....	135

LIST OF TABLES

Table 1. Adjectives for Elevated Periglacial Terraces and First Appearance Reference	13
Table 2. Development Hypothesis, Abbreviated Definition, and First Appearance	20
Table 3. Google Scholar Top 5 Cited Articles about Cryoplanation	29
Table 4. Fracture Pearson's Chi-Square (χ^2), Likelihood Ratio (LR), and Cramer's V (ϕ_c)	49
Table 5. Summary Table of Trends in Significantly Different Means	55
Table 6. Sample Details and Calculated ^{10}Be Ages from Eagle Summit	72
Table 7. Sample Details and Calculated ^{36}Cl Ages from Mt. Fairplay	74
Table 8. Erosion Rates Based on Calculated Ages	77
Table 9. Meltwater Discharge Rate and Transported Material Characterization	89
Table 10. Volume Differences between Marginal Drainage and Incipient Terraces	91
Table 11. Frost Ridge Minimum and Maximum Nivation-Driven Denudation Rates	92

LIST OF FIGURES

Figure 1. Cryoplanation Terrace Morphological Components	1
Figure 2. Scarp Retreat Schematic for the Nivation Formation Hypothesis.....	3
Figure 3. Map of Dissertation Study Areas	5
Figure 4. Cryoplanation Terrace Morphological Components	10
Figure 5. Global Distribution of Documented Cryoplanation Terraces	17
Figure 6. Conceptual Diagrams of Proposed Formation Hypotheses.....	21
Figure 7. Frequency of Cryoplanation Literature Publication	30
Figure 8. Five-Year Interval Cumulative Cryoplanation Co-Citation Networks	33
Figure 9. Co-Citation Network Edge and Node Frequency over Time	34
Figure 10. Time-Transgressive Cryoplanation Terrace Development Schematic.....	40
Figure 11. Relative Weathering Study Area Map and Photos	42
Figure 12. Sampling Strategy for Relative Weathering Study	44
Figure 13. Mt Fairplay: Tukey’s HSD Results for Relative Weathering Indices.....	51
Figure 14. Eagle Summit: Tukey’s HSD Results for Relative Weathering Indices	52
Figure 15. Skookum Pass: Tukey’s HSD Results for Relative Weathering Indices	53
Figure 16. Transportation Slopes on Eagle Summit and Seward Peninsula.....	57
Figure 17. Cross Section Topographic Profiles of Terraces Eagle Summit	58
Figure 18. Revised Nivation Model for Cryoplanation Terrace Formation	59
Figure 19. Eagle Summit and Mt. Fairplay Photos and Terrace Components	63
Figure 20. Geochronology Study Areas and Geologic Context	66
Figure 21. Sampling Strategy for Geochronology Study.....	69

Figure 22. Calculated Ages Graphed by Position on Topographic Profiles76

Figure 23. Frost Ridge Study Area Map and Photo of Features of Interest.....82

Figure 24. Photos of Late-Lying Snowbanks and Features of Interest.....83

Figure 25. Idealized Schematic of Edgar Lake Valley85

Figure 26. Late-Lying Snowbank Temperature and Density Profiles88

Figure 27. 3D Representations of Marginal Drainage and Incipient Terrace Features90

CHAPTER 1. INTRODUCTION

Research Context

Cryoplanation terraces (CTs) are large erosional landforms consisting of alternating steep scarps and shallow sloping treads, sometimes culminating in a summit flat on ridges and hillslopes in upland to mountainous periglacial (cold and unglaciated) environments (Figure 1). These distinctive landforms have intrigued geomorphologists around the world for more than a century and have often been compared to the treads and risers of gigantic staircases (e.g., Kozmin, 1890; Demek, 1969; Nelson & Nyland, 2017; Ballantyne, 2018, p. 220). Despite recognition in scientific literature, CTs continue to evoke a classic geomorphic question: “How exactly did this landscape form?”

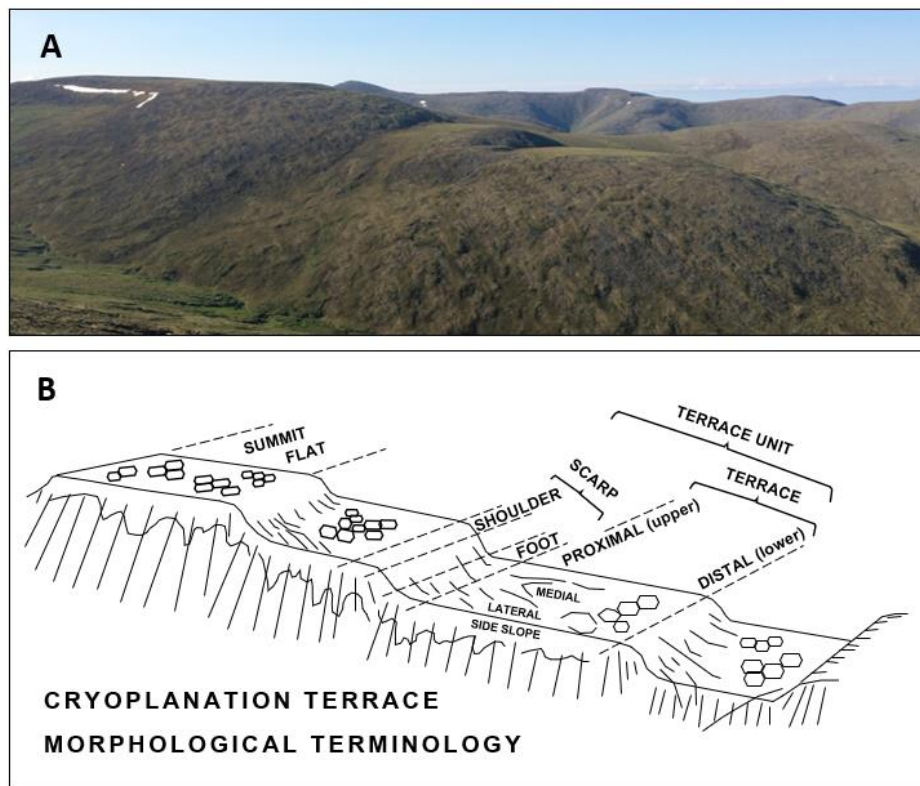


Figure 1. Cryoplanation Terrace Morphological Components. (A) Example of cryoplanation terraces near Eagle Summit, Alaska and (B) a schematic modified from Brunnschweiler (1965) of terraces with morphological components labeled. Photo by: K.E. Nyland, June 2017.

A diverse group of authors have proposed a wide assortment of process models for the formation of cryoplanation landscapes over the past century. By the mid-20th century, CTs were generally associated with the action of periglacial processes (e.g., Peltier, 1950; Demek, 1969), although disagreement persists about whether the dominant controls over their development are climatic or geologic structural (French, 2016; 2017, p. 295; Ballantyne, 2018, pp. 220-222). This knowledge gap was perhaps best articulated by Thorn and Hall (2002, p. 548):

To deny the fairly widespread existence of features commonly called cryoplanation benches, terraces, and pediments would be foolish; to claim that there is anything approaching an adequate explanation of their origin(s) would be even more foolish.

The most widely supported hypothesis for CT formation is based on climatic controls governing the mass balance of localized accumulations of snow (e.g., Ballantyne, 2018, p. 221). *Nivation*, used here as a shorthand term for intensified weathering and transportation in the vicinity of late-lying snowbanks, is thought to be responsible for the parallel retreat of scarps (Figure 2). Snowbanks lasting well into summer provide thermal insulation and moisture that contribute to intensified chemical and mechanical breakdown of rock that is subsequently removed by gravity-driven mass wasting processes fueled by the snowbank's meltwater (e.g., Thorn, 1976; Thorn & Hall, 1980; Ballantyne et al., 1989; Berrisford, 1991).

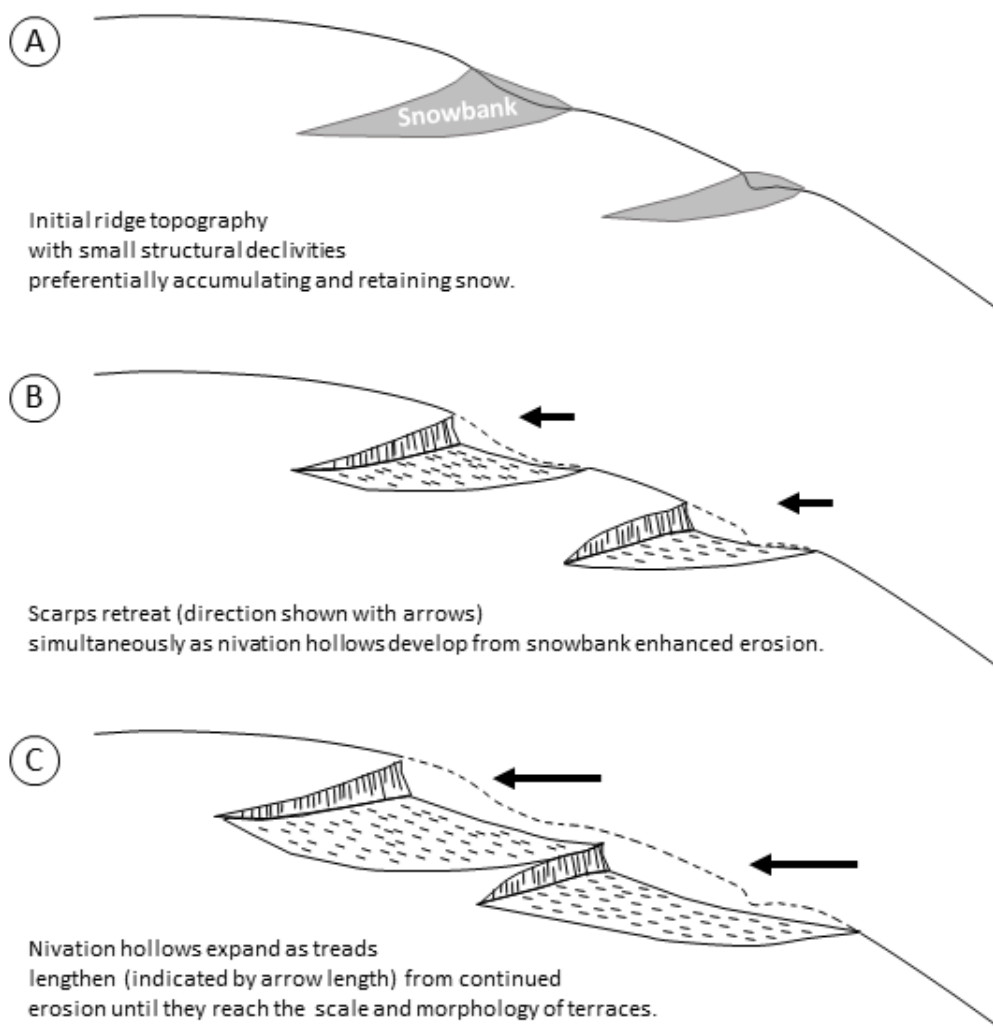


Figure 2. Scarp Retreat Schematic for the Nivation Formation Hypothesis. Model for cryoplanation terrace development, via parallel retreat of scarps, producing time-transgressive tread surfaces through long-term operation of nivation erosion processes. Nivation processes include enhanced chemical and mechanical weathering, creep, solifluction, rill- and sheetwash. Figure modified from Reger (1975, p. 170).

Additional evidence in support of the nivation-driven hypothesis for CT formation includes documentation of CT treads cutting across geologic structure and compositional layering (Demek, 1969), repeating sedimentological and morphological patterns (Reger, 1975; Queen, 2018), subcontinental-scale analyses indicating statistically significant preferred poleward orientation

(Nelson, 1998), and elevational trends closely tracking those of glacial cirques (Nelson & Nyland, 2017). The latter two lines of evidence are suggestive of strong climatic controls on terrace formation, much like those acting on glacial landforms, which have long been understood to be climatically controlled (Reger, 1975; Reger & Péwé, 1976; Nelson, 1989; 1998; Nelson & Nyland, 2017).

Despite the nivation-based hypothesis for CT formation having been posed more than a century ago (Cairnes, 1912a), it has yet to be explicitly tested on these landforms. This issue has become particularly important because some geomorphologists have attempted to associate upland periglacial landforms, such as CTs and cryopediments, with arid environmental processes, and assert that distinctly periglacial upland landscapes may not exist (e.g., French, 2016). The ability of periglacial processes to limit the height of high-latitude topography has been referred to by some as the “frost buzzsaw” (Hales & Roering, 2009; Hall & Kleman, 2014), analogous to what is now commonly referred to as the “glacial buzzsaw” (e.g., Brozović et al., 1997). This dissertation attempts to determine if nivation processes satisfy this “buzzsaw” concept, and therefore, if CTs represent a component of a distinctly periglacial landscape.

Dissertation Focus and Organization

The goal of this work is to address questions about the origins and formation of CTs and the lack of direct observational data (e.g., Demek, 1969, p.66; Prieznitz, 1988; Thorn & Hall, 2002) through extensive fieldwork, coupled with contemporary technologies. Chapters 2 through 5 are self-contained studies and their respective appendices offer minimally processed data. The following interrelated research questions are addressed in Chapters 2 through 5.

- (1) What factors have affected the trajectory of scientific research on CTs?

- (2) Are CT trends time-transgressive surfaces?
- (3) Has erosion on CTs been continuous or is it synchronous with cold (glacial) intervals?
- (4) What is the rate of erosion produced by nivation processes, and is it compatible with the scale of CTs?

CTs are especially well developed and ubiquitous throughout Beringia, the region extending from the Lena River in Siberia to the Mackenzie River in northwestern Canada, and containing the former Bering Land Bridge between Eurasia and North America during Quaternary cold intervals (Reger, 1975; Nelson, 1989; Lauriol et al. 1997). Field-based questions 2 and 3 are addressed within the context of eastern Beringia, i.e., western and central Alaska, and question 4 is addressed in northwestern British Columbia (Figure 3).

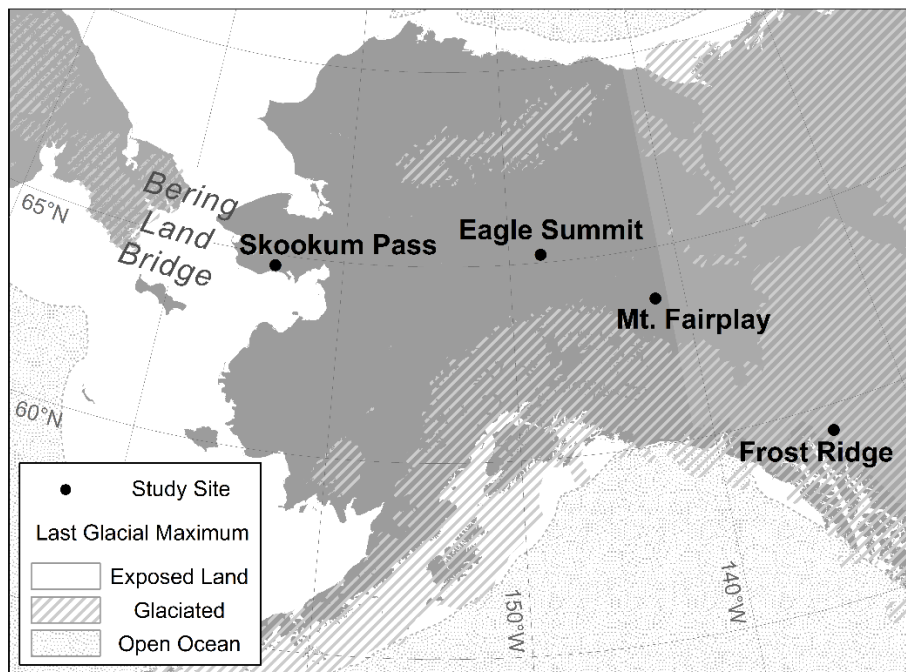


Figure 3. Map of Dissertation Study Areas. Relict cryoplanation terrace sites (Skookum Pass, Eagle Summit, and Mt. Fairplay) form a transect through unglaciated eastern Beringia. The recently deglaciated flanks of Frost Ridge are an area of active nivation operating on incipient terraces.

Chapter 2 is a literature review examining the state of knowledge about CTs. The problem of CT genesis has been complicated by a diverse lexicon and the large number of hypotheses posed over time about their formation. Terms for these features used in English-language literature have included *cryoplanation*, *altiplanation*, *equiplanation*, *nivation*, and *goletz*. Proposed hypotheses for CT formation include a modification of the Davisian cycle of erosion, a special phase of solifluction, complex sorting from mass-movement, surface and permafrost table lowering, and polygonal cracking, although contemporary literature favors only two hypotheses: structural control, and nivation. This review examines literature related to: (1) this diverse lexicon; (2) the distribution of CT studies around the world; (3) the numerous diverse genetic theories; and (4) the evolution and trajectory of cryoplanation literature over the past half-century. Tracking co-citation network modularity in the cryoplanation literature corpus serves as a quantifiable test for “gate-keeping” publications possibly discentivising research into the geomorphic enigma that is cryoplanation and its associated processes.

In Chapter 3, spatial statistical analyses of six relative weathering indices (fracture counts, Cailleux roundness, Cailleux flatness, Krumbein sphericity, rebound, and weathering rind thickness) across well-developed terraces at Mt. Fairplay, Eagle Summit, and Skookum Pass are used to test if cryoplanation terraces develop through scarp retreat. Statistically significant differences in relative weathering indices detected through chi-square and multiple-comparison procedures indicate that rock clasts are less weathered closer to scarps, i.e., that these areas were more recently exposed than those distant from the scarp. Based on these findings, a refined model of time-transgressive cryoplanation terrace development through nivation-driven scarp retreat is proposed. This new qualitative model addresses the removal of weathered material from terrace treads down side slopes through piping and gravity-driven mass wasting processes.

Chapter 4 presents the first numerical surface exposure ages and erosion rates from cryoplanation terraces obtained from terrestrial cosmogenic nuclides (TCN) in surface boulders. Ages include six ^{10}Be TCN ages from two terrace treads near Eagle Summit and six ^{36}Cl ages from two terrace treads on Mt. Fairplay. Based on these exposure ages the terraces at both locations were last actively eroding around the time of the Last Glacial Maximum. Both locations exhibit time-transgressive development, particularly in close proximity to scarp-tread junctions. Boulder exposure ages and distances between sample locations were also used to estimate erosion rates across these four terrace treads. The time-transgressive development of these Yukon-Tanana Upland surfaces, which correlate with multiple cold intervals, provides strong new evidence in support of the theory that these features form through scarp retreat driven by nivation.

Chapter 5 addresses the persistent question in periglacial geomorphology regarding the ability of nivation to produce CT-scale landforms (e.g., Prieznitz, 1988; Thorn & Hall, 2002). This chapter examines “Frost Ridge” on the Cathedral Massif in northwestern British Columbia to estimate long-term denudation attributable to nivation processes active since the Last Glacial Maximum. Frost Ridge presents an opportunity to address this issue by virtue of its east-west orientation and deglaciation history. Once deglaciated, marginal drainage features were present on both valley walls. Minimized solar radiation on the steep north-facing wall (Frost Ridge) allowed snowbanks accumulated in marginal drainage scars to persist and nivation processes to erode the slope. Today, several large nivation hollows, or incipient terraces, are present near the summit of Frost Ridge and marginal drainage features are preserved at lower elevations and on the opposite, south-facing valley wall. Using an unmanned aerial vehicle (UAV), a high-resolution survey was conducted, and volumes of marginal drainage and incipient terrace features compared. Based on

this volumetric comparison, denudation rates were estimated and compared to nivation rates from the Antarctic and lower-latitude periglacial areas.

Chapter 6 summarizes and discusses these data and results from the four preceding chapters, offers recommendations for future research, and identifies contributions these works offer to the discipline of periglacial geomorphology, and to society.

CHAPTER 2. HISTORY OF A GEOMORPHIC ENIGMA: REVIEW OF CRYOPLANATION AND ASSOCIATED HYPOTHESES

Introduction

Large elevated bedrock terraces culminating in extensive summit flats are common in hilly to mountainous periglacial (cold, unglaciated) environments. These *cryoplanation terraces* (CTs) resemble flights of giant steps, with alternating shallow sloping treads (typically 1° to 12° slopes) and steep, rubble-covered risers that can span several kilometers (Figure 4) (e.g., Demek, 1969; Prieznitz, 1988; Ballantyne, 2018). A tread and the riser immediately upslope are considered a “terrace unit” (Brunnschweiler, 1965). Although “riser” completes the staircase analogy, this portion of the terrace unit is more commonly referred to as a “scarp,” a term used in this study in a strictly morphologic and descriptive sense (Bloom, 2004, p. 67). Despite their dominating appearance in periglacial landscapes and more than a century of published identifications and studies, the origin, evolution, and significance of these landscapes remains a contentious topic in geomorphic literature (e.g., Thorn & Hall, 2002; French, 2016, 2017).

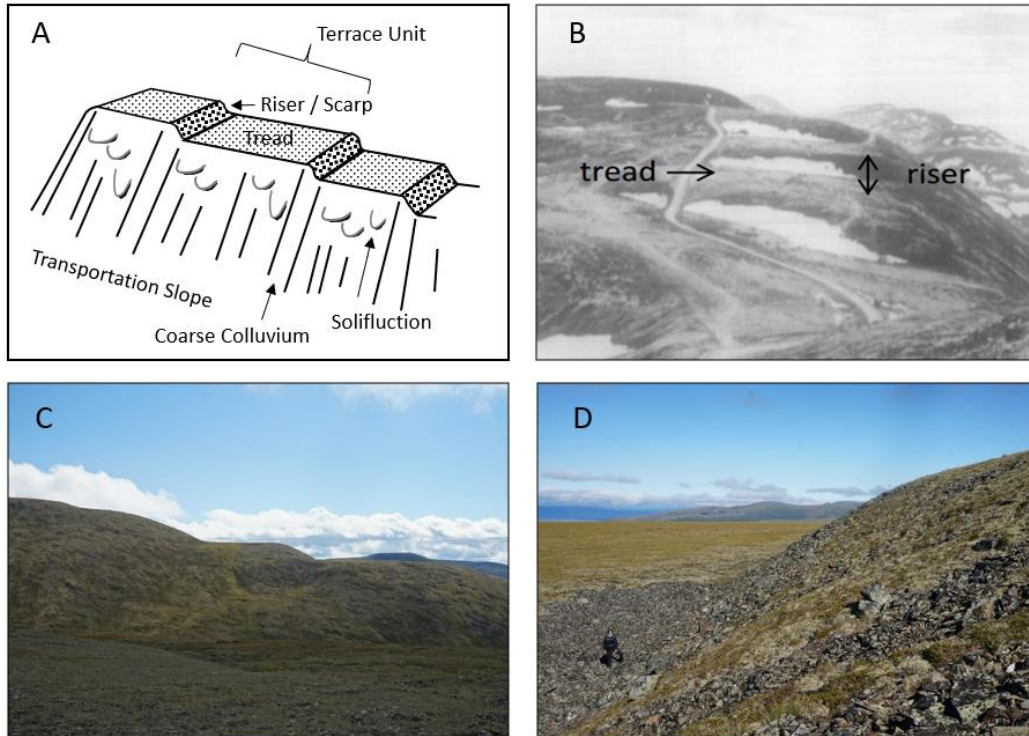


Figure 4. Cryoplanation Terrace Morphological Components. (A) Cryoplanation terrace morphology and terminology schematic, adapted from Nelson (1989) showing scarps or risers and nearly planar treads culminating in a summit flat. A “terrace unit” refers to a tread and the scarp rising from it (Brunnschweiler, 1965). Side slopes feature solifluction, rock stripes and other mass wasting forms. (B) Example of terraces at Indian Mountain., Alaska (Photo by: T.L. Péwé, June 1967). (C) Another example of CTs from Eagle Summit (Photo by: K.E. Nyland, August 2015) and (D) a rubble covered scarp at Eagle Summit with K.E. Nyland for scale (Photo by: C.W. Queen, August 2015).

CTs were first described in northwestern North America in the early 20th century by U.S. Geological Survey and Geological Survey of Canada personnel engaged in exploratory geology in the aftermath of the Klondike Gold Rush and its extension into Alaska (e.g., Moffit, 1905; Prindle, 1905, 1913; Cairnes, 1912a; Eakin, 1916). Early workers emphasized the ubiquity and prominence of these bedrock terraces and their apparent regionally consistent elevations. For example, Prindle (1905, p. 20) wrote: “[CTs] are especially prominent on the spurs and occur at corresponding levels

... Whatever the bedrock or its attitude, the same [cryoplanation] forms have been developed and are the most striking features of the landscape.”

These initial works attempted to align CT genesis with Davis’ “normal cycle of erosion” and the concept of peneplanation (Davis, 1909), but they could not resolve the presence of weathered deposits on terraces inconsistent with fluvial action (e.g., Moffit, 1905; Cairnes, 1912a) nor the apparent simultaneous formation at various elevations on a given ridge without regard to local or regional base level (e.g., Eakin, 1916). Although the specifics of the processes eluded these early workers, the features are consistent with ideas about parallel retreat of slopes that Davis (1932) erroneously attributed to Penck (1924; also see Simons, 1962) and later espoused by Bryan (1940) and King (1962), and by George Dawson, who emphasized the ability of cold-climate processes to intensify erosion (Dawson, 1896). The inferred ability of periglacial processes to limit the height of high-latitude topography is analogous to what is now commonly referred to as the “glacial buzzsaw” (e.g., Brozović et al., 1997; Hales & Roering, 2009; Hall & Kleman, 2014).

Breaking away from Davisian theory, subsequent genetic hypotheses centered on the cold climatic conditions of periglacial regions, often invoking permafrost-related processes such as solifluction, complex sorting, lowering of the permafrost table, and polygonal cracking (Eakin, 1916; Taber, 1943; Popov, 1960; Krivolutskiy, 1965). Contemporary literature favors only two hypotheses for CT formation, based on (1) geologic structure (e.g., Hall & André, 2010; French, 2016); and (2) nivation, a short-hand term for a suite of erosional processes associated with snowbanks persisting well into summer months (e.g., Cairnes, 1912a; Prindle 1913; Reger & Péwé, 1976; Nelson, 1989; 1998; Nelson & Nyland, 2017).

Impediments to advances about the origins and development of CTs include the several aliases for these landforms (altiplanation, equiplanation, nivation, goletz terraces), political and

linguistic barriers to knowledge dissemination, and a lack of both explicit field study and holistic treatment of the topic. Despite repeated calls for data on CT ages and rates of development over the last nearly 50 years (e.g., Demek, 1969; Prieznitz, 1988; Thorn & Hall, 2002; Nelson & Nyland, 2017), these basic questions remain to be addressed before consensus can be reached on a theory of CT genesis. A discussion of possible reasons for this literary stalemate is presented following a topical review of cryoplanation in the literature of periglacial geomorphology. This review details: (1) the diverse lexicon developed for cryoplanation landscapes; (2) the global distribution of field studies conducted on CTs; (3) the chronology of the numerous diverse formation theories proposed for their formation; and (4) the trajectory of contemporary (1970-2018) research using bibliometric methods.

A Diverse Lexicon

Although *cryoplanation* is the most common adjective applied to elevated bedrock terraces in periglacial environments, CTs have also been referred to in peer-reviewed literature as *altiplanation*, *equiplanation*, *nivation*, and *goletz* terraces (e.g., Demek, 1969; Prieznitz, 1988; French & Harry, 1992; Grab et al., 2005). Demek (1969, p. 5) lists several other names that have been applied to the features in various languages. The primary terms, which are used repeatedly in the literature, are summarized in Table 1 along with short definitions taken from their original sources. Each of these terms invokes different formation processes or regionality.

François Matthes (1900) introduced the term *nivation* to describe a suite of erosional processes revolving around intensified weathering and transportation in the vicinity of late-lying snowbanks he observed in the Big Horn Mountains of Wyoming. Although Cairnes (1912a) was the first to connect the nivation process suite with cryoplanation terraces, he advocated use of the term *equiplanation* in an adaptation of Davis' "normal cycle," in order to be more inclusive of

climatically controlled erosion processes. Cairnes also hypothesized that the movement of detritus is an equilibrium process, and that periglacial uplands are reduced to snowline, but not to base level (Cairnes, 1912b). The term “equiplanation” was never generally adopted.

Table 1. Adjectives for Elevated Periglacial Terraces and First Appearance Reference.

Adjective	Short Definition	Citation
Equiplanation	Flattening of a periglacial upland surface similar to Davis’ “normal cycle of erosion,” but involving nivation and solifluction processes.	(Cairnes, 1912b)
Altiplanation	Descriptor for a “special phase of solifluction” occurring at the landscape scale.	(Eakin, 1916)
Goletz	From the Russian голец террасы (‘mountain balds’)	(Boch & Krasnov, 1943)
Cryoplanation	General and unifying term for frost action and downslope transportation of debris.	(Bryan, 1946)
Nivation	Enhanced erosion afforded by snow through ‘freeze-thaw cycling’ and added moisture.	(Gregory, 1966)

During the same era of initial observation in Alaska, another term, *altiplanation*, was proposed by Eakin (1916) to reflect his hypothesis that these large terraces were the result of localized solifluction processes. “Altiplanation” continued in use as a very general term for decades, although not necessarily in conjunction with the concept of nivation. In some cases nivation and altiplanation were represented as complementary processes or perhaps competing hypotheses (e.g., Mertie, 1936, p. 32). Te Punga (1956) suggested nivation as an explanation for development of altiplanation terraces in southwestern England, although he regarded “downwearing” as responsible for terrace growth. This morphologic-genetic association between nivation (process) and altiplanation (form) continued (e.g., Embleton & King, 1968) until the late 1960s, when Demek (1968) introduced the “apt and justifiable” (Jahn 1975, p. 164) term “cryoplanation terrace,” which gained dominance after publication of Demek’s (1969) influential

monograph. “Altiplanation” largely fell out of general use after the 1960s, except in reference to older works, and by a few authors (e.g., Péwé, 1973; 1975; Washburn, 1973) who used ‘altiplanation terrace’ in a manner identical to contemporary usage of “cryoplanation terrace.”

Until the widespread adoption of “cryoplanation terrace,” literature originating in Eastern Europe and Asia, particularly those countries formerly aligned politically with the Soviet Union, have traditionally used a term phonetically translated from Russian, *goletz* terraces (e.g., Boch & Krasnov, 1943; 1951). The original Russian phrase indicates that the feature is above treeline or ‘bald’ (Prieznitz, 1988). Use of this naming convention is typically indicative of study area or an author’s language of training (e.g., Boch & Krasnov, 1943; Richter et al. 1963; Lomborinchen, 1998).

The term *cryoplanation* has come to be favored by most authors, as it is the most appropriate and inclusive term describing gentle erosional surfaces produced under cold climatic conditions (Demek, 1969). In Bryan’s original definition he made explicit note to include fluvial processes working at lower elevations to transport materials initially delivered by processes driven by frost action (1946, p. 640). It is clear from Bryan’s text that he intended the term to refer to broad-scale planation surfaces produced under cold climatic conditions. Peltier (1950) outlined a Davisian-style erosional cycle, in which he employed “cryoplanation” with reference to regional lowering of the land surface. It was nearly 20 years later that Demek (1968) used the term adjectivally, affixing it as a prefix to “terrace.” “Cryoplanation terrace” received widespread acceptance almost immediately thereafter. It became the preferred expression and was ensconced in the literature after it was adopted by periglacial textbooks during the 1970s (Embleton & King, 1975; French, 1976; Washburn 1979).

A curious leap in geographic scale accompanied adoption of the term “cryoplanation terrace.” Bryan (1946) and Peltier (1950) used “cryoplanation” with reference to planation surfaces of regional extent, but Demek’s (1968) application of the term to high mountain terraces of local areal extent was a rather extreme departure from the original usage. Precedent exists for such a terminological approach; Ollier (1981, pp. 152-153), for example, made reference to “tiny” planation surfaces.

Hall (1998) has argued that little difference exists between the terms cryoplanation and nivation, but rather that these may represent the extrema of a single process spectrum. Hall’s appraisal of the nivation literature suggests that term “nivation” is employed more in wetter environments and “cryoplanation” more in water-limited ones (Hall, 1998; Thorn & Hall, 2002). However, CTs have been identified in polar marine climates (Shear 1964), such as Iceland (Schunke, 1974; 1975; Schunke & Heckindorf 1976).

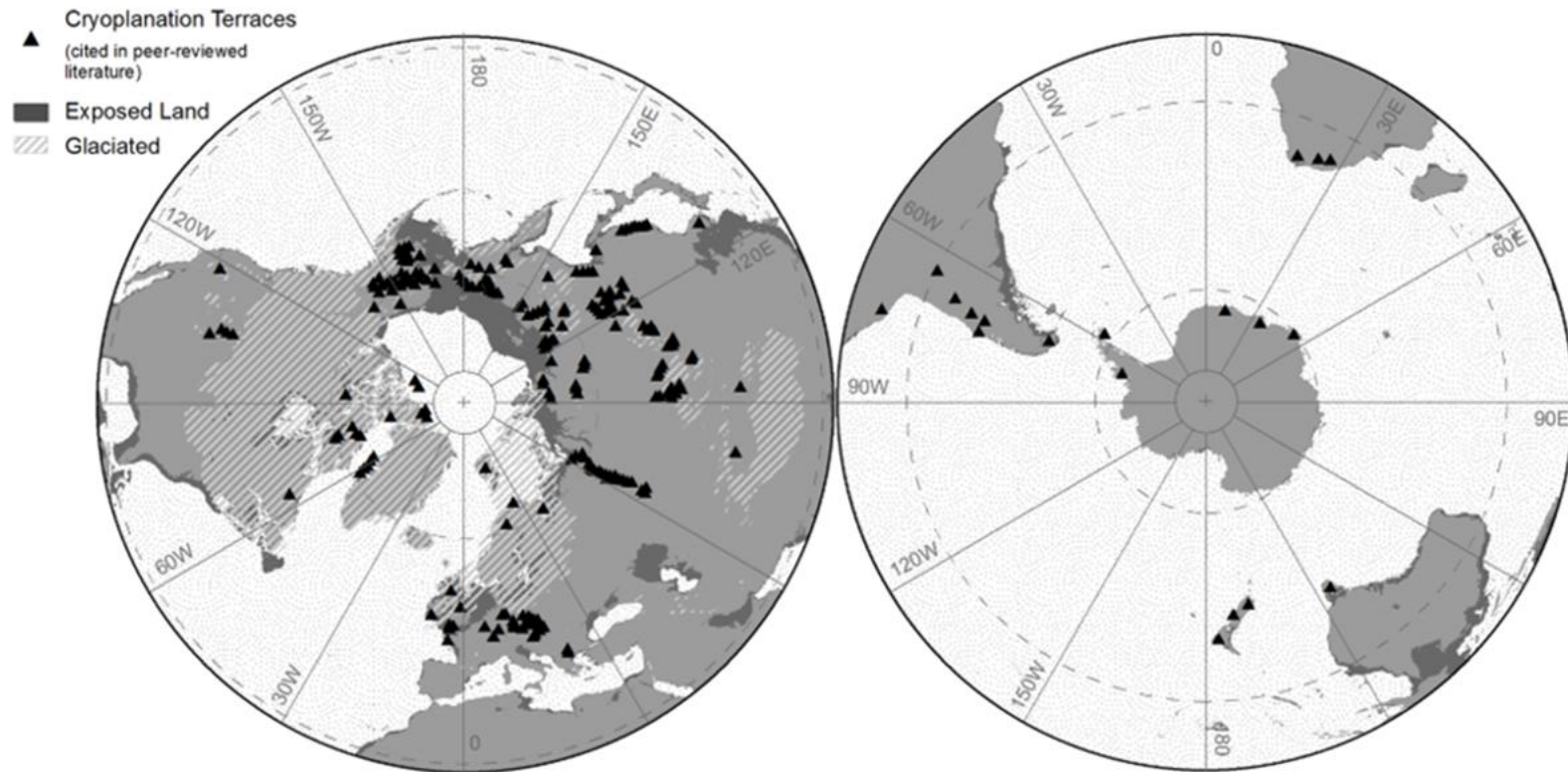
We recommend following Thorn’s (1983) suggestion to separate morphological and genetic inferences in the assignment of names to geomorphic features. Under this constraint “nivation” is a shorthand term encompassing the suite of processes that lead to intensified weathering and transportation in the vicinity of late-lying snowbanks. “Cryoplanation terrace” is primarily a morphological term referring to step-like slope profiles in cold regions involving a gentle tread and a steeper riser, separated by an abrupt break in slope. We propose that smaller features be referred to as “incipient cryoplanation terraces,” thereby avoiding the ambiguity involved in specifying the dimensions at which a nivation hollow becomes a cryoplanation terrace (Hall, 1998). A similar terminological suggestion was made by Lewis (1939) and supported by Te Punga (1956, p. 335).

Global Distribution

Demek (1969) inventoried relevant periglacial geomorphology literature published before 1968 for CT location information and used these data to map the distribution of CTs in North America, Europe, and Asia. This series of three maps has represented the known global distribution of CTs in many subsequent works (e.g., Reger, 1975; Washburn, 1973; 1979). Karrasch (1972) expanded on this by mapping generalized CT locations in the Northern Hemisphere with contemporary permafrost regions.

Using the descriptors catalogued in the previous section, peer-reviewed literature was searched for additional CT locations to expand on the previously understood global distribution. This update includes papers published after Demek's work and in areas previously not covered, including the Southern Hemisphere. Although the majority of papers included in the inventory was explicitly about cryoplanation or geomorphic mapping (e.g., Davies, 1958; Jahn, 1979; Grosso & Corte, 1991; Hall, 1997a; Skyles & Vanching, 2007; Hall & André, 2010) other studies that mention CT locations tangentially were also included (e.g., Leslie, 1973; Hagedorn, 1984; Schrott, 1991; Trombotto et al., 1997; Galán de Mera et al., 2014). A total of 249 cryoplanation sites identified in peer-reviewed publications are shown in Figure 5. Except for Reger (1975), who inventoried CT sequences throughout central and western Alaska, no other attempts at mapping CT study locations over large areas have been published. Importantly, an inventory of CTs has not previously been attempted at the global scale. Figure 5 shows that cryoplanation landforms are ubiquitous in both present and past periglacial environments and exist on every continent.

Global Occurrences of Cryoplanation Terraces as Published in Peer Reviewed Literature



Glacial and exposed land data source: Gibbard, P. L. (2008). *Quaternary Glaciations: Extent and Chronology*. J. Ehlers (Ed.). Elsevier.

Figure 5. Global Distribution of Documented Cryoplanation Terraces. cryoplanation terrace locations identified from published in peer-reviewed literature. Northern Hemisphere: Demek, 1969, and references therein; Jahn, 1979; Yangxing & Xiaofeng, 1983; Ballantyne, 1985; Guoqing & Guodong, 1995; Lauriol et al., 1997; Seong & Kim, 2003; Skyles & Vanching, 2007; Quinn, 2011. Southern Hemisphere: Davies, 1958; Sekyra, 1969; Wood, 1969; Leslie, 1973; Schunke, 1974, 1975; Karrasch, 1972; Corte, 1983; Hagedorn, 1984; Vtyurin, 1986; Yoshikawa et al., 1988; Grosso & Corte, 1991; Schrott, 1991; Hall, 1997a; Trombotto et al., 1997; Grab et al., 1999; Grab et al., 2005; Coronato et al., 2008; May, 2008; Perucca & Angillieri, 2008; Borromei et al., 2010; Hall & André, 2010; Galán de Mera et al., 2014.

In the Northern Hemisphere new locations largely constitute infilling with works published in the 50 years since Demek's inventory, including locations in the permafrost regions of China and Mongolia (Yangxing & Xiaofeng, 1983; Guoqing & Guodong, 1995; Skyles & Vanching, 2007) South Korea (Seong & Kim, 2003), Yukon Territory (Lauriol et al., 1997), southwest Ireland (Quinn, 2011), Scotland (Ballantyne, 1985), northeast Norway (Jahn, 1979), Iceland (Schunke, 1974, 1975; Schunke & Heckendorff 1976), and Russian islands in the Arctic Ocean (Karrasch, 1972). The Southern Hemisphere represents the largest expansion of the previous distribution, with CT studies in Antarctica (Sekyra, 1969; Corte, 1983; Vtyurin, 1986; Hall, 1997a; Hall & André, 2010), South Africa (Grab et al., 1999), Tasmania (Davies, 1958), and New Zealand (Wood, 1969; Leslie, 1973; Yoshikawa et al., 1988). Constituting the most recent cryoplanation work are studies conducted throughout much of the Andes over the last 27 years (Grosso & Corte, 1991; Schrott, 1991; Trombotto et al., 1997; Coronato et al., 2008; May, 2008; Perucca & Angillieri, 2008; Borromei et al., 2010; Galán de Mera et al., 2014).

Of particular note are those regions with the highest density of CTs, in the Carpathian and Ural Mountains and in Beringia, the former ice-free corridor and land bridge that connected Eurasia with North America during Quaternary cold intervals (e.g., Reger 1975, Nelson 1989, Lauriol et al. 1997). Both the Carpathians and the Urals have long been studied by periglacial geomorphologists, even before the naming of the subdiscipline. Walery von Lozinski coined the term 'periglacial' in 1909 when studying the mechanical weathering of sandstones in the Carpathians (Lozinski, 1909; 1912; French, 2000). Predating this, CTs in the Urals were discussed in Russian literature by Kozmin as early as 1890 (Boch & Krasnov, 1943). However, Beringia has emerged as the best place for the study of periglacial landforms and processes, owing to the cold but largely unglaciated conditions that extended through most of the Pleistocene (e.g., Birot, 1968).

Beringia contains the most ubiquitous and best-developed CTs, an association that indicates the antiquity of these features (Demek, 1969; Reger, 1975; Nelson & Nyland, 2017; Ballantyne, 2018, p. 221).

Despite the Bering Sea separating eastern and western Beringia by just 80 km, there was very little scientific communication between Soviet and North American geomorphologists during the first half of the 20th century on virtually any cryospheric subject (e.g., French & Nelson, 2008). Until Demek's 1969 monograph, CT studies had developed in a parallel fashion between western Beringia (Obruchev, 1937; Zhigarev & Kaplina, 1960), from Yakutia to Chukotka (Richter et al., 1963; Demek, 1968; Czudek & Demek, 1973) and eastern Beringia (Moffit, 1905; Prindle, 1905; Eakin, 1916; Mertie, 1937; Péwé, 1973; Reger, 1975) from Alaska to the Yukon Territory (Cairnes, 1912a; Raup, 1951; Lauriol, 1990).

A Century of Competing Hypotheses

The variety of untested hypotheses about the origins and development of CTs is likely due in part to political and linguistic divisions in 20th century literature and in part to a lack of detailed field study. Reger, in his 1975 doctoral dissertation, provided an exhaustive review and critique of seven different hypotheses proposed for the origin and evolution of CTs. Table 2 and Figure 6 provide a synopsis of his detailed review, with additional supporting publications in the chronological order in which the hypotheses were proposed.

Table 2. Development Hypothesis, Abbreviated Definition, and First Appearance.

Hypothesis Name	Short Definition	Citation
Davisian Erosion	Cryoplanation surfaces result from subaqueous or subaerial dissection and erosion of a peneplain	Collier, 1902
Scarp Retreat	Nivation processes intensify frost action and erosion causing scarp retreat.	Cairnes, 1912a
Altiplanation	Under a “special phase of solifluction” where there is loose rock material, “subarctic temperatures,” no vegetation, minimal precipitation, and extended weathering, slopes form terrace-like forms and flattened summits	Eakin, 1916, p.78
Geologic Structure	Terraces result from surface erosional processes along horizontal bedrock structures that control the development.	Padalka, 1928
Mass Movement	Terraces are formed via a complex series of sorting and mass wasting processes forming embankments on slopes	Taber, 1943
Polygonal Cracking	Regular form and spacing of terraces due to large-scale cracking from tectonics and ice wedging on sloping denudation surfaces	Popov, 1960
Surface Lowering	Terraces and flattened summits are formed when repeated freeze/thaw action breaks down rock and heaves clasts to the surface to be transported down sideslopes. Continued removal of surface material lowers the permafrost table to weather progressively deeper rock.	Krivolutskiy, 1965

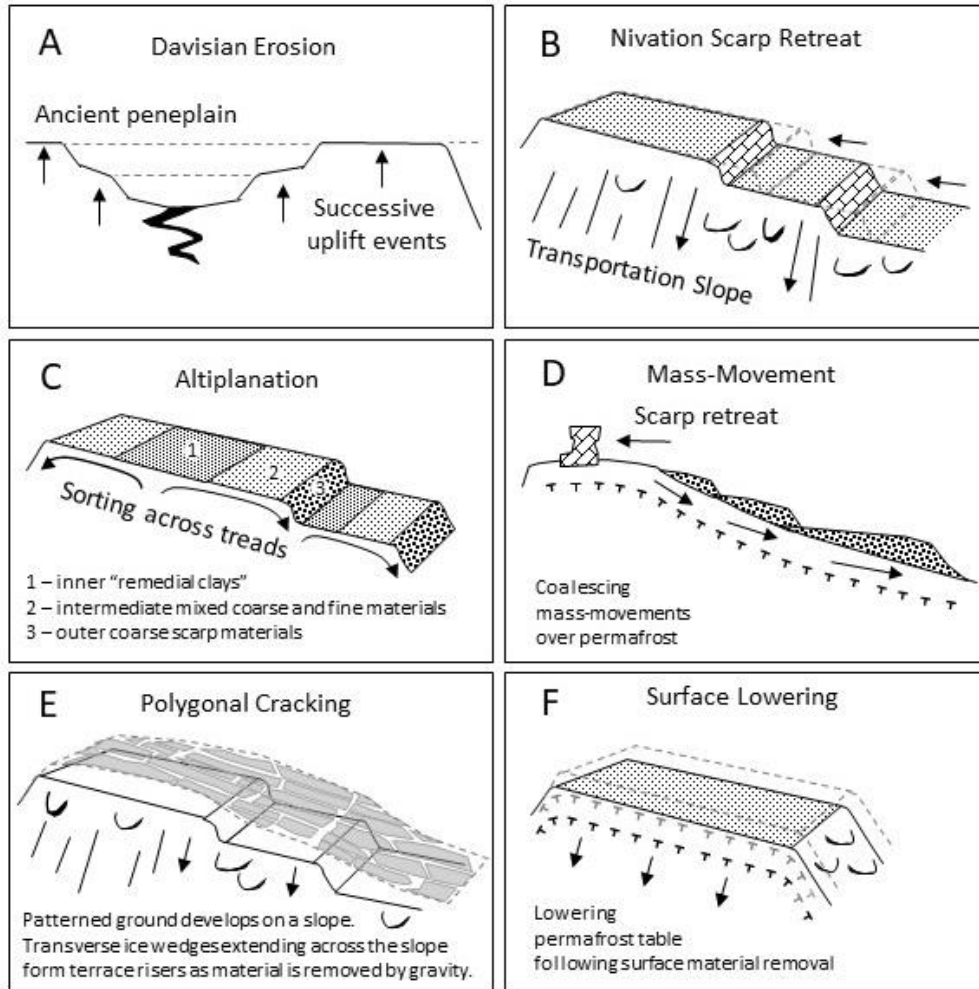


Figure 6. Conceptual Diagrams of Proposed Formation Hypotheses. (A) Davisian erosion, (B) scarp retreat, (C) altiplanation, (D) mass-movement, (E) polygonal cracking, and (F) surface-lowering theories proposed for the formation of CTs in peer-reviewed literature.

Davisian Erosion

Davis' "normal cycle of erosion" (1909) was the widely accepted model for landscape evolution in the early 20th century. Based on initial surveys, and observations that summit flats displayed approximately accordant elevations and truncated geologic structure, several authors interpreted these landscapes as ancient peneplains subsequently dissected by fluvial processes (Figure 6A). This erosional surface interpretation was applied to CTs in the Yukon-Tanana Upland

(Prindle, 1905; 1913; Cairnes, 1912a; 1912b) and in the northwest Seward Peninsula (Collier, 1902; 1906; Smith & Mertie, 1930; Hopkins & Sigafos, 1951; Sainsbury et al., 1965). Tors, tumps, and bolvans (Demek, 1969, p. 63-65) present on these surfaces were explained as residual monadnocks (Prindle, 1905; 1913; Cairnes, 1912a; 1912b). The interpretation that these are erosional surfaces was also applied to Siberian uplands thought to have been leveled by a Pleistocene glaciation (Aleschkow, 1936).

Thornbury (1969, pp.181-184) outlined five criteria for recognizing a Davisian peneplain, of which only three were satisfied in the original observations of CTs from the beginning of the 20th century. Several researchers made note of the distinct terrace riser and tread junctions, and the truncation of rocks of varying resistance (e.g., Moffit, 1905; Cairnes, 1912a; Eakin, 1916). Moffit (1905) also claimed terraces and summit areas were accordant, despite measurements to the contrary generated by his topographer. No one found alluvial deposits on these elevated surfaces nor significantly thick zones of weathered debris, but rather thin, if present, autochthonous rubble, evidence in contradiction to the necessary qualifications for a peneplain (Moffit, 1905; Cairnes, 1912a; 1912b; Eakin, 1916). The enigma these elevated terraces presented to geomorphologists from the early 20th century eventually necessitated a fundamental break from Davisian geomorphic theory, in favor of a model involving parallel retreat of scarps and creation of time-transgressive tread surfaces.

Scarp Retreat

Equiplanation, as proposed by Cairnes (1912a), centered on scarp retreat under nivation and the planating effect about the snowline altitude (Figure 6B), as described by Matthes (1900). Although contemporary understanding of the nivation process suite (Thorn, 1976; Thorn & Hall, 2002) is substantially different from what Matthes and Cairnes originally proposed, abundant

evidence exists that intensified weathering and erosion occur in the vicinity of late-lying snowbanks (e.g., Thorn, 1976; Ballantyne et al., 1989; Berrisford, 1991; Hall, 1993; cf. Hall, 1999; Boelhouwers & Jonsson, 2013). Snowbanks lasting well into the warm season provide thermal insulation and moisture that contribute to enhanced chemical and mechanical breakdown of rock, which is subsequently removed by mass wasting processes (e.g., Thorn & Hall, 1980; Berrisford, 1991).

Since introduction of the nivation concept more than a century ago, many have supported its application to CT development (e.g., Cairnes, 1912a; Boch & Krasnov, 1943; Te Punga, 1956; Waters, 1962; Demek, 1969; Czudek & Demek, 1973; Reger, 1975; Reger & Péwé, 1976; Nelson, 1989, 1998; Nelson & Nyland, 2017). Just a year after Cairnes' publication appeared, Prindle (1913, p. 54) also invoked the erosive effects of snow banks at scarp-tread junctions causing parallel retreat in his discussion of "step-cut hills" in Alaska's Circle district, although he did not use the term "nivation."

Although a direct, process connection between nivation and CTs has yet to be substantiated by instrumental field observations and experiments, indirect evidence provides strong support for such a connection (Reger, 1975; Reger & Péwé, 1976; Nelson 1989; 1998; Nelson & Nyland, 2017). However, the rate and erosive capacity at which the nivation process suite operates, and whether it is applicable at the scale of large cryoplanation terraces, remains to be determined in detail (cf. Nelson, 1989).

Altiplanation

Solifluction was defined by Andersson in 1906 as the gravity- and frost-driven flow of saturated material downhill. Eakin (1916, p. 76) then redefined the term as the vertical and horizontal movement of material by frost heave and thrust respectively. Building on his version of

“solifluction” in the same work (Eakin, 1916, p. 78), he coined “altiplanation” to designate a special phase of solifluction that, under certain conditions, expresses itself in terrace-like forms and flattened summits and passes that are essentially accumulations of loose rock materials (Figure 6C).

Eakin based his ideas on observations of only autochthonous materials and perceived repeating sedimentological patterns. He interpreted CTs as made up of three debris zones. Moving outward from scarp-tread junctions or the centers of summit flats, these were: (1) residual clays; (2) mixed fines and coarse materials; and (3) large rubble constituting the descending scarps at the angle of repose. The inner zone is leveled “under stress of gravity” and the intermediate zone under “the action of frost,” where, with time, treads expand and consume lower tread surfaces as frost wedging and solifluction sorts and removes material down the outer scarp zone (Figure 6C) (Eakin, 1916, p. 81).

There are several significant issues with Eakin’s (1916) explanation, including disregard for the original definition of solifluction, ambiguous process mechanisms, and material sources. He offered no explanation for the initial formation of stepped profiles and asserts that solifluction is more intense in the inner margins of treads, and “practically dies out” near the rim (p. 79). It is rather difficult to understand how the outer margins of the terraces can be extended if the main transportation agency is considered inactive. Also, the terraces he observed, revisited by Reger, are bedrock features with only a thin rubble cover. On average, CTs throughout central and western Alaska have only 1.5 m of material overlying bedrock (Reger, 1975). Despite these shortcomings, Eakin’s explanation for altiplanation terraces continued to be treated as plausible into the 1960s (e.g., Wahrhaftig, 1965, p. 16; Foster, 1967, p. B16).

Geologic Structure

Padalka (1928) postulated that the distinctive planar morphology of terrace treads in the Urals was simply the result of geologic structural control. Structure was also employed in explanations by Waters (1962) after studying CTs on nearly horizontal joint planes in Spitsbergen and by Foster (1967, p. 16) for some terrace series on Mt. Fairplay in Alaska's Yukon-Tanana Upland, where folded igneous materials have formed nearly horizontal bedding planes. This interpretation has also received much more recent support in the context of CTs on Alexander Island off the Antarctic Peninsula (Hall & André, 2010). Hall & André (2010) concluded that the CTs they were initially monitoring for active planation processes were instead the result of exposed lithologic junctions.

The greatest weakness of a purely structural hypothesis for CT formation are the many documented sites where CTs cross-cut bedding structures, rock type, or foliation (e.g., Demek, 1969; Reger, 1975; Reger & Péwé, 1976). However, structural influence and erosional process are not mutually exclusive (Waters 1962, p. 100). Reger (1975, p. 131) pointed out at two Alaskan sites; Mt. Fairplay and Mastodon Dome (also in the Yukon-Tanana Upland), where "... processes forming cryoplanation terraces can take advantage of zones of weakness in bedrock ..." Similarly, in the Yukon, CTs, and particularly cryopediments, have also been recently described as "landscapes of inheritance," or controlled by structure and then modified by climate-driven processes (French & Harry, 1992; French, 2011; 2016).

Mass Movement

Taber (1943) hypothesized that terraces he observed were the result of accumulations of mass-movements involving large clasts. According to his hypothesis for permafrost regions, large, loose clasts, mobilized by frost action and scarp retreat, roll over underlying fines moving under

creep. The faster-moving overlying coarse material accumulates when slope decreases, or when the underlying fine fraction is outpaced and contact is made with bedrock, other coarse material, or vegetation. As underlying fines continue to creep over the permafrost table these talus-like accumulations overtake one another at lower elevations, increasing the size and reducing the inclination of lower treads. When accumulations become thicker than the depth of seasonal freezing, permafrost aggrades, stabilizing these talus slopes and allowing frost action to initiate scarp retreat again. Tors on summit flats, he then argued, were remnants of previous scarp recession, providing the material for the mass movements (Figure 6D).

Much like the issues found with Eakin's altiplanation hypothesis, Taber's mass-movement explanations interprets CTs as accumulation features. They are, in fact, cut in bedrock with only a veneer of rubble – hallmarks of an erosional feature. A mass-movement process such as that envisioned by Taber would also dictate that terraces would increase in size and angularity with decreasing elevation. Reger's (1975) inventory of Alaskan CT morphologies showed the opposite trend, where higher-elevation CTs tend to be more angular.

Polygonal Cracking

Popov (1960) conceived that CTs of regular size and consistent scarp and tread dimensions could be the result of patterned ground development on slopes. He hypothesized that what would later be termed "anti-syngenetic" ice wedges (Mackay, 1990) orient longitudinally and transversely to a slope and could extend several tens to hundreds of meters, forming orthogonal patterned ground (French, 2017, p.144-145). Where significant inter-polygon fissures completely traverse a slope, a scarp can develop as bedrock weathers and large clasts are removed by nivation and accompanying slope processes. Treads then develop from the settling and flattening of inter-

polygon fissures as they continue to widen over time (Figure 6E). Popov attributed rounding of terraces to subsequent removal of material in rock stripes.

The major assumption that terraces are of equal areal dimensions and regular scarp-to-tread ratios is unsubstantiated by field observation. Tread length and scarp height can vary significantly within and among terrace series (Reger, 1975; Reger & Péwé, 1976). Although polygon diameters observed on slopes and well-drained uplands can exceed 40 m, frost-initiated polygonal networks are largely absent in metasedimentary and igneous rock (French, 2017, p. 145), rock types in which CTs readily form.

Surface Lowering

In an attempt to explain the presence of summit flats and flat passes in granitic materials in Siberia, Krivolutskiy (1965) proposed that these surfaces are simultaneously lowering. The lack of matrix material around the large angular clasts he observed on terrace treads allows precipitation to infiltrate underlying bedrock until the permafrost table is reached. Within the depth of seasonal freezing, bedrock is then mechanically weathered through ice wedging. Clasts heaved to the surface they are transported across treads and down sideslopes, as evidenced by rock stripes. Sustained removal of material lowers the ground surface and consequently the underlying permafrost table, weathering successively deeper bedrock on treads where water does not run off as easily (Figure 6F).

Although Krivotskiy's hypothesis might explain the summit flats and passes he observed in granitic materials, it does not explain the formation of terraces that typically form a series below a summit flat or in areas not explicitly controlled by underlying bedrock structure. Terraces have also been documented with permafrost tables above the depth of bedrock (Reger, 1975).

Bibliometric Assessment of Contemporary Cryoplanation Literature

Since the 1970s, only theories based on geologic structure and scarp retreat through nivation have continued to receive attention and support in modern literature, but no significant progress has been made toward a general acceptance of either. Instead, the topic has repeatedly been described as an ongoing debate (e.g., Prieznitz, 1988; Thorn & Hall, 2002; Ballantyne, 2018).

Boelhouwers and Jonsson (2013) identified publications that may have been performing “gate-keeping” roles in the nivation literature. They traced the provenance of the idea that a $2^{\circ}\text{C min}^{-1}$ threshold is a primary factor involved in mechanical weathering and showed, based on detailed review of literature, that this “thermal stress hypothesis” had been misinterpreted and misrepresented as it diffused from the literature of engineering to that of geomorphology. Boelhouwers and Jonsson’s (2013) paper included an analysis of the frequency at which these papers have been cited, demonstrating that the $2^{\circ}\text{C min}^{-1}$ threshold is not substantiated, owing to contradictory results and the variability of strength in different rock types. As of 2013, three papers (Hall, 1997; 1999; Hall & André, 2001) were the most cited for the topic of thermal stress weathering. However, the temperature requirement for particular rock types that result in strain affecting long-term weathering remains unsettled in nivation literature. In an examination of the bibliometric trends in contemporary cryoplanation literature, defined here as those published after 1970, we test whether any publications related to cryoplanation are performing similar gate-keeping (Wang et al., 2017) or “fashionista” (Sherman, 1996) functions that could disincentivize critical field investigations.

Bibliometric analysis (e.g., Osareh, 1996) is a powerful tool for tracing the origins and evolution of scientific ideas, although it appears to have not been used extensively in periglacial geomorphology. Citation analyses are usually favored by practitioners over bibliometrics,

particularly for capturing trends in subfields (Dorn, 2002). The top five most-cited papers in the cryoplanation corpus (Table 3) have not been followed by an increase in publications according to publication counts from Web of Science and Scopus. Google Scholar also shows short-term declines following these publications, but an overall increase over the longer term (Figure 7). These publication counts were generated from basic term searches of cryoplanation-related terms in tandem with the word “terraces”. To test if any of these are acting as gate keepers, or if papers significantly discourage or encourage work on the subject, we examined the development of the cryoplanation co-citation network over time.

Table 3. Google Scholar Top 5 Cited Articles about Cryoplanation.

Rank	Citations	Author(s)	Date	Journal
1/2	54	Demek, J.	1969	<i>Rozpravy ČSAV. ř. mat. a přír. věd.</i>
1/2	54	Reger, R.D., Péwé, T.L.	1976	<i>Quaternary Research</i>
3	50	Thorn, C.E., Hall, K.	2002	<i>Progress in Physical Geography</i>
4	41	Czudek, T.	1995	<i>Geografiska Annaler: Series A</i>
5	40	French, H.M., Harry, D.G.	1992	<i>Geografiska Annaler: Series A</i>

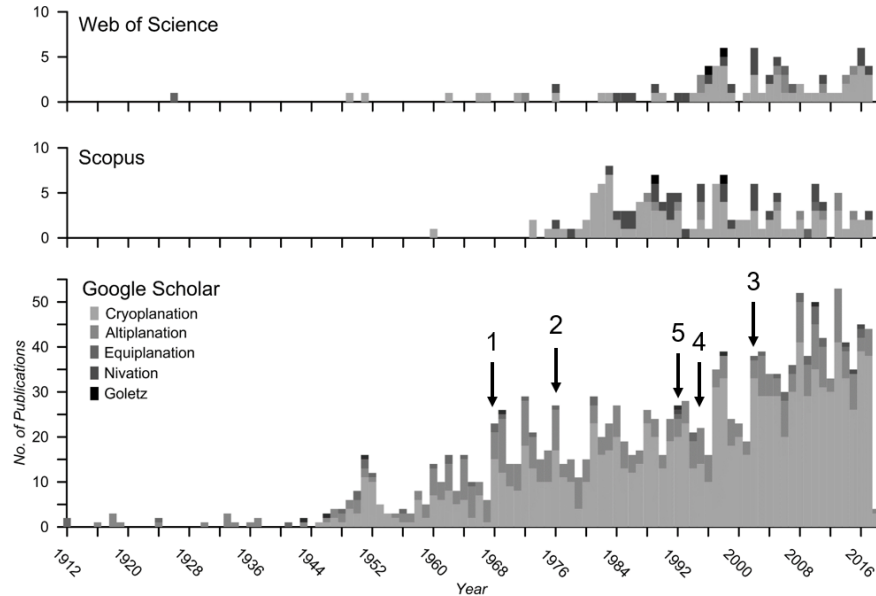


Figure 7. Frequency of Cryoplanation Literature Publication. Publication timeline is based on term searches. Numbered arrows indicate the rank of the top five most cited works (see Table 3).

Co-Citation Analysis

Elsevier’s citation database, Scopus, was chosen to examine contemporary CT literature because it offers article metadata and a more consistent database than Google Scholar, and better coverage of natural science journals relative to Web of Science (Mongeon & Paul-Hus, 2016). Data were obtained from Scopus via a series of queries to the Elsevier application programming interfaces (APIs). First, a keyword search was used to identify 243 articles matching the term “cryoplanation” or any one of a set of similar terms (see Table 1), and the word “terrace” or “terraces”. The retrieved data were evaluated manually by the authors for relevance, using the criterion that only those articles that explicitly mention formation process(es) were retained, yielding a set of 121 articles published from 1971 to 2018. Subsequent calls to Elsevier APIs were used to gather article and citation metadata for the relevant articles. Although there is a recognized English-language bias in Scopus (e.g., Dorn, 2002; Mongeon & Paul-Hus, 2016), of the 121

relevant articles, 15% are in foreign languages; Chinese (1), Czech (2), French (4), German (3), Hungarian (2), Polish (3), Russian (1), Slovenian (1), and Spanish (1). The resulting dataset was therefore deemed acceptable for further analysis in terms of relevance and international representation.

A bibliometric analysis of these data was conducted by isolating pairwise co-citations from the reference lists of the relevant articles. Only those co-citations in which both the cited articles in each pair were also members of the initial set of 121 articles were retained and analyzed. A co-citation network was then created using Python packages, including Pandas (McKinney, 2010) for data cleaning and processing and NetworkX (Hagberg et al., 2008) to formulate and analyze the evolution of this literature network over time. Network visualizations were created using Gephi open-source software (Bastian et al., 2009).

Results and Interpretation

Figure 8 shows the evolution of the contemporary CT corpus beginning when the network grew larger than 15 nodes (cited articles) and edges (articles that cite the connected nodes, or co-citation). When articles were evaluated for relevance, the articles' "stance" on formation processes was also attributed. An article was classified as taking a climatic stance if it presents evidence or otherwise supports a climate-driven formation process for CT formation, such as scarp retreat under nivation (e.g., Reger & Péwé, 1976; Nelson, 1989; Czudek, 1995; Thorn & Hall, 2002). Neutral articles present at least two formation hypotheses, typically as a review of the ongoing debate, without providing additional support for any particular one (e.g., Tufnell, 1971; French, 2000; Thorn, 2003; Ballantyne, 1984). Lastly, "skeptical" is a catchall category for articles presenting evidence contradictory to climate-driven erosional processes operating at the scale of

CTs, or otherwise supporting an alternative hypothesis (Hall, 1997a; 1997b; Humlum, 1998; Migon & Goudie, 2001; Hall & André, 2010).

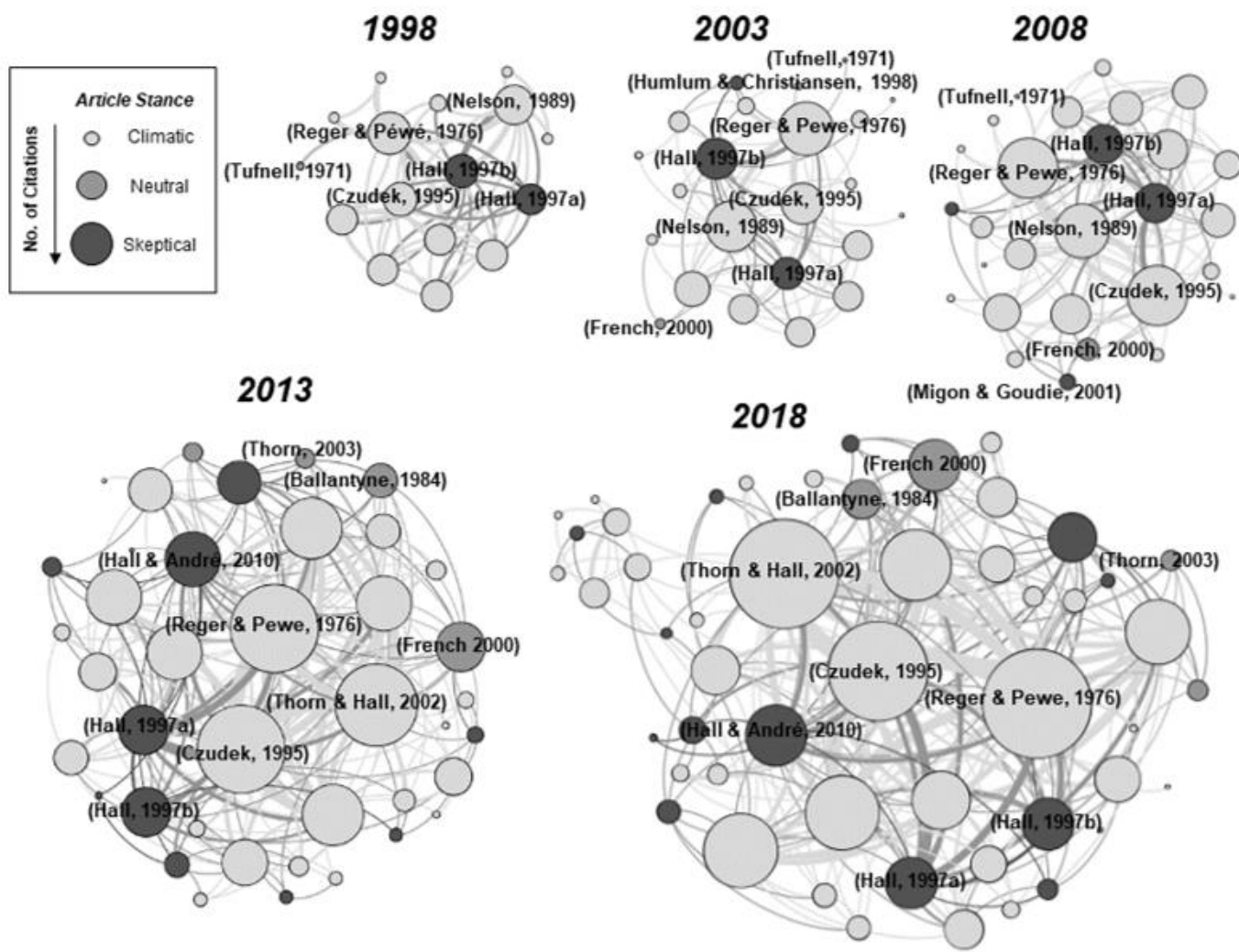


Figure 8. Five-Year Interval Cumulative Cryoplanation Co-Citation Networks. Time series begins after the network grew larger than 15 nodes and edges. Edge thickness is relative to the number of papers citing connected nodes together. The top three cited articles within each stance category are labeled for reference.

Over the last several decades there has been a steady increase in the number of articles taking a skeptical or neutral stance on the subject of CT formation processes (Figure 9). Support for structural-based hypotheses, in which the mass wasting processes involved are thought to be controlled largely by geologic structure and lithology (e.g., Hall, 1998; Hall & André, 2010), has been bolstered by the conceptual introduction of landscape inheritance, or the persistence of a surface formed before the Quaternary and only minimally modified thereafter (e.g., Migon & Goudie, 2001).

Within this contemporary time frame, however, there has been little to no clustering in this literature corpus. Clustering would manifest as nodes connected to the main network by significantly fewer edges, meaning that articles were only citing a select group of authors. The only instance of clustering in the evolution of this network occurs by 2018, and is clearly based on the common geography (Great Britain) of the study areas featured in these works (e.g., Ballantyne, 1985; Gerrard, 1988; Evans et al., 2012; Harrison et al., 2015; Evans et al., 2017).

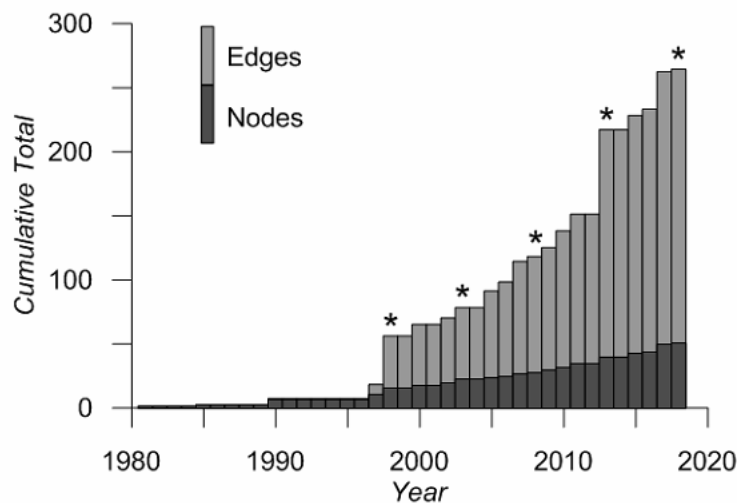


Figure 9. Co-Citation Network Edge and Node Frequency over Time. Asterisks indicate time points with maps shown in Figure 8. Note the gradual increase in nodes juxtaposed by the significant increases in edges in 1997-1998, 2013, and 2017.

Although the number of nodes has experienced steady growth, there have been three instances of significant increases in the numbers of edges, usually with the publication of review-type articles (Hall, 1998, 2013; Rixhon & Demoulin, 2013; Goodfellow & Boelhouwers, 2013). The lack of clustering (particularly around any one stance) or plateauing of either nodes or edges indicates that individual works are not acting as gate-keepers influencing the trajectory of research, but new works are discussing the variety of evidence and attitudes together. This extends to the most recent jump in edges in 2017 with the publication of two analytical studies presenting new data, but clearly acknowledging the diversity of findings and hypotheses (Nelson & Nyland, 2017; Nešić et al., 2017).

Discussion

The contemporary cryoplanation literature corpus is focused on the 90-year-old polarized discussion between CT formation theories based on geologic structure and that of nivation. This discourse is interesting not just for its longevity, but the growing implications for recognition of distinctly periglacial landscapes. For example, French has postulated that some upland periglacial landscapes are “landscapes of inheritance” in which landforms are the result of processes operating in the distant past under presumably warmer, more arid conditions (French & Harry, 1992; André, 2003; Martini et al., 2011; French, 2011, 2016). This idea of inheritance does not negate nivation processes further altering slopes under cold conditions. For example, glacial cirques are accepted as climatically controlled features even though these are also controlled by geologic structure (e.g., Evans, 1994; 2006).

Beginning with Wright (1914, p. 6), nivation was thought to expand and deepen initial hollows (under the necessary climatic conditions) until a small glacier was formed (e.g., Flint, 1971, p. 134; Embleton & King, 1975, p. 142-143). This “nivation hollow to cirque continuum”

was contested by Thorn (1976, p. 1176), who argued that calculated nivation rates were insufficient to excavate a feature on the scale of a cirque within previously hypothesized timeframes. Later, Nelson (1989) compared the size of CTs and cirques using Reger's (1975) Alaskan CT inventory and Derbyshire and Evans' (1976, p. 482) compilation of cirque inventories. Nelson found that the median CT size is an order of magnitude smaller (0.032 km^2) than median cirque sizes (0.3 to 0.46 km^2) (Derbyshire & Evans, 1976, p. 482) and concluded that published nivation rates are consistent with the scale of CTs (Nelson, 1989). Besides these back-of-the-envelope calculations, relatively few works have attempted to quantify nivation erosion and none have attempted it at the scale of CTs in an active periglacial environment (e.g., Thorn, 1976; Thorn & Hall, 1980; Berrisford, 1991; Lauriol et al., 1997).

Advancement on the fundamental questions surrounding the processes that form landscape-scale features such as CTs may represent the next paradigm shift in periglacial geomorphology, with the potential to bring the subdiscipline back into the mainstream. In glaciology this occurred recently with the development of the "glacial buzzsaw" theory (e.g., Mitchell & Montgomery, 2006; Egholm et al., 2009; Nielsen et al., 2009; Sanders et al., 2012). Several authors have suggested a similar regional limiting of topography in the periglacial realm, or "frost buzzsaw" (Hales & Roering, 2009; Hall & Kleman, 2014), which could also explain CT elevation trends tracking those of cirques (Nelson & Nyland, 2017).

Conclusions

Elevated bedrock terraces in periglacial environments have been identified on every continent by names including altiplanation, equiplanation, nivation, goletz, and, most commonly as cryoplanation terraces (CTs). CTs are most prevalent in the Carpathian and Ural Mountains, and, especially, throughout unglaciated sections of Beringia. The variety in terminology and

geography has complicated establishing the processes involved in the formation of these landscape-scale features. This review examines possible reasons for this debate having extended over more than a century. We suggest that terminological complexity and ambiguity can be largely eliminated by treating “nivation” as a process term, and “cryoplanation terrace” as a morphological descriptor.

Encouragingly, the co-citation analysis conducted as part of this literature review did not reveal any work(s) or author(s) as having attempted to “steer” research initiatives through selective citation. However, despite several high-quality review papers published on the subject (e.g., Demek, 1969; Czudek, 1995; Thorn & Hall, 2002), CT literature remains unfocused, and these works do not appear to have spurred explicit testing of either of the remaining hypotheses.

The debate about CT genesis and development is no longer centered on the constructional *vs.* erosion theories posed for CT formation from 1905 to 1965 (e.g., Prindle, 1905; Eakin 1916; Krivolutskiy, 1965). There is consensus that CTs are erosional phenomena, although the roles of geologic structure and nivation and their relative importance are still contested (cf., Ballantyne, 2018, pp. 220-222; French, 2017, p. 295). On one side of the debate are those who consider cryoplanation to be a characteristic periglacial form (e.g., Péwé, 1975; Reger & Péwé, 1976; Nelson, 1989; 1998; Nelson & Nyland, 2017) and those who contend that distinctly periglacial landscapes may not exist or that geological structure is primarily responsible for stepped topography in cold regions (e.g., French & Harry, 1992; Hall & André, 2010; French, 2015; 2017). Given the many examples of CTs cutting across geological structure and composition (Reger 1975; Péwé and Reger 1983), the burden of proof rests with those advocating a purely structural interpretation. Fifty years later, Embleton and King’s (1968, p. 533) summary statement appears prophetic: “There are obviously close links between [cryoplanation] terraces and nivation hollows

and further studies may well suggest that the distinction between these two groups of features should be discontinued.”

Nonetheless, works quantifying the erosive capacity of nivation have been limited, and few have been conducted at the scale of CTs in an active periglacial environment (e.g., Thorn, 1976; Thorn & Hall, 1980; Berrisford, 1991; Lauriol et al., 1997). At the risk of simply echoing the pleas of others (e.g., Demek 1969; Thorn and Hall 2002), we point again to the need for instrumented, process-oriented investigations and critical field experiments on cryoplanation terraces.

CHAPTER 3. SCARP RETREAT ON CRYOPLANATION TERRACES IN EASTERN BERINGIA: STATISTICAL ANALYSIS OF RELATIVE WEATHERING INDICES

Introduction

Cryoplanation terraces (CTs) are elevated, staircase-like sequences of alternating shallow sloping treads and steep risers, or scarps (Figure 10). These landforms are cut into bedrock, and occupy large expanses of hillslopes, summits, and ridge lines in cold environments around the world (e.g., Demek 1969; Reger, 1975; Nelson & Nyland, 2017). Despite their dominating presence in many unglaciated landscapes and more than a century of discussion in the geomorphic literature, their origins and development remain contentious (e.g., Prieznitz, 1988; Thorn & Hall, 2002; Ballantyne, 2018, p. 220-222). Two hypotheses for the origin and development of CTs continue to receive support in the literature on periglacial geomorphology. One is that CT formation is driven by geologic structure and the concept of landscape inheritance (e.g., French & Harry, 1992; Hall, 1998; Hall & André, 2010), the other by climate, through the mass balance of localized snowbanks (e.g., Reger & Péwé, 1976; Nelson, 1989; 1998; Nelson & Nyland, 2017).

We use the term *nivation* as a shorthand term encapsulating the suite of erosional processes related to snowbanks persisting well into summer. There is substantial evidence that the localized thermal/moisture conditions provided by late-lying snowbanks facilitate intensified mechanical and chemical weathering and facilitates the transport of materials released by these processes (e.g., Thorn, 1976; Rapp, 1986; Ballantyne et al., 1989; Berrisford, 1991; Nyberg, 1991; Hall, 1993). Where snowbanks persist in topographic irregularities on ridges and hillslopes, erosion and associated debris transport processes, including scarp failure, soil creep, solifluction, piping, rillwash, and sheetwash, contribute to scarp retreat. Progressive weathering and parallel retreat of scarps behind late-lying snowbanks forming niches and hollows, results in a time-transgressive

(diachronous) erosion surface. Many researchers have invoked a continuation of nivation processes and associated scarp retreat in the formation of CTs (Figure 10) (e.g., Demek, 1969; Reger & Péwé, 1976; Nelson & Nyland, 2017).

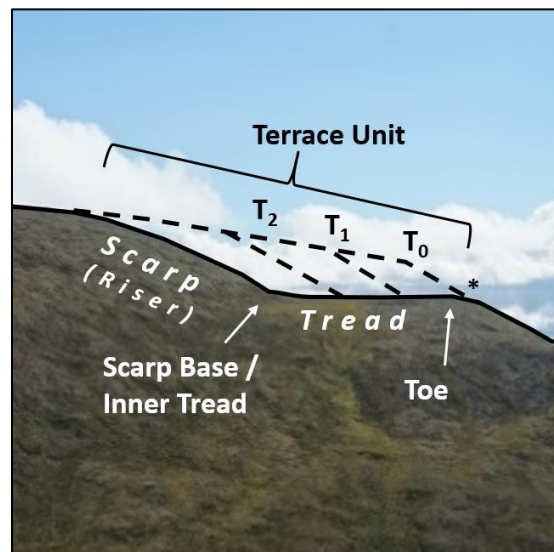


Figure 10. Time-Transgressive Cryoplanation Terrace Development Schematic. Treads belong to the scarp (riser) immediately above in a terrace unit. A terrace unit is formed as a scarp retreats over time, elongating tread length. Asterisk indicates possible initial structural ledge or hollow that would retain snow and promote nivation.

Nivation has been linked to CT formation for more than a century (e.g., Cairnes, 1912a), although the connection remains unsubstantiated by quantitative field study in the high-latitude periglacial environments where these features are most ubiquitous (Demek, 1969; Prieznitz, 1988; Thorn & Hall, 2002). Existing evidence in support of this model for CT formation includes widespread documentation of CTs crosscutting geologic structure (Demek, 1969; Reger, 1975; Reger & Péwé, 1976), and subcontinental-scale spatial analyses demonstrating that CTs exhibit preferred poleward orientations (Nelson, 1998) and elevation trends closely tracking those of glacial cirques (Nelson & Nyland, 2017).

The work reported here evaluates the hypothesis that CTs form by slope retreat, producing low-angle, time-transgressive surfaces (treads). This hypothesis was tested through statistical treatments of six well-established relative weathering indices, indicative of boulder exposure time at the ground surface, as measured in a spatially oriented sampling scheme across eight CT treads from three locations spanning central Alaska.

Study Areas

Beringia, the former ice-free corridor containing the Bering Land Bridge, connected Eurasia and North America during Quaternary cold intervals, and extends from the Lena River in Siberia to the Mackenzie River in Canada. Its vast, largely unglaciated extent contains abundant and especially well-developed CTs (Demek, 1969; Reger, 1975; Nelson, 1989; Lauriol et al., 1997). Using Reger's (1975) inventory of nearly 700 relict CTs in western and central Alaska and aerial reconnaissance in western Alaska's Seward Peninsula, three study sites were selected to form a roughly east-west transect through eastern Beringia. All three sites remained unglaciated throughout the Quaternary (Péwé et al., 1967; Kaufman & Manley, 2004) (Figure 11).

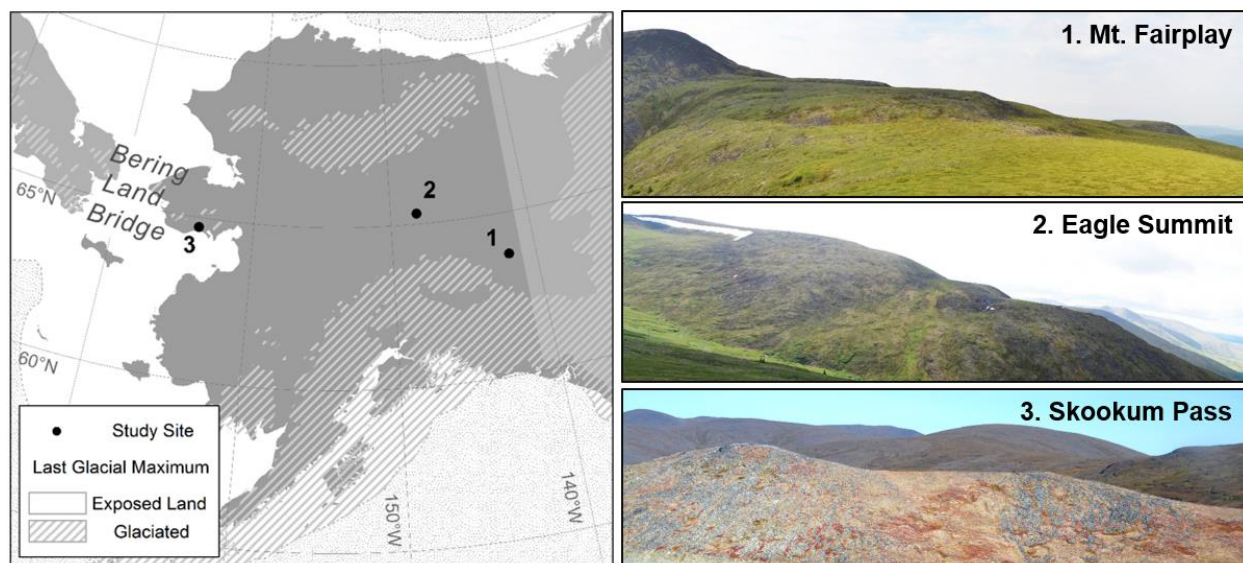


Figure 11. Relative Weathering Study Area Map and Photos. (Left) locations of the three study areas distributed across eastern Beringia from east to west: Mt. Fairplay, Eagle Summit, and Skookum Pass. (Right) show cryoplanation terrace series studied at each site.

Mount Fairplay ($63^{\circ}40'51''$ N, $142^{\circ}12'39''$ W) and Eagle Summit ($65^{\circ}27'53''$ N, $145^{\circ}21'40''$ W) are both located within the Yukon-Tanana Upland (YTU) physiographic province, a dissected, hilly to mountainous area situated between the Tanana River to the south and the Yukon River to the north (Wahrhaftig, 1965; Foster, 1992). Isolated alpine glaciers were present in this province during the Wisconsin glacial episode, or what are locally referred to as the Eagle and Salcha glacial advances (Péwé et al., 1967; Péwé, 1975, p. 16; Weber, 1986; Briner et al., 2005; Kaufman et al., 2011), but most of the YTU is veneered with aeolian, fluvial, and undifferentiated surficial deposits (Péwé, 1975, p. 3). The terrace series on Mt. Fairplay studied here extends from 1360 to 1580 m.a.s.l. on a ridge extending due north from the mountain summit (Figure 12). Tertiary (i.e., Neogene/Paleogene) mafic volcanic bedrock is exposed at several locations along the terrace scarps (Foster, 1967; 1992). The series studied near Eagle Summit faces west-northwest on an early-Paleozoic quartzite ridge, extending from 1140 to 1250 m.a.s.l. (Wiltse et al., 1995a; 1995b).

The Seward Peninsula physiographic province had isolated mountain glaciers in its interior uplands during the Pre-Illinois, Illinois, and Wisconsin glacial episodes, for instance, most recently, the Mt. Osborn advance preceded by the Salmon Lake advance in the Kigluaik Mountains and on the coastal plain (Wahrhaftig, 1965; Péwé, 1975, p. 16; Kaufman & Hopkins, 1986). Close to the transition to the coastal lowlands, in largely undifferentiated deposits similar to those in the Yukon-Tanana Upland (Péwé, 1975, p. 3), is Skookum Pass (64°43'34" N, 164°3'9" W), just above the headwaters of the Skookum River. The pass contains a series of two terraces between 395 and 420 m.a.s.l. on a hillside of Cambrian metasedimentary, mafic-rich material (Werdon et al., 2005).

These three study areas were chosen to represent a variety of local conditions, including location in eastern Beringia, elevation, lithology, and various relations to underlying bedrock structures. Terraces near the summit of Mt. Fairplay have formed parallel to the horizontal sequences of welded igneous tuffs and flows (Foster, 1967; Reger, 1975, p. 77). However, terraces near Eagle Summit and at Skookum Pass crosscut structure. Eagle Summit CTs do not parallel the foliated sequences of micaceous quartzite and quartz-mica / quartz-chlorite schists (Reger, 1975, p. 79; Wiltse et al., 1995b). Similarly, terraces at Skookum Pass cross a variety of bedding planes heavily deformed by two fault junctions on either side of the pass (Werdon et al., 2005).

Methodology

To evaluate the comparative length of exposure in different parts of terrace treads, relative weathering indices for boulders (≥ 256 mm diameter) were measured in three plots at: A) the base of the scarp; B) part way across the terrace tread; and C) at the distal edge (toe) of the tread. Specific plot locations were determined by the availability of boulders exposed at the ground surface. Control plots were established in the same lithologies on nearby south-southwest to south-

southeast facing slopes, where solar insolation is maximized and nivation processes are unlikely to have influenced slope development (Figure 12).

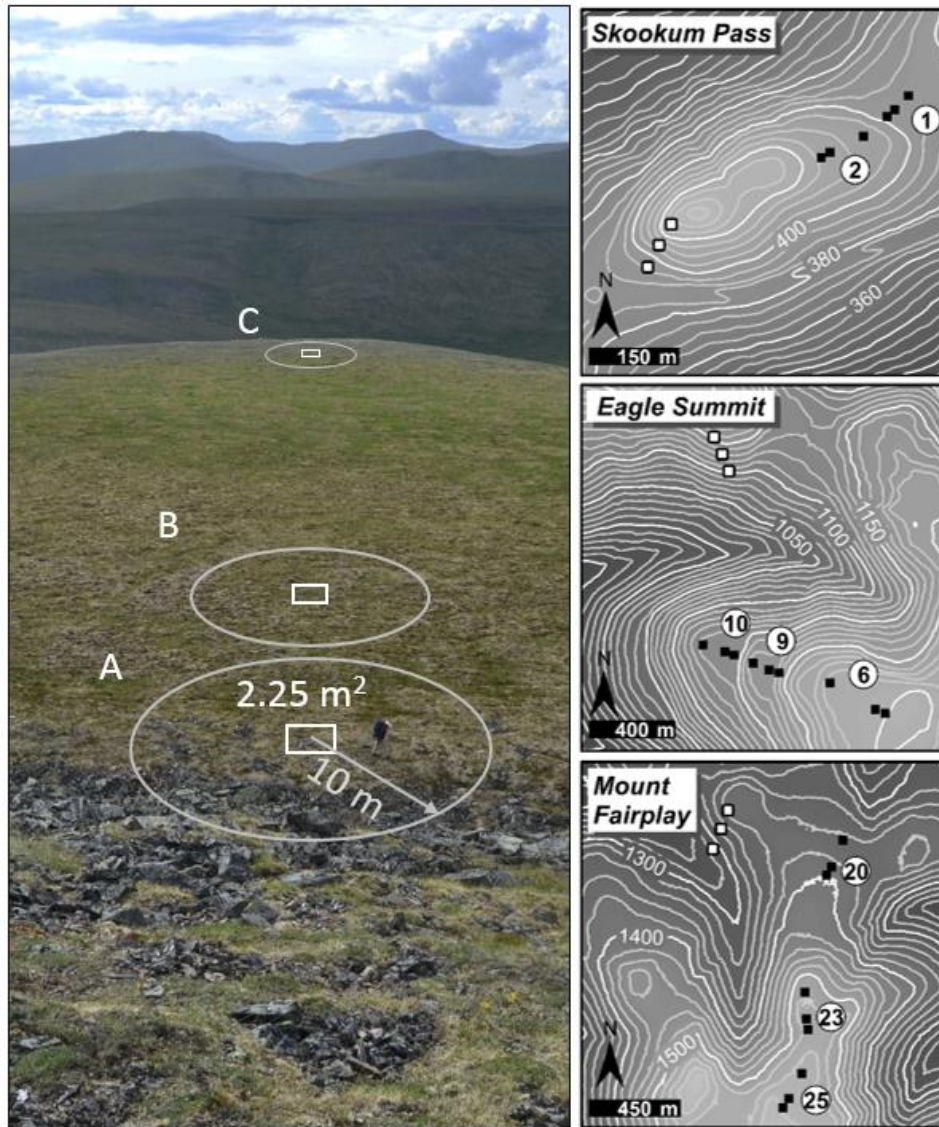


Figure 12. Sampling Strategy for Relative Weathering Study. (Left) 2.25 m² plots for fracture counts and 10 m radius for randomly selected clasts (n=50) for additional indices at (A) the scarp-tread junction; (B) mid-tread; and (C) tread toe positions. (Right) terraces numbered according to Reger's (1975) inventory with plots indicated by black squares and control sites with white squares.

A 2.25 m² quadrat was delineated for fracture counts at each plot location and, based on the center of the quadrat, additional indices (shape, rock hardness, and weathering rind thickness) were measured for 50 random clasts within a 10 m radius. Clasts for additional indices were identified by a randomly generated bearing and distance from the center of the quadrat. Randomness was introduced at this scale to avoid the 1 to 3 m diameter patterned ground present on terrace treads. All subsequent statistical analyses of these data were performed using the Systat (v. 13) statistical software package.

Clast Fracture Counts

Following the methodology of Berrisford (1991), all boulders exposed at the ground surface within a 2.25 m² quadrat were evaluated as having either (1) surface fractures; (2) > 30% loss of mass; or (3) no surface fractures. Count values for each of these three classes were recorded and Pearson's chi-square (χ^2) analysis performed. Due to low expected frequencies (< 5), particularly of clasts with > 30% loss of mass, a likelihood-ratio chi-square (LR) was also performed (Delucchi, 1983). Because three classes were used, χ^2 and LR values were compared to the chi-square critical value of 9.210 for two degrees of freedom and 0.01 significance level (Rea and Parker, 2014, p. 215). Where LR values exceed the critical value, the null hypothesis that fracturing (mechanical weathering) is independent of distance along a terrace tread is rejected. Sites where the null hypothesis is rejected are interpreted as likely time-transgressive surfaces and the Cramer's V (ϕ_c) statistic was used to evaluate the strength of association, or effect size, between fracturing distributions and distance along a tread (Rea & Parker, 2014, p. 219).

Clast Shape

Well-rounded, spherical clasts are interpreted as having undergone more physical weathering than angular clasts (Boggs, 2006, p. 65). Controlling for lithological differences, Cailleux roundness, flatness (Cailleux, 1946), and Krumbein sphericity (Krumbein, 1941) were calculated as follows:

$$\text{Cailleux Roundness} = 1000 \left(\frac{2r}{a} \right) \quad (1)$$

$$\text{Cailleux Flatness} = 1000 \left(\frac{a+b}{2c} \right) \quad (2)$$

$$\text{Krumbein Sphericity} = \sqrt[3]{\left(\frac{bc}{a^2} \right)} \quad (3)$$

where a, b, and c are the long, intermediate, and short clast axes, respectively, and r is the radius of curvature of the sharpest angle.

A roundness value of 1000 represents a smooth clast without sharp angles while lower values represent increasingly angular clasts (Boggs, 2006, p. 66). A flatness value of 100 represents an equant form and values > 100 represent increasingly flatter forms. The sphericity index ranges from 0 to 1, where 1 represents a perfectly spherical pebble and lower values represent reduced sphericity (Barrett, 1980; Benn & Ballantyne, 1993; Boggs, 2006, p. 65-66). Although indices such as Cailleux's have been de-emphasized in recent literature (Benn & Evans, 2004, p. 80), considering several shape indices together improves confidence in trend detection and makes these data comparable with data from historical periglacial studies (King, 1966, pp. 291-292; Benn & Ballantyne, 1993, 1994).

Rebound

Rebound is a standard measure of the degree of rock hardness and is directly related to compressive strength (Day & Goudie, 1977). Significant differences in hardness within the same lithology is then an indicator of differences in weathering (Matthews et al., 1986; McCarroll, 1989; Sumner & Nel, 2002; Goudie, 2006). Two Humboldt N-Type Schmidt hammers were used in this study to measure rebound. These instruments are appropriate over a wide range of rock strength, from approximately 20 to 250 MPa (Goudie, 2006). Following guidelines in the product user's manual (www.humboldtmg.com/humboldt-concrete-rebound-hammer.html) and the methods used by Ballantyne et al. (1989), the average of five readings was taken from a dry rock surface, free of lichens and other debris. Two Schmidt hammers were alternated in the field and after a given hammer was used for 2,000 measurements it was returned to the manufacturer for recalibration.

Weathering Rind Thickness (WRT)

The degree of chemical weathering is indicated by the relative thickness of a weathering rind, if present. In the context of nivation, increased chemical weathering is facilitated by the greater availability of meltwater (Thorn, 1976; Lauriol et al., 1997). To determine weathering rind thickness, boulders were broken with a sledge hammer and the maximum weathering rind thickness (WRT) was recorded to the nearest mm using a caliper.

Clast shape indices, rebound, and weathering rind thickness were measured on 50 randomly selected clasts within a 10 m radius of each quadrat used for fracture counts. Descriptive statistics were calculated for the shape indices, rebound, and WRT data. These data distributions were tested for normality using the Shapiro-Wilk test (Shapiro and Wilk, 1965) and for heterogeneity of variance using Levene's (1960) test. Roundness, flatness, and WRT variables

showed slight deviations from normality and a tendency toward heteroscedasticity at the 0.1 significance level. Based on these initial results, one-way analysis of variance (ANOVA) was chosen to compare differences in means as it is robust with respect to minor departures from normality and variance when there are equal sample sizes (Kirk, 1982, p. 78). Tukey's Honestly Significant Difference (HSD), also known as Tukey's range test (Tukey, 1949), was used as a multiple comparison procedure (post hoc) test.

Results

Chi-Square Analysis of Fracture Counts

Table 4 shows the results of the chi-square analysis from highest to lowest elevation terraces at the three study sites. All terraces at Mt. Fairplay displayed statistically significant χ^2 and LR values at the 0.01 significance level. The null hypothesis was therefore rejected in favor of the alternative, that there is a relationship between the degree of boulder fracturing and location on a terrace tread. Clasts with surface fracturing and those displaying >30% loss of mass both decrease in occurrence with distance along a tread. This is interpreted as indicative of all three terrace treads being time-transgressive surfaces, where weathering was last active, or is presently most active, at or near the scarp (plot A). Strength of association (ϕ_c) values indicate moderate relationships between the degree of fracturing and distance across all three treads at Mt. Fairplay. The relationship across terrace treads is supported by the inability to reject the null hypothesis at the nearby control plot series on the south-facing slopes, where nivation processes are unlikely to have operated intensively.

A similar interpretation can be made for results from Eagle Summit. The null hypothesis was rejected for Terraces 9 and 10 but cannot be rejected for the controls or Terrace 6. At Skookum Pass, the null hypothesis can only be rejected for Terrace 2. Terraces 6 (at Eagle Summit) and 1

(Skookum Pass), display weak or non-significant relationships respectively. These terraces are also outliers morphologically. Terrace 6 is by far the longest tread, at more than 300 m in length and is situated atop a sequence of terrace units at lower elevations. Terrace 1 forms half of a saddle constituting the northern end of Skookum Pass. These different morphologies may involve significantly longer periods or intensified processes affecting the numbers and location of fractured clasts.

Table 4. Fracture Pearson's Chi-Square (χ^2), Likelihood Ratio (LR), and Cramer's V (ϕ_c). Fracture count distributions shown from Mt. Fairplay, Eagle Summit, and Skookum Pass. Both χ^2 and LR values are compared to the critical value, 9.210, for two degrees of freedom. Asterisks indicate p-values <0.05 (*), <0.01 (), and <0.001 (***). $\dagger H_0$: data are not significantly different and are likely members of the same population. H_a : means are significantly different and representative of independent populations.**

Plot Series	χ^2	LR	ϕ_c	Reject/Fail to H_0[†]
<i>Mt. Fairplay</i>				
Terrace 25	19.258**	20.059***	0.253 (Moderate Association)	Reject
Terrace 23	17.297**	17.587**	0.278 (Moderate)	Reject
Terrace 20	15.730**	17.063**	0.235 (Moderate)	Reject
Control	3.842	4.931	0.101 (Weak)	Fail to Reject
<i>Eagle Summit</i>				
Terrace 6	5.799	7.976	0.122 (Weak)	Fail to Reject
Terrace 9	44.625***	45.975***	0.285 (Moderate)	Reject
Terrace 10	16.875**	16.945**	0.168 (Weak)	Reject
Control	4.271	5.997	0.131 (Weak)	Fail to Reject
<i>Skookum Pass</i>				
Terrace 2	13.552**	12.839*	0.176 (Weak)	Reject
Terrace 1	2.170	2.154	0.078 (Negligible)	Fail to Reject
Control	6.976	7.677	0.129 (Weak)	Fail to Reject

ANOVA Results: Shape, Rebound, and Weathering Rind Thickness

Figures 13-15 show Tukey's HSD multiple-comparison plots at Mt. Fairplay, Eagle Summit, and Skookum Pass, respectively, for morphology indices, rebound, and maximum WRT. Box-plot extent represents the 95% confidence interval about the mean value for a given index and plot (Andrews et al., 1980; Nelson and Schimek, 2015). Weathering is indicated by increasing roundness, sphericity, and WRT values, and decreasing flatness and rebound values. Clasts are, in general, increasingly rounded, spherical, and equant, show thickening weathering rinds, and reduced rock hardness with increasing distance from scarp base to tread toe at the sites examined.

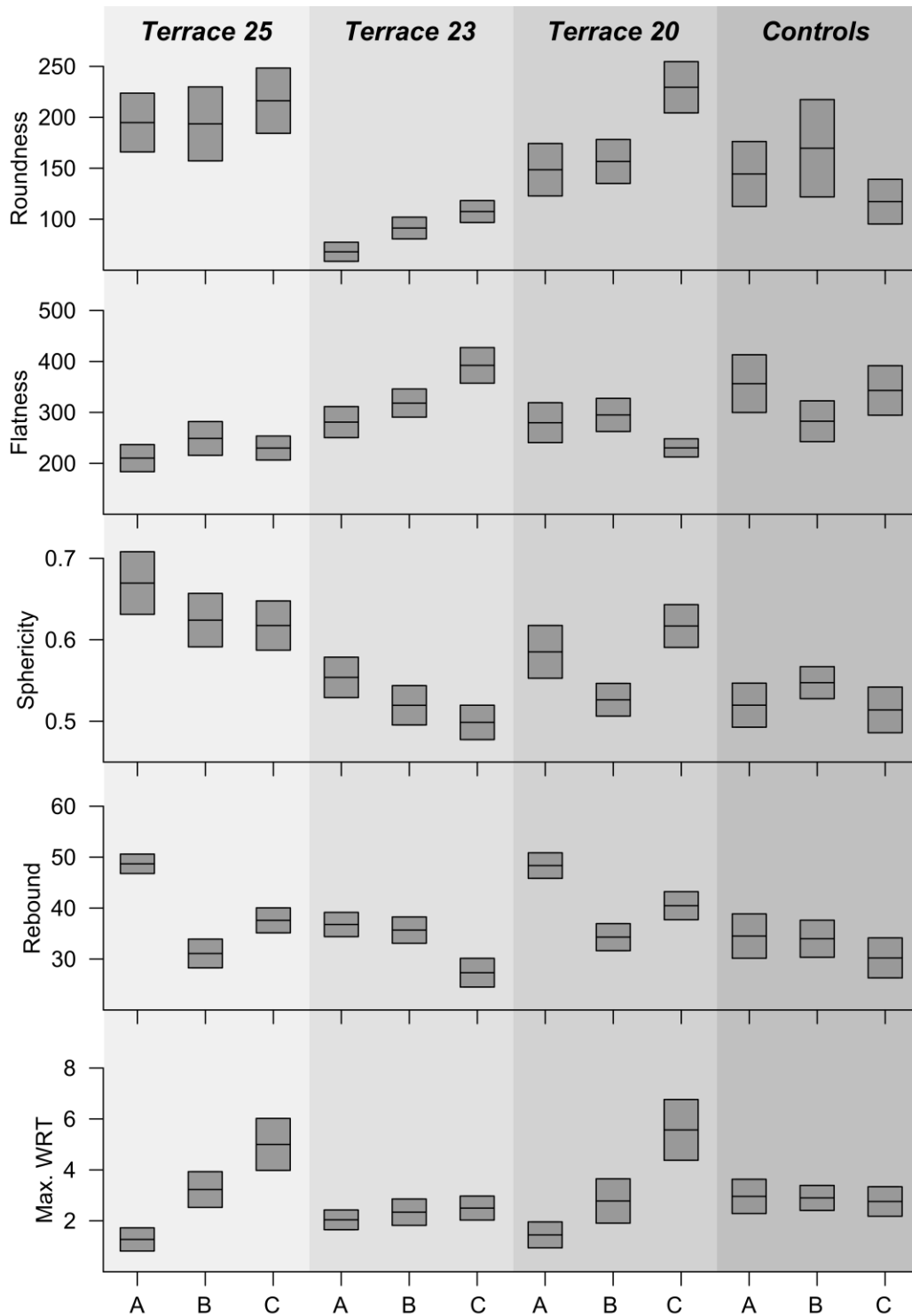


Figure 13. Mt Fairplay: Tukey's HSD Results for Relative Weathering Indices. Morphology indices (top three graphs), rebound, and maximum weathering rind thickness (Max. WRT) (bottom graph) at (A) scarp base; (B) mid-tread; and (C) tread toe. Box plots represent confidence intervals (box top and bottom) about the mean (center line) for a 0.05 confidence level. Significant differences between plots occur where box extents do not overlap on the y-axis scales.

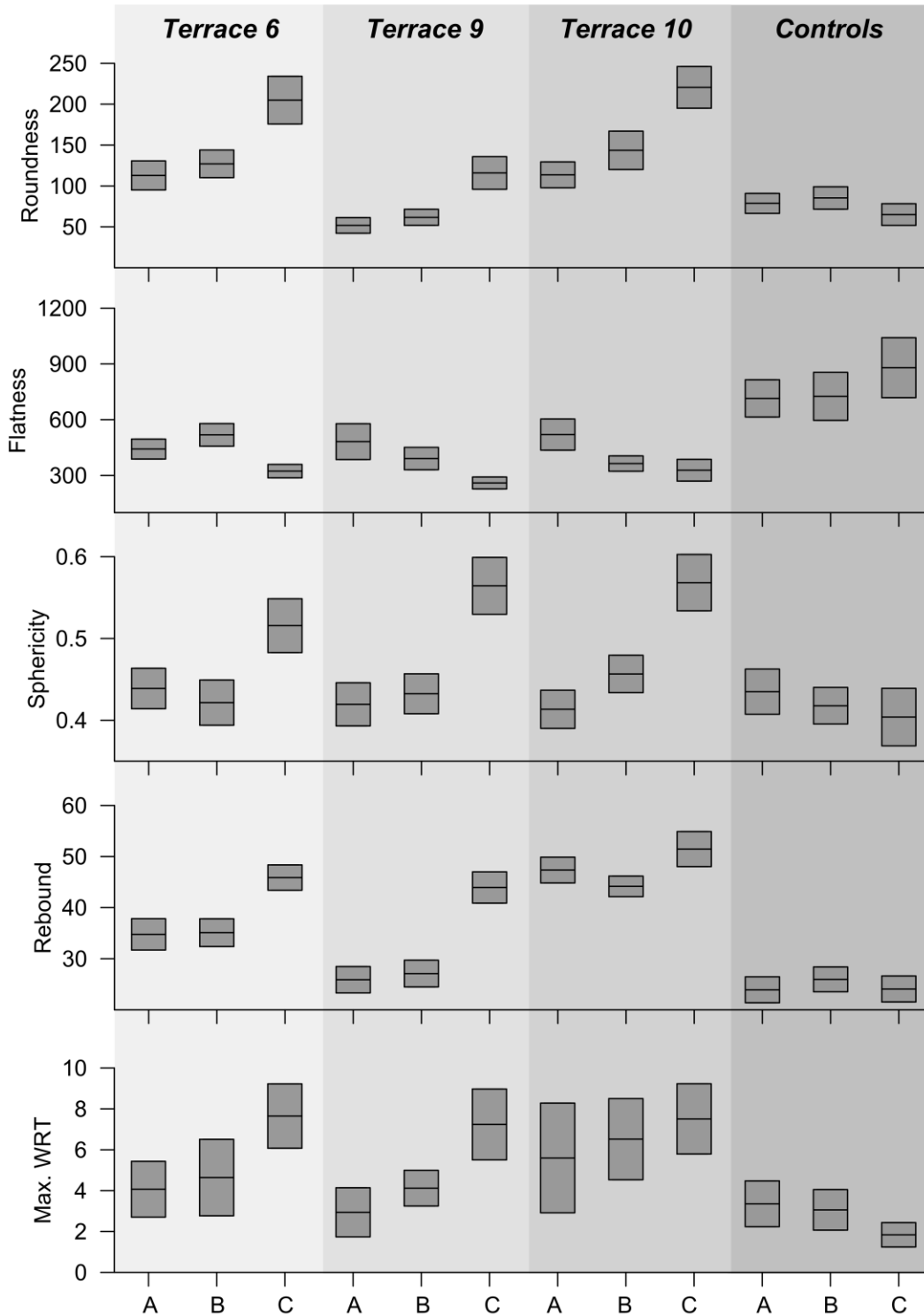


Figure 14. Eagle Summit: Tukey's HSD Results for Relative Weathering Indices. Eagle Summit: Morphology indices (top three graphs), rebound, and maximum weathering rind thickness (Max. WRT) (bottom graph) at (A) scarp base; (B) mid-tread; and (C) tread toe. Box plots represent confidence intervals (box top and bottom) about the mean (center line) for a 0.05 confidence level. Significant differences between plots occur where box extents do not overlap on the y-axis scales.

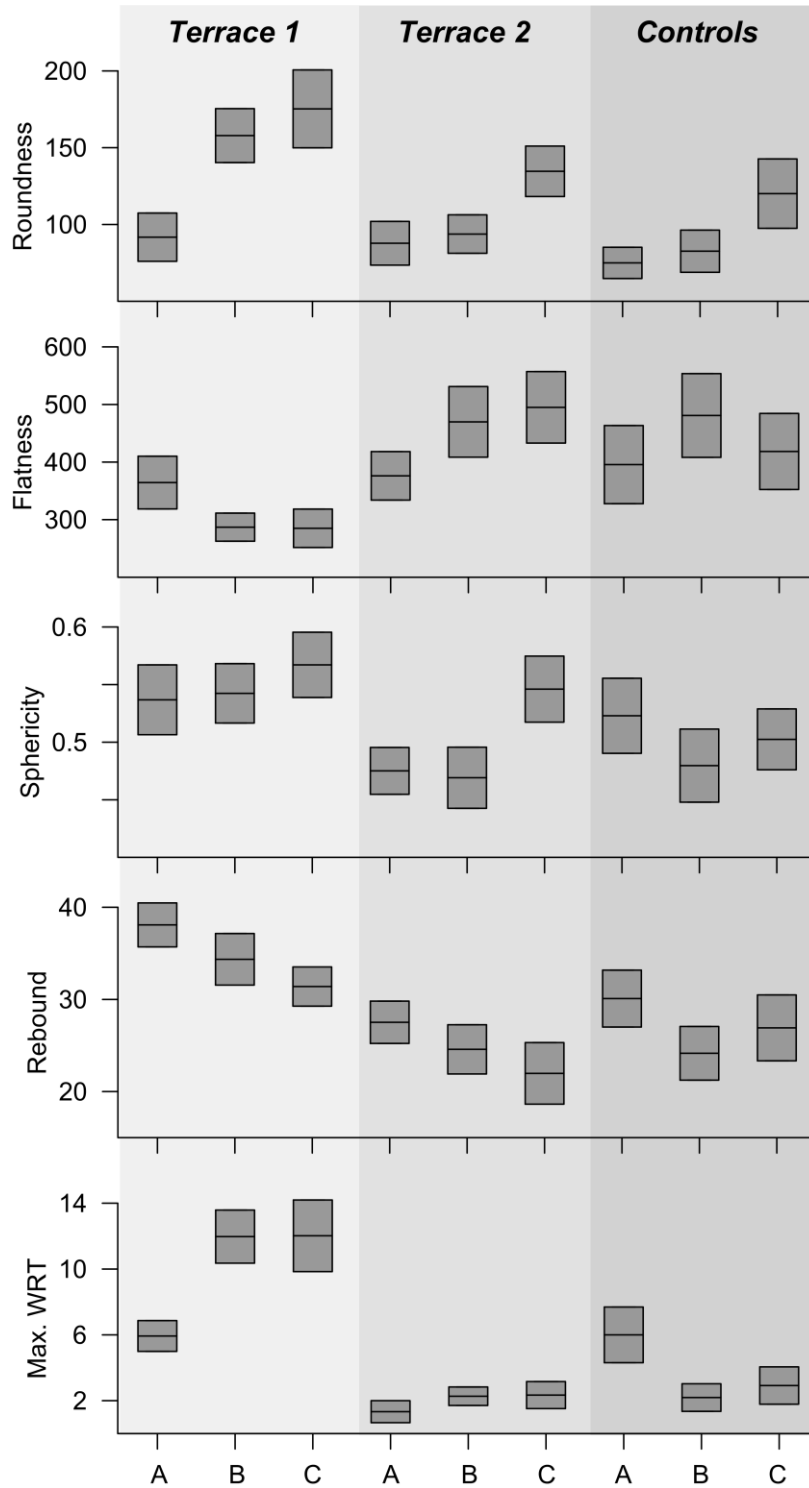


Figure 15. Skookum Pass: Tukey's HSD Results for Relative Weathering Indices. Morphology indices (top three graphs), rebound, and maximum weathering rind thickness (Max. WRT) (bottom graph) at (A) scarp base; (B) mid-tread; and (C) tread toe. Box plots represent confidence intervals (box top and bottom) about the mean (center line) for a 0.05 confidence level. Significant differences between plots occur where box extents do not overlap on the y-axis scales.

Table 5 is a summary of the multiple comparisons previously shown graphically, where significant differences in mean values for a given variable and the direction (positive or negative) of a linear trend in mean values are indicated with arrows. Significant differences between plots, particularly between A (at the base of the scarp) or B (mid tread) and the distal plot, C (tread toe), were detected for at least two variables on every CT tread. Increasing trends in roundness, sphericity, and WRT, and decreasing trends in flatness and rebound are consistent across at least four treads at different sites. These results indicate that all eight treads examined are likely to have undergone time-transgressive development, with clasts closer to the toe of a tread having been exposed longer than those near scarps. This interpretation is supported by the lack of trends in control plot series at all three study sites. There are no significant differences between plots for any variable at the Mt. Fairplay or Eagle Summit control sites, nor for flatness, sphericity, or rebound at the Skookum Pass control sites.

Table 5. Summary Table of Trends in Significantly Different Means. Based on Tukey’s HSD results for shape, rebound, and Max. WRT variables. An arrow indicates at least one pair of plots has significantly different means at the 0.05 significance level and the direction of the arrow indicates a positive or negative linear trend in plot means.

Plot Series	Roundness	Flatness	Sphericity	Rebound	Max. WRT
<i>Mt. Fairplay</i>					
Terrace 25				↓	↑
Terrace 23	↑	↑	↓	↓	
Terrace 20	↑		↑	↓	↑
Control					
<i>Eagle Summit</i>					
Terrace 6	↑	↓	↑	↑	↑
Terrace 9	↑	↓	↑	↑	↑
Terrace 10	↑	↓	↑	↑	
Control					
<i>Skookum Pass</i>					
Terrace 2	↑		↑		
Terrace 1	↑	↓		↓	↑
Control	↑				↓

Notable deviations from expected trends include significant increases in mean rebound values across all three CT treads at Eagle Summit and significant differences in roundness and WRT at the Skookum Pass control series. The quartz-mica schist boulders exposed at the ground surface along treads near Eagle Summit have large quartz inclusions (Reger, 1975). Boulders in the distal position contained significantly more quartz or were pure quartz. A study comparing physical properties of quartzites in Antarctica found that average Schmidt hammer rebound values of quartz-mica schist are less than those of quartz and that readings of quartz or quartz inclusions

will give higher rebound values (Hall, 1987). The increasing rebound trend may, however, still be indicative of weathering. Quartz is the last mineral to weather according to the Goldich weathering series, therefore larger and more pure quartz clasts toward the tread toe may be the remainder after the micaceous minerals found closer to scarps have weathered (Goldich, 1938).

The significant differences in roundness and weathering rind thickness between the control plots at Skookum Pass may be explained by the steep nature of the control site. The southerly aspect of the pass is an approximately 22° slope. Clasts here are likely to have been rolling and tumbling downhill. Abrasion may then have resulted in rounder clasts at downslope positions with thinner weathering rinds.

Discussion

The six relative-weathering indices employed in this study, treated with two different comparative statistical analyses, show good agreement. These results offer strong support for interpreting CT treads at all three sites as time-transgressive surfaces, i.e., diachronous surfaces formed over extended periods of time through scarp retreat. This interpretation is consistent with the nivation-based hypothesis for CT formation, driven by climate through the mass balance of highly localized snowpacks (e.g., Demek 1969; Reger & Péwé 1976; Nelson, 1989; 1998; Nelson & Nyland, 2017).

A common critique of this hypothesis is the lack of a widely applicable qualitative model accounting for the removal of weathered sediment from terrace treads (e.g., Hall, 1998; Thorn & Hall, 2002; Ballantyne, 2018, p. 221). Although solifluction and associated processes are understood to be effective for transporting materials across shallow gradients, many cannot resolve the transportation of material down a series of terraces without the presence of ramparts or other accumulation features (Thorn & Hall, 2002, p. 245-246).

Lateral side slopes at the sites studied in this work are, however, clearly slopes of transportation, with significant amounts of eroded materials originating from terrace treads (Figure 16). Clastic material is consistently exposed in the same positions on terrace treads and scarps. Steep scarps expose bedrock or are covered in coarse clastic rubble, and treads commonly feature sorted circles or nets elongating into sorted stripes on side slopes.



Figure 16. Transportation Slopes on Eagle Summit and Seward Peninsula. (A) Side slope of terrace series near Eagle Summit and (B) oblique aerial view of a terrace tread and side slope on the Seward Peninsula (after Nelson and Nyland, 2017).

Despite their nearly planar appearance, CT treads are slightly convex (Péwé & Reger, 1983, p. 120). Sub-meter stadia rod and handlevel measurements made at 2 m increments were used to generate cross-tread topographic profiles for each terrace in the series studied near Eagle Summit (Figure 17). Lateral slopes across these treads range from 1° to 5° . The convex-upward curvature of these surfaces serve as additional evidence for lateral flows of eroded material under gravity-driven mass wasting processes. Lateral flows of material from CTs have been previously suggested by several authors, including Gravis (1964), Demek (1969, p. 64), and Reger and Péwé (1976, p. 101). Demek (1969, p. 64) described the observed transition from patterned ground on

terrace treads to sorted stone stripes and then to solifluction lobes on side slopes. As terrace treads mature and elongate, lateral pathways become the shortest and most efficient routes for materials eroded at scarp bases to be removed from the treads.

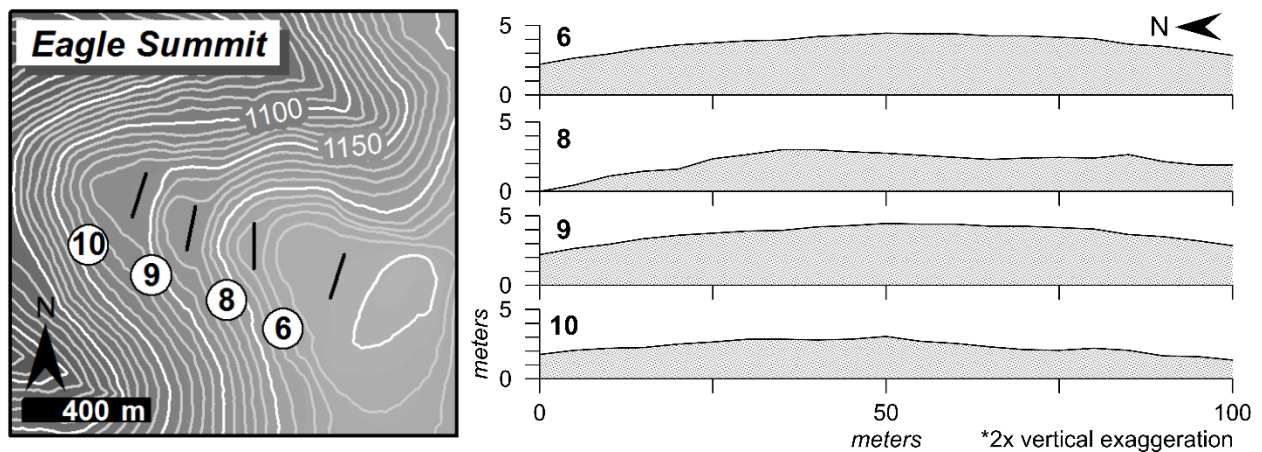


Figure 17. Cross Section Topographic Profiles of Terraces Eagle Summit. Profiles correspond to black lines shown on map. Note the convex shape of all terraces in the series near Eagle Summit.

Figure 18 represents a qualitative model of CT formation, based on observed morphologies and results from statistical analysis of relative weathering indices applied across eastern Beringia. Late-lying snowbanks, particularly during cold climatic intervals, provide the thermal insulation necessary for the sustained sub-freezing conditions that facilitate accretion of segregation ice and fracture of underlying bedrock (Walder & Hallet, 1985; 1986; Hallet et al., 1991; Murton et al., 2006; Sanders et al., 2012). Coarse clastic material is detached from the bedrock through “cryoexpulsion” (Font et al., 2006), or the ejection of coarse material from joint sets and other fractures by frost heave. The coarse material forms sorted patterned ground in the moist microenvironment near the base of the scarp. Fines derived from weathering in the snowbank vicinity are transported by fluvial (rill flow and slopewash) processes and solifluction laterally

across treads and down the side slopes (e.g., Péwé & Reger, 1983, p. 125). Piping of fine material through stone stripes (Smith, 1968; Nelson, 1975, pp. 16-17; Wilkinson and Bunting, 1975; Paquette et al., 2017) to side slopes plays a particularly important role in this model (Figure 16B). Flowing water supplied by these conduits promotes removal of weathered material down the side slopes by solifluction. Continued recession of the scarp parallel to itself extends the tread, creating a diachronous surface.

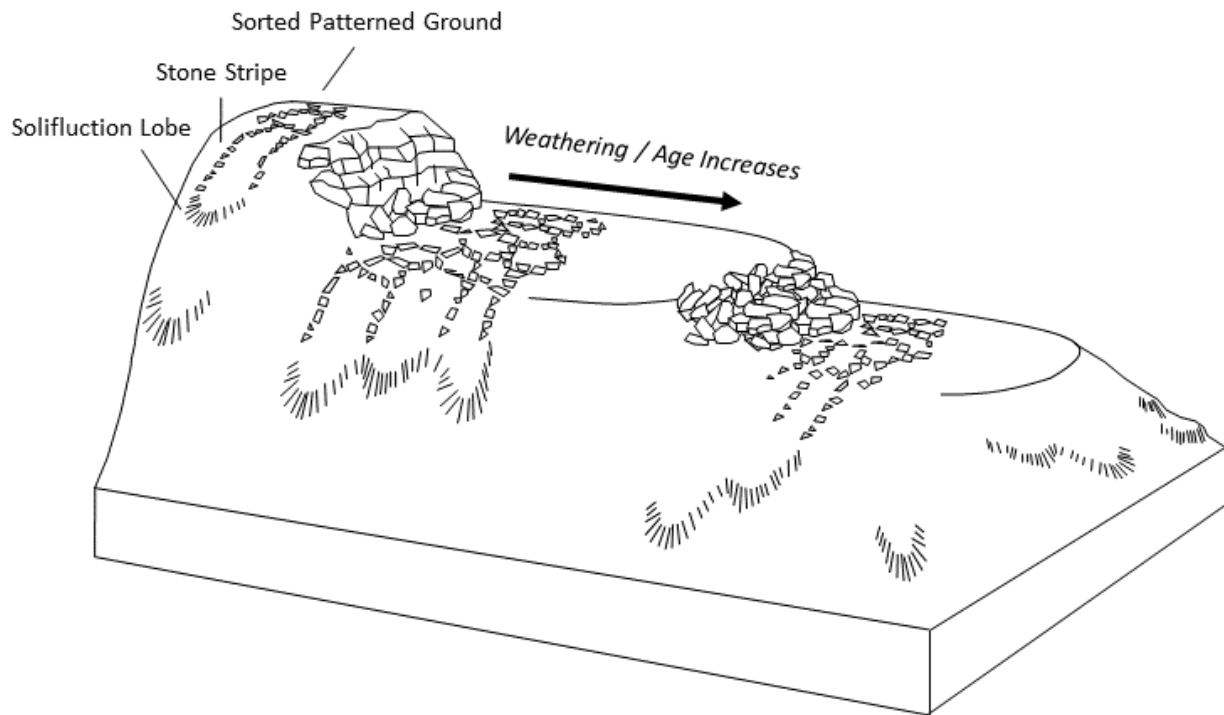


Figure 18. Revised Nivation Model for Cryoplanation Terrace Formation. Block diagram showing idealized features from typical cryoplanation terraces in Eastern Beringia.

Conclusions

Calls to substantiate or refute the nivation process suite in the context of CTs using age determinations have appeared in the literature of periglacial geomorphology for at least a half century (e.g., Demek, 1969; Thorn & Hall, 2002; Nelson & Nyland, 2017). The data on relative ages across CT tread surfaces presented here support inferences drawn from subcontinental-scale spatial analyses of CTs in Alaska. Statistically significant preferred poleward orientations of terrace scarps, and elevational trends closely tracking those of glacial cirques, are suggestive of strong climatic controls, analogous to those understood to act on glacial landforms (Nelson, 1989; 1998; Nelson & Nyland, 2017). This study detected statistically significant differences in relative weathering indices (fracture counts, Cailleux roundness, Cailleux flatness, Krumbein sphericity, rock hardness, and weathering rind thickness) across CT treads at three widely separated sites with different lithologies and bedding structures. These findings are also consistent with time-transgressive (diachronous) surface development under scarp retreat specified by the nivation hypothesis of CT formation.

Future work will include absolute dating of clasts using terrestrial cosmogenic nuclide (TCN) dating and refinement and quantification of the model for CT formation in eastern Beringia. The consistency of these results coupled with the lithologies at Eagle Summit and Mt. Fairplay make these locations especially good candidates for ^{10}Be and ^{36}Cl TCN dating, respectively.

Although the results presented here are interpreted as evidence supporting the nivation hypothesis of CT formation, the two primary interpretations of CT development, (nivation and geologic structure) are not mutually exclusive. Like glacial cirques, the ultimate origins of cryoplanation terraces may be topographic irregularities related to geologic structure, in which large volumes of snow accumulate. Undoubtedly, both play a role in the evolution of cryoplanation

landforms. Structural features can provide the initial hollow promoting the accumulation and persistence of snow. Inherited landforms may also provide topographic irregularities that are modified subsequently by nivation processes.

CHAPTER 4. COSMOGENIC ^{10}Be AND ^{36}Cl GEOCHRONOLOGY OF CRYOPLANATION TERRACES IN THE YUKON-TANANA UPLAND, ALASKA

Introduction

Cryoplanation terraces (CTs) are large bedrock features often likened to giant staircases carved into ridges and hillslopes in present and previously periglacial (cold but unglaciated) environments. CTs consist of alternating gently sloping treads (generally $< 12^\circ$) and steep ($> 20^\circ$) rubble-covered, or exposed bedrock scarps, also referred to as risers. The term “scarp” is used here in a purely descriptive or morphological, and not necessarily tectonic sense (Bloom, 2004, p. 67). A terrace unit consists of a tread and the scarp immediately upslope (Brunnschweiler, 1965). Sequences of terrace units can culminate in extensive summit flats. Terrace treads range from tens to hundreds of meters in length, and sequences of terraces can span several kilometers of ridgeline (Figures 19A, B) (e.g., Demek, 1969; Priestnitz, 1988; Reger and Péwé, 1976; Nelson and Nyland, 2017; Ballantyne, 2018, p. 220-222). Although these impressive features have been readily identified and discussed for more than a century in the periglacial geomorphic literature, their origins and development, and therefore Quaternary significance, remain speculative.

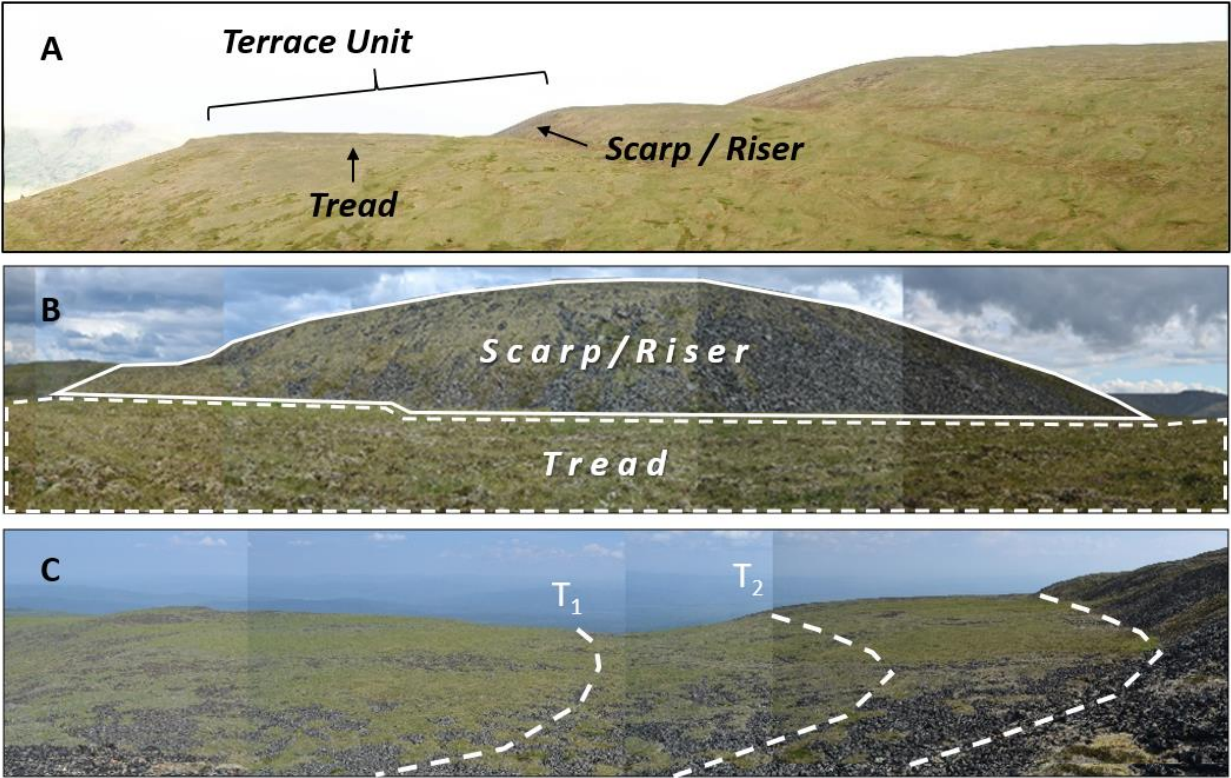


Figure 19. Eagle Summit and Mt. Fairplay Photos and Terrace Components. (A) Example of a cryoplanation terrace sequence near Eagle Summit, Alaska (facing north) culminating in a summit flat, with tread components, and terrace unit (approx. 200 m in length) labeled, (B) photo facing east from outer edge of a terrace tread in the sequence pictured above looking toward higher scarp (approximately 50 m in height), and (C) oblique view toward northeast of terrace tread (approximately 150 m) on Mt. Fairplay with current and hypothesized previous scarp-tread junctions represented by dashed lines.

Two distinct hypotheses for CT formation are supported in contemporary literature: (1) CTs are the result of geologic structure (e.g., Waters, 1962; Hall and André, 2010; French, 2016), and (2) that CTs are the result of a distinctively periglacial set of weathering and transportation processes circumscribed by the term *nivation* (e.g., Demek, 1969; Reger and Péwé, 1976; Nelson, 1989; 1998; Nelson and Nyland, 2017). Some of the best developed and most impressive CTs are found in Beringia – the former land bridge exposed during Quaternary cold intervals that connected Eurasia with North America between the Lena River in Siberia and the Mackenzie River in Canada (Demek, 1969; Reger, 1975; Nelson, 1989; Nelson & Nyland, 2017). The first

documented CTs in eastern Beringia are in reports from exploratory mapping of central Alaska by the U.S. Geological Survey during the early 20th century (Moffit, 1905; Prindle, 1905; Cairnes, 1912a; Eakin, 1916; Mertie, 1937). It was apparent to these investigators, even during the height of Davisian geomorphic theory, that these features appeared to contradict Davis' "normal cycle of erosion" (Davis, 1909). For example, Moffit (1905, p. 44) remarked on the angularity of clasts on the high terraces and how these were more likely the result of frost rather than fluvial action. Similarly, Prindle (1905, p. 20) noted that neither lithology nor structure appeared to control CT elevation or orientation. Cairnes (1912a) was the first to hypothesize that CTs are climatically controlled and formed through scarp retreat driven by nivation processes. Although he did not use the term nivation, Prindle (1913) posited a hypothesis for CT formation that deviates little from the contemporary explanations cited above.

Nivation encompasses the suite of erosion processes associated with snowbanks that last well into warm months (Matthes, 1900). Although the processes involved differ significantly from those initially proposed by Matthes, abundant evidence exists that late-lying snowbanks provide moisture and thermal insulation that intensifies the mechanical and chemical weathering of underlying materials (e.g., Thorn, 1976; Ballantyne et al., 1989; Berrisford, 1991; Hall, 1993; Thorn & Hall, 2002). Weathered materials are transported away from the scarp via soil creep, solifluction, piping, rill wash, and sheetwash, fueled by meltwater from the late-lying snowbank (Thorn & Hall, 1980; 2002). Continued scarp recession by nivation forms a hollow and eventually a terrace (Figure 19C).

Nivation has continued to receive support in the literature as a dominant process in CT formation through scarp retreat (Demek, 1969; Reger & Péwé, 1976; Nelson & Nyland, 2017). Additional evidence includes terraces that cross-cut structure (Demek, 1969; Reger, 1975),

sedimentological and morphological patterns (Reger, 1975; Queen, 2018), statistically significant poleward orientation (Nelson, 1998), and subcontinental-scale elevation trends tracking those of glacial cirques – landforms understood to be controlled by cold climate conditions (Nelson & Nyland, 2017). Repeated calls have been made for absolute ages and erosion rates to complement existing evidence (e.g., Demek, 1969; Prieznitz, 1988; Thorn & Hall, 2002) and most recently to assess whether CT treads are time-transgressive surfaces developing, like glacial cirques, in phase with cold climatic periods (Nelson & Nyland, 2017). This paper addresses such questions about CTs in eastern Beringia using ^{10}Be and ^{36}Cl terrestrial cosmogenic nuclide (TCN) exposure dating techniques.

Study Areas

Two well-developed sequences of CTs, near Eagle Summit ($65^{\circ}27'53''$ N, $145^{\circ}21'40''$ W) and on Mt. Fairplay ($63^{\circ}40'51''$ N, $142^{\circ}12'39''$ W), were selected from an inventory of nearly 700 cryoplanation landforms in central and western Alaska (Reger, 1975) based on road access and previous studies conducted in these areas. Both study areas are located within the dissected, hilly to mountainous Yukon-Tanana Upland (YTU) physiographic province bounded by the Yukon River to the north and the Tanana River to the south (Wahrhaftig, 1965; Foster, 1992). The YTU remained largely unglaciated throughout the Pleistocene with only isolated valley glaciers developing during the Wisconsin, locally referred to as the Eagle (early / middle Wisconsin) and Salcha (late Wisconsin) glacial episodes (Weber, 1986; Briner et al., 2005; Kaufman & Manley, 2004; Kaufman et al., 2011) (Figure 20). None of these isolated glaciers covered either study area (Péwé et al. 1967). With minimal glacial reworking, YTU surface deposits are primarily undifferentiated, aeolian, or fluvial (Péwé, 1975, p. 3). The majority of the YTU is underlain by the Yukon-Tanana Terrane, bounded by the Denali fault system to the south and the Yukon Flats

to the northwest and the Tintina fault zone to the northeast (e.g., Foster et al., 1973; Mortensen, 1992; Hansen & Dusel-Bacon, 1998).

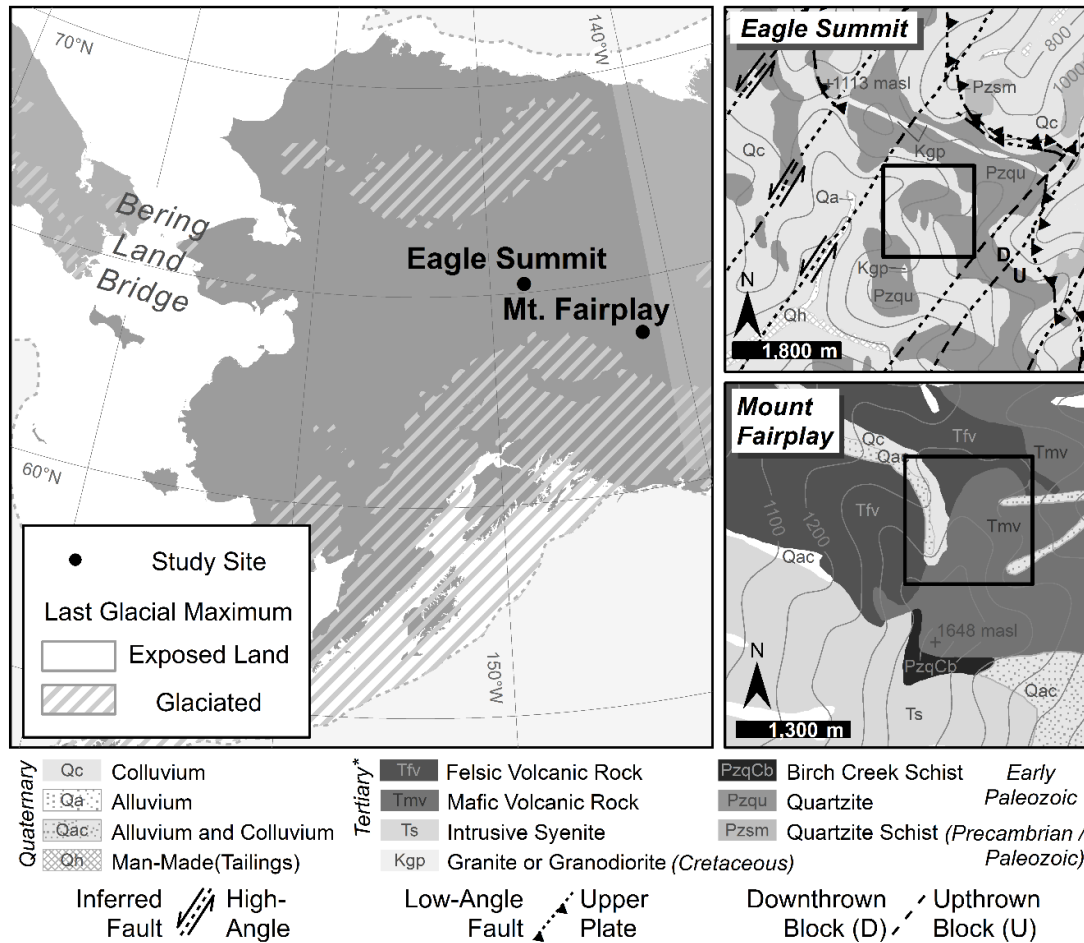


Figure 20. Geochronology Study Areas and Geologic Context. Study area locations in eastern Beringia (left) and the geologic context of Eagle Summit (Wiltse et al., 1995a) and Mt. Fairplay (Foster, 1967) areas (right). Terraces studied are indicated by solid black rectangles in panels at right and correspond to map extents in Figure 21.

Near Eagle Summit is a sequence of four CTs between 1140 and 1250 m.a.s.l. carved into an early-Paleozoic quartzite ridge facing WNW (Reger, 1975; Wiltse et al., 1995a; 1995b) (Figure 20). The treads of these terraces cross-cut the foliated micaceous quartzite and quartz-mica to

chlorite schist bedrock (Reger, 1975, p. 79; Wiltse et al., 1995b). Additionally, the northerly orientation of this terrace sequence is at approximately a right angle to two parallel thrusts, or low-angle faults trending NNW-SSE (Wiltse et al., 1995a).

Mt. Fairplay consists primarily of flows of Tertiary (i.e., Neogene/Paleogene) mafic and felsic igneous materials. A sequence of five well-developed CTs lies between 1360 and 1580 m.a.s.l. near this summit (Figure 20) (Reger, 1975, p. 77). Farther north, on Taylor Mountain, structure may have played a greater role in the location and development of terraces (Foster, 1967; 1992), owing to horizontal foliation in the Birch Creek Schist and nearly horizontal welded igneous tuffs and flows. On Mt. Fairplay, however, structure is more complex, with tuffs dipping about 40° to the ESE, and joints trending N-S and dipping to the E at 30-40°. Also, within the sequence of terraces studied is a large scarp between what Reger (1975) designated T21 and T23. At 100 m in height this scarp is significantly larger than other CTs scarps in the area (which range from 10 to 30 m). The base of the scarp trends roughly NW-SE (Figure 21). There are no mapped faults on Mt. Fairplay that could explain this scarp. The entire region is deformed, and the beds and igneous bodies are folded and faulted. According to Foster (1967), the main structures in the region trend NE-SW and NW-SE although both structures are poorly expressed in the Mt. Fairplay area, probably due to the igneous intrusions and volcanic rocks. Despite efforts to identify a structure directly related to this anomalously large scarp, it was not possible to confirm one. A detailed morphometric analysis of Mt. Fairplay by P.M. Figueiredo using the 2 m resolution ArcticDEM (Porter, et al., 2018) revealed evidence of well-defined, steep landslide scarps. Although it is not possible to definitively associate this anomalously high scarp with landslide processes, it is possible that nivation has reworked a preexisting morphology.

Methodology

TCN geochronology methods are applied to estimate how long a surface or rock at the Earth's surface has been exposed to cosmic rays (e.g., Lal, 1991; Goose & Philips, 2001). Rare cosmogenic nuclides like ^{10}Be , ^{26}Al , or ^{36}Cl are produced in the uppermost few meters below the surface, as cosmic rays bombard the rock material, interacting with the atomic structures within the mineral lattice. The known production rates and the measurements of the concentration of TCN allows for the estimation of exposure length or denudation at the surface (Darville, 2013; Frankel & Owen, 2010; Schaetzl & Thompson, 2015, p. 598). Some advantages of using TCN geochronology methods are that it can be applied broadly to preserved erosional as well as aggradational features, in a variety of lithologies, and across timescales of thousands to a few million years.

For this study, a total of 12 boulders were sampled across four terraces at two locations. The same spatial sampling scheme was employed to collect three samples across both the highest and lowest elevation terraces at the two study sites. Samples were collected at (A) the base of the scarp, (B) the edge of the rubble further out on the tread, and (C) at the outer (distal) edge of the tread (Figure 21). Samples are referred to by terrace number (T6, 10, 20, and 25) assigned by Reger (1975) and position on the tread (A-C). When selecting boulders in these three tread positions, preference was given to larger clasts, or bedrock, with minimal lichen cover, as these are less likely to have been moved by other geomorphic processes or require additional shielding calculations (Figure 21). A sledgehammer and chisel were used to collect at least 500 g of rock sample from the upper 5 cm of exposed boulder surface. The location of each sample was recorded using a handheld GPS, and angular elevations to the horizon at cardinal and intercardinal directions were

taken using a clinometer for topographic shielding calculation. Boulder size and shape were measured and recorded, and photos were also taken.

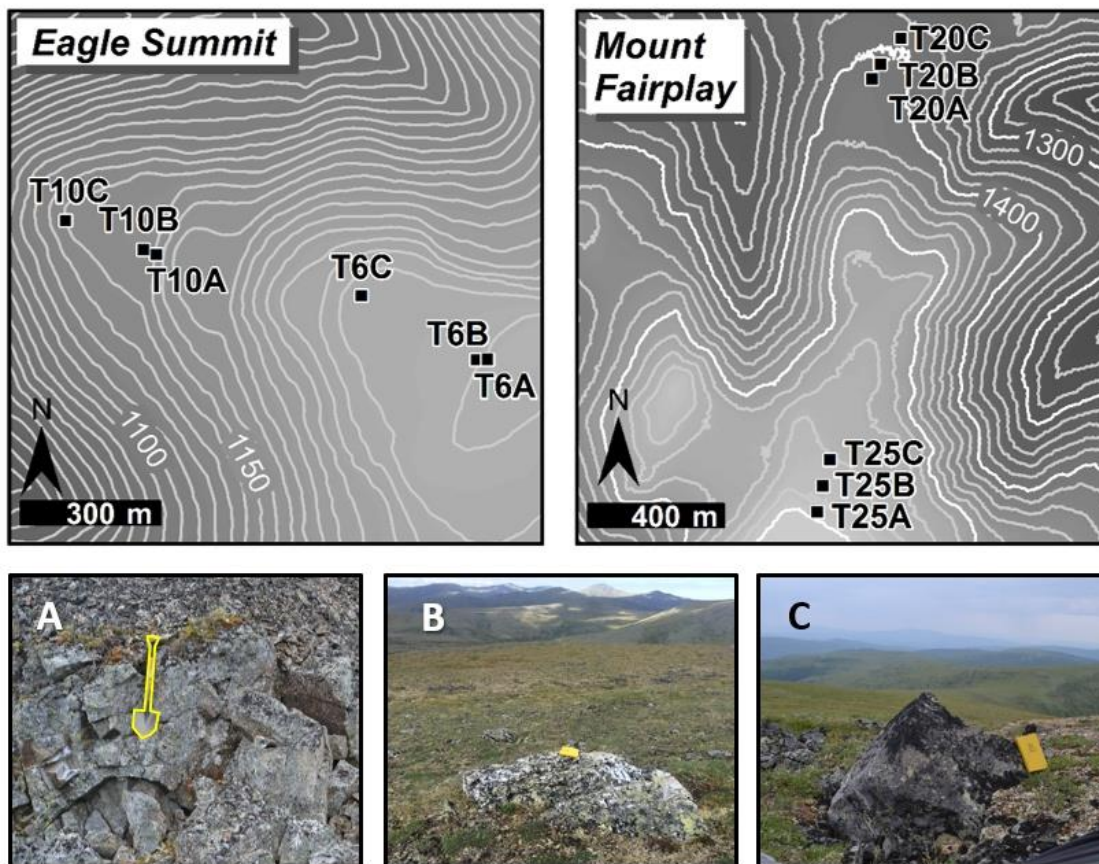


Figure 21. Sampling Strategy for Geochronology Study. Maps show sampling locations on the highest and lowest terraces near Eagle Summit and on Mt. Fairplay. Map areas indicated on Figure 20 geologic maps. Terrace numbers taken from Reger's (1975) inventory and letters indicate sample positions. Examples of boulders sampled at (A) the bedrock scarp (shovel outlined for scale), (B) mid-tread, and (C) tread toe (field books for scale).

Physical and chemical preparation of the ^{10}Be and ^{36}Cl samples to target nuclides were conducted at the University of Cincinnati geochronology laboratories. Accelerator mass spectrometry (AMS) measurements were performed at the Purdue University PRIME lab. All rock samples were first crushed and sieved. Then, the chemical preparation was performed on the 250-500 μm size fraction. For ^{10}Be , quartz was isolated from quartzite samples in accordance with the

methodology developed by Kohl and Nishiizumi (1992). Through a chemical procedure, $\text{Be}(\text{OH})_2$ was precipitated for each quartzite sample, and then combusted to obtain BeO that was loaded into steel cathodes for AMS measurements. For samples poor in quartz, such as the ones from Mount Fairplay (mafic volcanic rock), the procedure by Stone et al. (1996) was followed for bulk rock preparation (without mineral separation) to target ^{36}Cl . Chlorine was isolated through precipitation of silver chloride, then loaded into copper cathodes for AMS analysis, specifically of $^{36}\text{Cl}/^{35}\text{Cl}$ ratios. Geochemistry, necessary for age calculation, for samples treated as bulk rock, was performed by Activation Laboratories Limited in Ancaster, Ontario.

Results

Two primary assumptions are associated with TCN analyses: (1) that the rock was not previously exposed to cosmogenic rays, and therefore contains a cosmogenic nuclide signature not altered by inheritance; and (2) that erosion has not continued to occur, or is negligible, after subaerial exposure of the rock (e.g., Gosse & Phillips, 2001; Cockburn & Summerfield, 2004; Darville, 2013, Schaetzl & Thompson, 2015, p. 598). The calculated ages presented here are therefore interpreted as minimum-limiting exposure dates (Ivy-Ochs et al., 2007; Heyman et al., 2011).

Table 6 provides a summary of sample details and calculated exposure ages from the two terraces near Eagle Summit. CRONUS-Earth version 3 online calculator was used to calculate ^{10}Be ages based on the Lal (1991)/Stone (2000) time-dependent production rate model using a global calibration dataset (Balco et al., 2008). Also, the CREp online calculator was used to generate ^{10}Be ages based on the Lifton-Sato-Dunai (2014) time-dependent model. A few of the Lifton-Sato-Dunai (2014) modeled ages are older, but due to the minimal differences between the two, and considering results as minimum exposure ages, subsequent analysis refers to the Lal (1991)/Stone

(2000) modeled ages. All ages from terraces 6 and 10 are from within the Wisconsin glacial episode. Two dates are from the Last Glacial Maximum during the Late Wisconsin or the local Salcha glacial episode (Weber, 1986). The other four ages from this terrace sequence fall within with the Eagle, or early/middle Wisconsin glacial episode.

Table 6. Sample Details and Calculated ^{10}Be Ages from Eagle Summit. Assuming no denudation of boulder surfaces.

Sample	Location (°N/°W)	Elevation (m.a.s.l.)	Thickness ¹ (cm)	Topographic shielding factor ²	Quartz ³ (g)	Be Carrier (g)	$^{10}\text{Be}/\text{Be}^{4,5}$ ($\times 10^{-15}$)	^{10}Be Concentration ^{5,6,7} (10 atoms g^{-1} SiO_2)	Age ^{3,5,8} Lal/Stone ⁹ (ka)	Age ^{3,5,8} Lifton et al. ¹⁰ (ka)
T6A	65.4674/ 145.3783	1244	4	0.999	18.5559	0.3572	218.58±6.75	2.92±0.01	22.4 ± 1.9	24.9 ± 1.4
T6B	65.4652/ 145.3635	1243	4.5	0.999	19.3534	0.3649	309.88±9.70	4.07±0.13	34.5 ± 2.9	34.7 ± 1.9
T6C	65.4665/ 145.3688	1221	3.5	0.998	19.8572	0.3634	353.72±11.85	4.51±0.15	39.1 ± 3.4	39.3 ± 2.2
T10A	65.4652/ 145.363	1141	3	0.999	20.9348	0.3710	452.68±11.10	5.59±0.14	43.7 ± 3.6	44.1 ± 2.3
T10B	65.4675/ 145.3789	1137	4	0.996	18.3772	0.3502	482.39±11.77	6.41±0.16	49.6 ± 4.1	50.3 ± 2.6
T10C	65.4681/ 145.3825	1113	5	0.989	19.5812	0.3659	219.38±6.96	2.85±0.09	22.4 ± 3.4	22.6 ± 1.3

¹The tops of all samples were exposed at the surface.

² Topographic shielding factor was calculated online using CHRONUS tool available at <https://hess.ess.washington.edu/>.

³A density of 2.7 g cm^{-3} was used based on the granitic composition of the surface samples.

⁴Isotope ratios were normalized to ^{10}Be standards prepared by Nishiizumi et al. (2007) with a value of 2.85×10^{12} and using a ^{10}Be half-life of 1.36×10^6 years.

⁵Uncertainties are reported at the 1σ confidence level.

⁶A mean blank value of $1,1824 \pm 0,54 \times 10^{-15} \text{ }^{10}\text{Be}$ was used to correct for background, according with PRIME lab measurements.

⁷Propogated uncertainties include error in the blank, carrier mass (1%), and counting statistics.

⁸Propogated error in the model ages include a 6% uncertainty in the production rate of ^{10}Be and a 4% uncertainty in the ^{10}Be decay constant.

⁹Lal and Stone time-dependent scaling model ± total uncertainty calculated on CHRONUS v.3 online calculator.

¹⁰Lifton-Sato-Dunai time-dependent scaling model ± total uncertainty calculated on CREp online calculator.

Table 7 summarizes sample and age details for the two terraces studied on Mt. Fairplay. CRONUS-Earth v. 2 was used to calculate ^{36}Cl ages. Both ages from the Lal (1991)/Stone (2000) time-dependent and independent scaling models are reported. The similarity of these ages indicates either is representative. Subsequent analysis, however, refers to ages calculated using the time-dependent scaling model as these dates are synchronous with cold-climate periods. Five of the six ^{36}Cl ages are from the Eagle or early/middle Wisconsin glacial episode while one date is significantly older, from the Mt. Harper or Illinois glacial episode.

Table 7. Sample Details and Calculated ^{36}Cl Ages from Mt. Fairplay. Assuming no denudation of boulder surfaces.

Sample	Location (°N/°W)	Elevation (m.a.s.l.)	Topographic shielding factor ¹	Leached Rock (g)	³⁵ Cl Carrier (g)	Cl (ppm)	³⁶ Cl Concentration (atoms/g ³⁶ Cl x 10 ⁶) ^{2,3,4}	Exposure Age ± Uncertainty (ka) ⁵	Exposure Age ± External Error (ka) ⁶
T25A	63.6785/ 142.2125	1571	0.970	30,3732	1,0422	900.692	5.79±0.08	49 ± 16	49±16
T25B	63.6794/ 142.2117	1564	0.998	30,0114	1,0498	614.645	9.99±0.15	125 ± 29	125±29
T25C	63.6810/ 142.2108	1532	0.999	30,2418	1,0352	513.755	2.58±0.17	29.4 ± 6.1	29.5±6.2
T20A	63.6884/ 142.2103	1389	0.992	30,4982	1,0919	104.913	0.71±0.08	28.5 ± 2.8	28.4±2.7
T20B	63.6888/ 142.2098	1385	0.999	30,0308	1,0221	46.999	1.26±0.77	57.3 ± 5.3	57±5
T20C	63.6895/ 142.2086	1376	0.999	30,2097	1,0468	115.570	0.78±0.01	30.3 ± 3.3	30.3±3.2

¹ Topographic shielding factor was calculated online using CHRONUS tool available at <https://hess.ess.washington.edu/>.

²Uncertainties are reported at the 1 σ confidence level.

³A mean blank value of 87.364±6.744 of ratio $^{35}\text{Cl}/^{37}\text{Cl}$ was used to correct for background, according with PRIME lab measurements.

⁴Propogated uncertainties include error in the blank, carrier mass (1%), and counting statistics.

⁵Lal and Stone time-independent scaling model ± total uncertainty calculated on CHRONUS v.2 online calculator.

⁶Lal and Stone time-dependent scaling model ± total uncertainty calculated on CHRONUS v.2 online calculator.

Figure 22 shows the ages based on the Lal (1991)/Stone (2000) time-dependent scaling models reported in Tables 6 and 7, expressed graphically for easier comparison and organized spatially according to where they were collected along the topographic profiles at each site. On all four terraces, exposure age from the base of the scarp are younger than the next boulder part way across the tread indicating time-transgressive development through scarp retreat. All three ages from Terrace 6 near Eagle Summit are progressively older with distance away from the scarp of that terrace unit. This age distribution is closest to the original hypothesis that these treads are diachronous surfaces from continuous backward retreat of scarps, and synchronous with glacial episodes.

In contrast, ages from the toe (boulder C) of terraces 10 and 25 are significantly younger than ages from near the scarp of the same terrace units. In the case of Terrace 20, the toe and the scarp ages are similar. We interpret these boulders as likely being too close to the slope shoulder and subject to ongoing erosion, and therefore not representative of long-term tread development. Rather, these younger exposure ages might be from continued erosion and gravity-driven processes operating on the scarp of the next lower terrace unit. Boulders near the scarp base (A and B) on all four terraces are nonetheless indicative of time-transgressive surface development through scarp retreat.

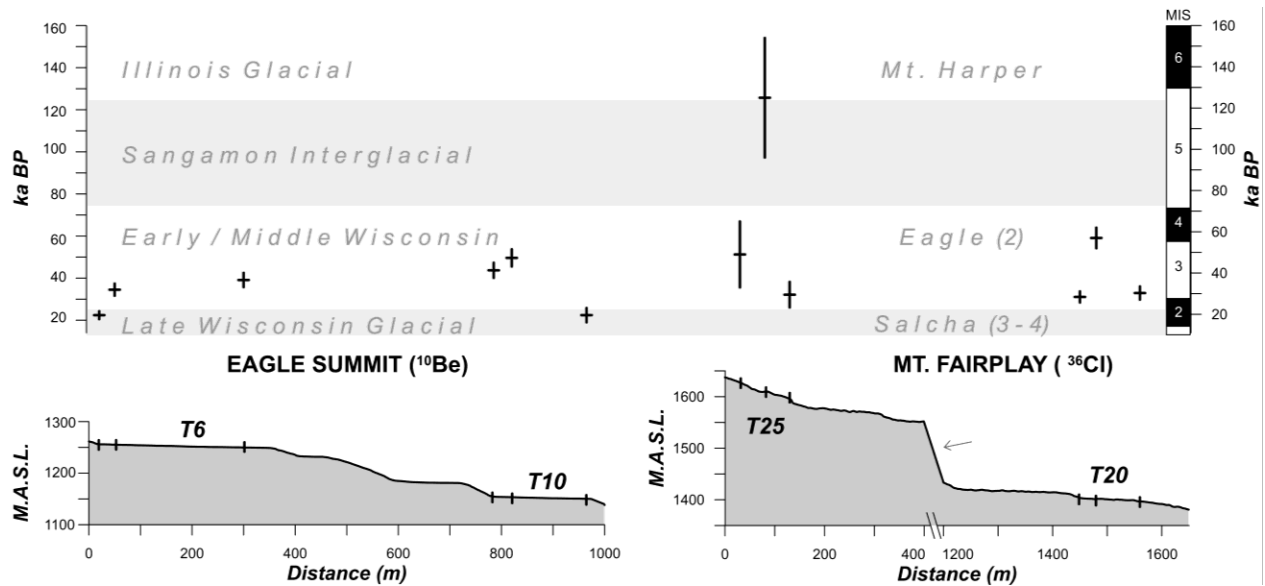


Figure 22. Calculated Ages Graphed by Position on Topographic Profiles. Calculated ^{10}Be ages for boulder exposure at Eagle Summit (left) and ^{36}Cl ages for Mt. Fairplay (right) shown according to position along topographic profiles of terrace sequences at both sites. Parentheticals after local glaciation names refer to number of advances during this time (Weber, 1986). Marine Isotope Stages (MIS) after Lisiecki and Raymo (2005). Arrow indicates position of anomalous scarp discussed in the study area description.

Discussion

An unresolved issue in periglacial geomorphology is whether nivation is capable of producing landscape-scale landforms with the dimensions typical of CTs. Studies on nivation have generated a variety of erosion rates for this process suite. For example, Thorn (1976) reported a nivation erosion rate of 7.5 mm ka^{-1} ($0.00075 \text{ cm yr}^{-1}$); Rączkowska (1995), 0.004 to 0.64 cm yr^{-1} ; and Kňážková et al. (2018) $0.77 \pm 0.12 \text{ mm yr}^{-1}$ ($0.077 \pm 0.012 \text{ cm yr}^{-1}$).

Erosion rate estimates from terraces studied in this work are shown in Table 8. These rates are calculated between boulders A and B (approaching terrace unit scarps) on all terraces, based on the difference in boulder distance to the scarp as measured on site and maximum and minimum differences in exposure age, accounting for external uncertainty associated with each age. Calculated rates appear high but are comparable to those reported previously by Rączkowska

(1995). Owing to the similarity of reported rates with those of nivation elsewhere and ages synchronous with local glacial advances, we conclude that nivation is, or has been active here, and could have been responsible for exposing these elevated boulders.

Table 8. Erosion Rates Based on Calculated Ages. Calculated erosion rates between boulders A and B for the four terraces studied at Mt. Fairplay and Eagle Summit. Distances between samples and their ^{10}Be and ^{36}Cl surface exposure age range assuming the associated uncertainty, are presented.

Terrace	Age Difference (ka \pm error)	Distance (m)	Rate (cm yr$^{-1}$ \pm error)
<i>Eagle Summit</i>			
T6	12.1 \pm 4.8	28	0.23 \pm 0.15
T10	5.9 \pm 7.7	33	0.56 \pm 2.11
<i>Mt. Fairplay</i>			
T25	76 \pm 43	84	0.11 \pm 0.04
T20	28.6 \pm 7.7	52	0.18 \pm 0.05

Apparent trends in elevation and timing of erosion within the terrace sequences near Eagle Summit and on Mt. Fairplay are inconsistent however. Previous work has found statistical significance between sub-continental scale spatial trends in CT elevations and Wisconsin-age snowlines (Nelson, 1998; Nelson & Nyland, 2017). Péwé and Reger (1972) mapped Wisconsin-age snowlines based on the elevations of the lowest glacial cirques across Alaska. Nelson and Nyland (2017) found that trends in median CT elevations closely track this paleo-snowline elevation gradient, which is dependent on latitude and continentality.

Erosion near the scarps in the sequence near Eagle Summit occurred mainly during the Eagle glacial episode (corresponding to MIS 2) from \sim 55 to 48 ka on the lowest terrace (T10, \sim 1150 m.a.s.l.) and during the Salcha glacial episode from \sim 32 to 22 ka on the highest terrace (T6,

~ 1250 m.a.s.l.). This could indicate a rising snowline through the Wisconsin glaciation. Meanwhile, on Mt. Fairplay, on the highest terrace (T25, ~ 1600 m.a.s.l.), the scarp was eroding from the Mt. Harper glaciation until the Eagle glacial episode, or between ~ 130 to 48 ka. This period includes an interglacial episode when periglacial erosion slowed and azonal processes prevailed. The lowest terrace scarp (T20, ~ 1400 m.a.s.l.) was eroding from the Eagle to the Salcha glacial episode, or between ~58 and 29 ka, indicating a possible lowering of the snowline from the end of the Illinois to the Late Wisconsin. More age determinations are required to better understand the timing of development on these ridges relative to local snowline altitudes.

Conclusions

This work features the first geochronology results from CT surfaces in the Alaskan Yukon-Tanana Upland. TCN surface exposure ages from CTs near Eagle Summit (six ^{10}Be exposure ages) and on Mt. Fairplay (six ^{36}Cl exposure ages) provide the quantification called for by many to evaluate the nivation hypothesis for cryoplanation terrace formation (e.g., Demek, 1969; Prieznitz, 1988; Thorn & Hall, 2002; Nelson & Nyland, 2017). These ages provide some support for nivation as a key process in CT development because: (1) exposure ages confirm time-transgressive development, particularly on the inner tread, with estimated erosion rates ranging from 0.11 to 0.56 cm yr^{-1} ; (2) the estimated erosion rates on the inner tread of all four terraces studied are comparable to previously published nivation studies (Rączkowska, 1995; Kňázková et al., 2018); and (3) exposure timing coincided with cold climatic intervals.

The data produced in this study reinforce previous work that found spatio-statistical indications of climatic controls on these landforms (e.g., Demek, 1969; Reger, 1975; Nelson, 1998; Nelson & Nyland, 2017) and significantly contribute to a generalized model for cryoplanation landform development in eastern Beringia. Additional surface exposure ages will, however, be

necessary at these study areas to clarify local elevation trends in terrace development. More ages, along with process monitoring and quantitative modeling, will eventually enable a genetic model for terraces in the Yukon-Tanana Upland or eastern Beringia to be developed.

Such a genetic model for CT development is becoming increasingly necessary for the acceptance of the ability of periglacial processes to limit topography regionally. Similar to the so-called “glacial buzzsaw” (e.g., Brozović et al., 1997), this has been referred to by some as a “frost buzzsaw” (Hales & Roering, 2009; Hall & Kelman, 2014) and holds the potential to rejuvenate periglacial geomorphic studies, as well as a new means by which periglacial research can contribute more effectively to Quaternary science.

CHAPTER 5. LONG-TERM EROSION RATES BY NIVATION, CATHEDRAL MASSIF, BRITISH COLUMBIA

Introduction

Cryoplanation terraces (CTs) are large landforms consisting of alternating steep and shallow slope segments and repeating sedimentological patterns. From a distance, these landforms resemble immense staircases. Risers (scarps) are inclined at angles of 15° - 40° and display exposed bedrock or a veneer of coarse, angular, clastic rubble. The gently sloping (1° - 10°) treads are mantled with sorted patterned ground and solifluction lobes. Although these landscape-scale features have long been associated with periglacial environments, the geomorphic processes responsible for their formation remain contentious. Debate is focused on whether CT formation is controlled primarily by geologic structure or by climatic factors (French, 2017, p. 295; Ballantyne, 2018, pp. 220-222). Process-oriented field investigations on CTs are rare. There are, however, several indirect lines of evidence supporting the climatic-influence hypothesis of CT development, through the suite of periglacial and fluvial processes known collectively as *nivation*.

Nivation is a shorthand term for locally intensified weathering, transport, and depositional processes associated with large snowbanks that persist well into summer months. The prolonged thermal insulation and moisture provided by snowbanks promote chemical weathering and mechanical weathering through ice lensing (e.g., Matsuoka & Murton, 2008). Meltwater transports eroded materials throughout the summer via rillwash, sheetwash, and piping, and promotes solifluction and frost creep (e.g., Thorn & Hall, 1980; 2002; Berrisford, 1991).

Indirect evidence indicating that nivation plays a critical role in CT formation includes CTs that cut across geologic structure (e.g., Demek, 1969; Reger, 1975), statistically preferred poleward orientations of CT scarps (Nelson, 1998), and CT elevation trends that closely track those

of glaciers (Nelson & Nyland, 2017). Nonetheless, Demek's (1969, p.66) statement that "there are no data on the rate of development of cryoplanation terraces" remains as applicable to the contemporary literature as it was half-century ago.

One of the key remaining issues is whether nivation can produce landforms with the dimensions typical of CTs. Although features in the lower part of the size spectrum are often termed nivation hollows, we follow a recommendation to separate morphological and genetic inferences (Thorn, 1983) by referring to cryoplanation *landforms* and nivation *processes* (Lewis, 1939; Te Punga; 1956, p. 335; also see Embleton & King, 1968, p. 533).

This study addresses two fundamental, unresolved issues in cryoplanation research (cf. Priesnitz, 1988; Thorn & Hall, 2002): 1) documentation of active nivation processes on cryoplanation landforms; and 2) calculation of long-term denudation rates by nivation processes. Frost Ridge constitutes a highly unusual configuration of features developed under naturally controlled conditions, resulting in incipient cryoplanation terraces approaching the size of typical CTs found throughout unglaciated Beringia. Insights into this active nivation environment are critical, as the CTs in unglaciated Beringia, including those in nearby Yukon Territory, are considered by many (e.g., Reger, 1975; Reger & Péwé, 1976; Hughes, 1990, pp. 14-16; Lauriol, 1990) to be relict.

Study Area and Geomorphic Evolution

This study evaluates the hypothesized link between long-term nivation denudation rates and the size and morphology of incipient terraces ("nivation hollows") on the Cathedral Massif in the Atlin / Téix'gi Aan Tlien Provincial Park, northwestern British Columbia (Figures 23 and 24). Slope evolution on the northerly aspect of Frost Ridge (N 59° 21' 5", W 134° 5') is the focus of this work. The Cathedral Massif is located within faults bounding the Atlin Terrane and has been

described as a “coast intrusion” of the Coast Plutonic Complex made up of primarily porphyritic and granophyric subvolcanic rock of Jurassic to Neogene age (Jones, 1975; Nelson, 1979; Gehrels et al., 2009).

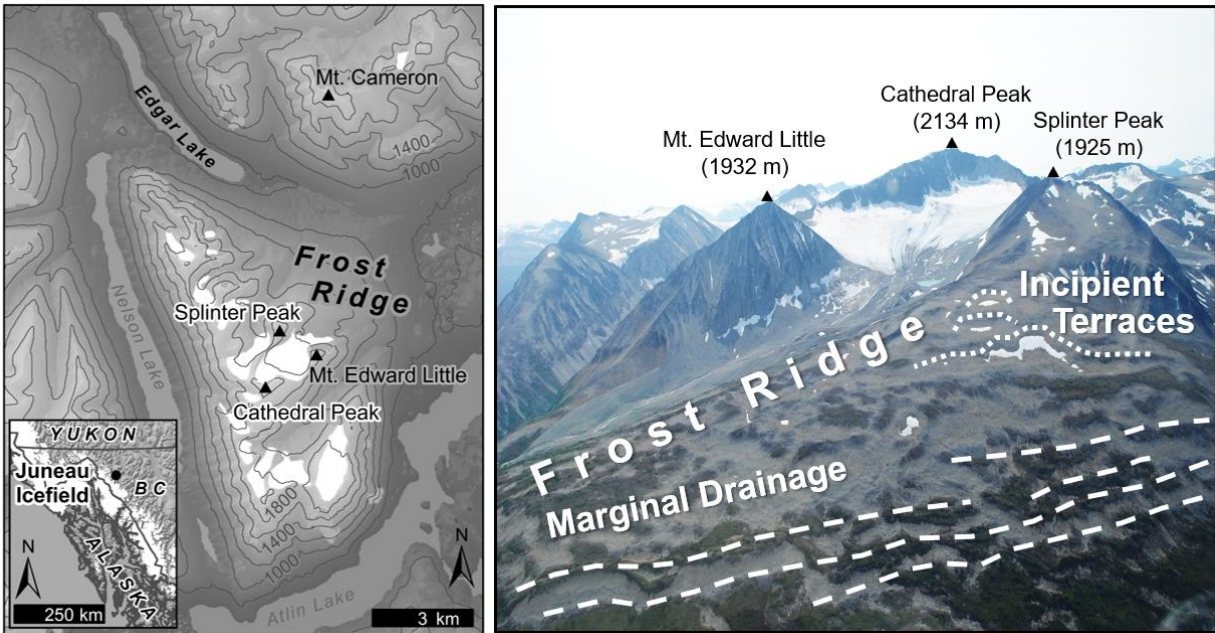


Figure 23. Frost Ridge Study Area Map and Photo of Features of Interest. Study area map with perennial snow and ice fields in white and aerial oblique photo of Frost Ridge on the Cathedral Massif with features of interest outlined with white dashed lines. Place names are from Cialek (1977) and are shown with SRTM elevation data.

Cathedral Peak is a paleonunatak, formerly surrounded by the ancestral Hobo-Llewelyn Glacier, part of the larger Cordillerian ice sheet (Bass, 2007). The tributary of the ancestral Hobo-Llewelyn Glacier that occupied the present Edgar Lake valley (Figure 23) receded between the middle (ca. 25 ka) and late Wisconsin (ca. 11 ka) (Jones, 1975, p. 35; Miller, 1975, p. 131-132; Slupetzky & Krisai, 2009, p. 207).

During waning phases of the Wisconsin glaciations, the upper reaches of Frost Ridge stood above the level of the glacier then occupying the present-day Edgar Lake valley (informal name).

A large cryoplanation terrace and a small cirque were incised into the flanks of Splinter Peak (Figure 24A). The tread of this CT displays a well-developed field of sorted patterned ground, consisting largely of sorted stripes (Figure 24B).

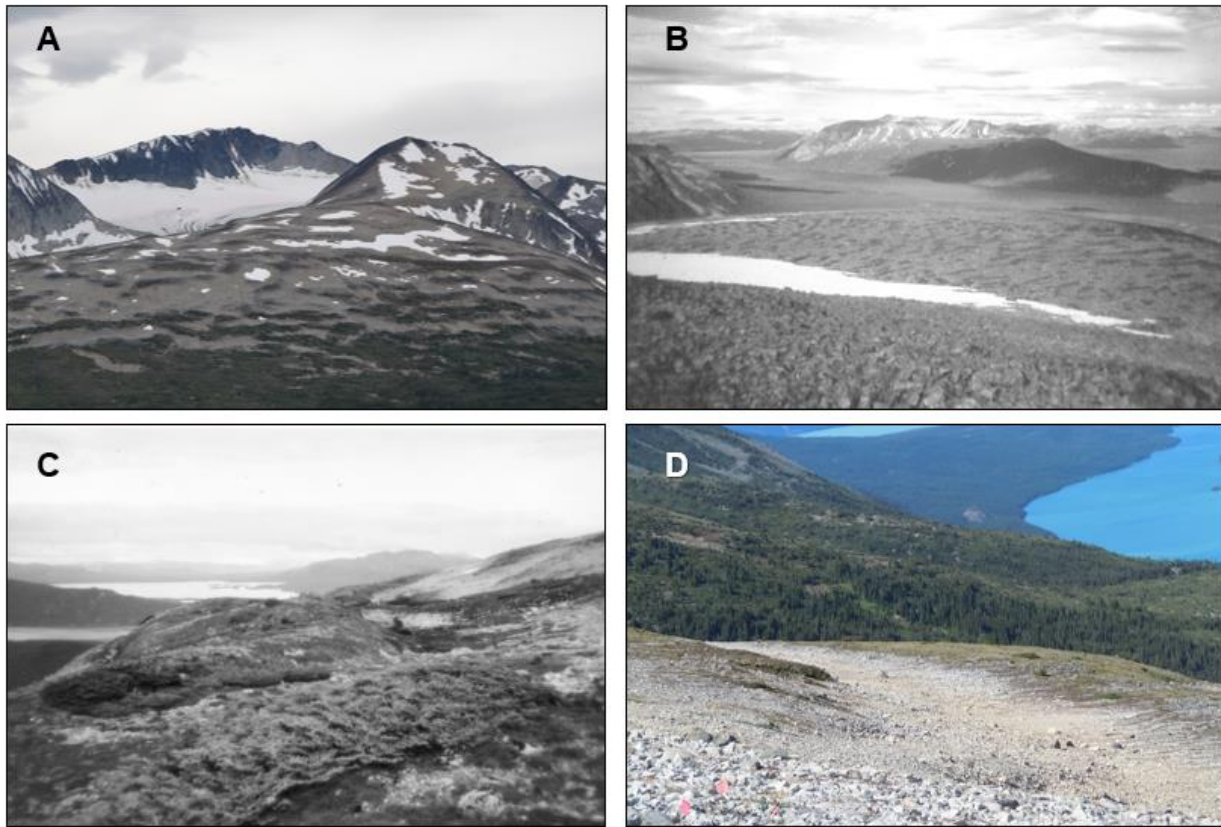


Figure 24. Photos of Late-Lying Snowbanks and Features of Interest. (A) View upslope of north-facing flank of Frost Ridge, showing snow-filled marginal drainage features (Photo by C.W. Queen, July 2017). (B) Large cryoplanation terrace cut into NE-facing flank of Splinter Peak. Note large perennial snowbank occupying the break in slope between the base of Splinter Peak and the CT tread, tessellated with sorted patterned ground. (C) A largely unmodified marginal drainage feature on the lower reaches of Frost Ridge, displaying a prominent reverse slope indicative of fluvial incision (Photos B and C by F.E. Nelson, August 1976). (D) Incipient cryoplanation terrace, created by modification of an initial V-shaped form by nivation processes. Note sorted stripes on terrace tread (Photo by F.E. Nelson, July 2017).

Edgar Lake valley is oriented east-west, with side slopes on Frost Ridge and Mt. Cameron facing north and south, respectively (Figure 23). The north-facing flank of Frost Ridge displays a

series of visually striking subhorizontal lineations, sloping down-valley at 1.7° (Figure 24A and C). These features are currently occupied by deep accumulations of snow that remain well into the summer. Similar lineations occupy the opposite (south-facing) valley side (Mt. Cameron), but are not occupied by late-lying snowbanks.

During deglaciation, marginal drainage at the contact between the glacier and valley walls (Maag 1969; Embleton & King, 1975, pp. 338-344; Syverson & Mickelson, 2009) created a series of elongated incisions in the valley sides subparallel with the contour and the glacier's direction of flow. Because solar radiation is minimized on steep north-facing slopes in the Northern Hemisphere, large snowbanks accumulated and persisted in these initially V-shaped incisions on Frost Ridge (Figure 24C). On the north-facing valley wall the incisions were enlarged substantially by nivation and their profiles modified to resemble the typically step-like form of CTs (Figure 24D). At lower elevations, however, where snow does not persist as long into the summer, the initial form of the marginal drainage features has been preserved. The developmental history of Frost Ridge topography is represented in Figure 25.

St-Onge (1969) concluded that it is next to impossible to ascertain the extent to which nivation processes have modified preexisting topographic irregularities, or whether they initiate such irregularities. The unusual history of deglaciation on Frost Ridge and the topoclimatic contrasts between the north- and south-facing slopes, removes this theoretical obstruction. The size and morphology of the marginal drainage channels determined through straightforward measurements and comparison with those of the contemporary (modified) incipient terraces upslope, provides a frame of reference within which long-term nivation erosion rates can be estimated in a historical context.

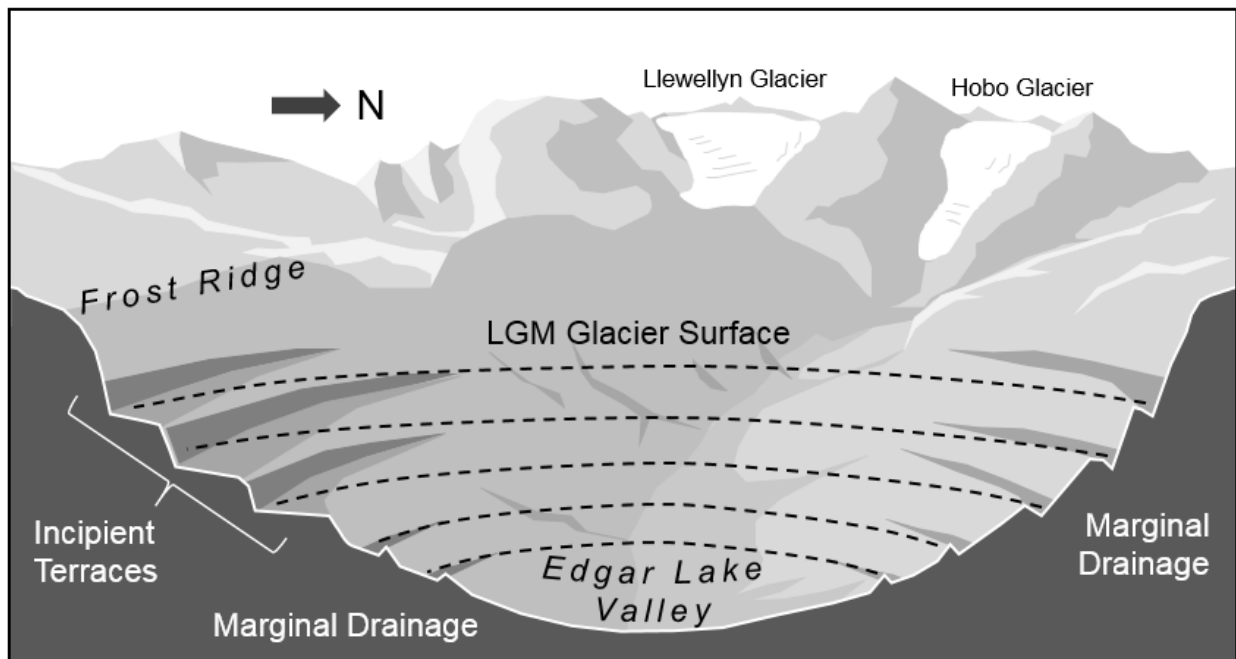


Figure 25. Idealized Schematic of Edgar Lake Valley. Idealized profile of the controlled natural experiment in Edgar Lake valley, formed by a branch of the ancestral Hobo-Llewellyn glacier. Dashed lines indicate glacier levels during progressive deglaciation. Notches created by marginal drainage are shown on the south-facing (right) valley wall and low elevations on the north-facing (left) valley wall. These have been enlarged into step-like hollows and terraces on the north-facing wall by periglacial processes associated with late-lying snowbanks.

Methodology

Nivation Observations

Active nivation processes were observed and recorded in late July of 2017 and 2018. Three of the large, late-lying snowbanks occupying incipient terraces on the north side of Frost Ridge were surveyed with a handheld GPS and three snow pits were excavated in a transect bisecting the approximate middle of each snowbank. Temperature and density measurements were recorded at regular intervals down snow profiles and notes were taken on any ice structures present, focusing on conditions at the base of the snowbank.

In the summer of 2018, the snowbanks were surveyed again, and three meltwater samples were collected from the downslope margin of each snowbank, following the procedure outlined

by Ballantyne (1978). At the lower edge of the snowbanks, the time to fill 2-liter bottles with meltwater and waterborne sediment was recorded. Air and soil surface temperatures were recorded during the collection of each sample.

Analysis of these samples was performed at a Michigan State University soil lab. Samples of meltwater and sediment were weighed, and dissolved content was measured using an Apera Instruments, AI422-M EC400S conductivity meter. Samples were then dried, lightly ground, and sieved (2 mm) to separate coarse and fine earth fractions. Particle size analysis for the fine fraction was performed by laser diffraction using a Malvern Mastersizer 2000E unit. Fines were homogenized using a sample splitter and a mass of approximately 2 g was chemically dispersed in a water-based solution of $[\text{NaPO}_3]_{13} \cdot \text{Na}_2\text{O}$ that was then shaken for at least 40 min. Laser diffraction generated detailed particle size measurements and precise textural classification.

Volumetric Comparison of Marginal Drainage and Incipient Terraces

Returning to Frost Ridge on September 4th, 2018 when the snowbanks had completely melted, we conducted an unmanned aerial vehicle (UAV) survey to generate a high-resolution DEM of the northern aspect of Frost Ridge. A DJI Mavic 2 Pro was flown over two adjoining areas covering a total of 1.3 km². Using DJI mission planning software, the UAV was flown at approximately 80 m altitude in a grid pattern, with flight lines oriented northeast-southwest, spaced at approximately 25 m intervals. The camera was oriented to nadir. Exposure intervals coupled with the flight line spacing resulted in 75% front and side overlap between images. Four ground control points were collected using a handheld GPS, at two low-elevation locations within the area covered and two high-elevation locations (where the UAV took off and landed for both flights). Photos were processed and photogrammetry performed in Pix4Dmapper (Pix4D Inc., San Francisco, California), which generated DEMs with spatial resolutions of 6.10 cm² (east area) and

5.84 cm² (west area). Absolute geolocation variance in all three dimensions was < 0.9 m. The accuracy of the DEM was deemed acceptable because subsequent analysis is more dependent on relative rather than absolute landform positions and morphologies.

Coordinates taken at incipient terraces and marginal drainage features of interest were used to identify these features on the DEM in ArcMap 10.2.2. One-hectare extractions of the three incipient terraces and six segments of the highest-elevation marginal drainage feature were resampled via cubic convolution to 25 cm² spatial resolution for computational ease. Differences in volume were computed in Surfer v. 12 (Golden Software, 2014) software using triangulated irregular network interpolations of the DEMs.

Calculation of Nivation-Driven Denudation Rates

Denudation rates were calculated by dividing the eroded volume by area of eroded material and dividing by the temporal deglaciation envelope published previously for this ancestral tributary of the Hobo-Llewellyn glacier (Jones, 1975, p. 35; Miller, 1975, p. 131-132; Slupetzky & Krisai, 2009, p. 2007). This procedure yielded a maximum denudation rate, based on the later bound of the deglaciation envelope (25 ka), and a minimum rate based on the earlier bound (75 ka).

Results

Active Nivation Processes on Frost Ridge

The collective periglacial and fluvial processes constituting the nivation process suite continue to operate on Frost Ridge, as evidenced by thermal, erosional, and other general observations documented in late July 2017 and 2018. Late-lying snowbanks provide consistent sub-zero temperatures to underlying rock material through July (Figure 26). Basal ice, ranging from 1 cm to 9.5 cm thick, was found at the bottom of the snowpack in all snow pits. Temperatures

in the snowpack ranged from -0.5 to -3°C (Figure 26). Running water was clearly audible within the snow pits, flowing through interstitial spaces beneath.

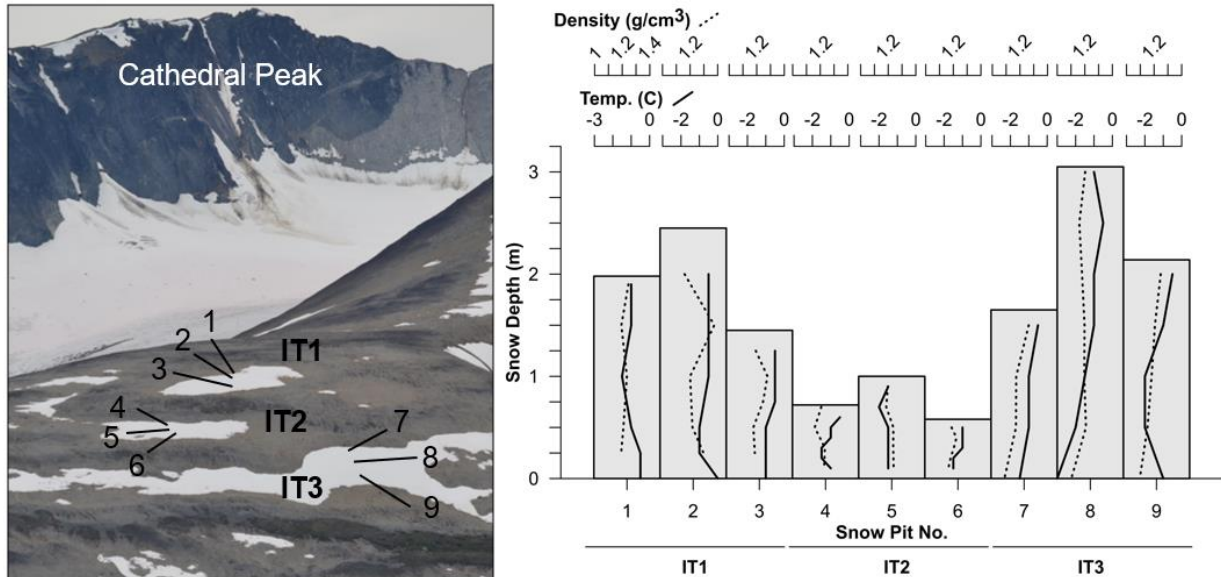


Figure 26. Late-Lying Snowbank Temperature and Density Profiles Density, temperature, and total depth of snow pits excavated in late-lying snow banks July 25th-27th, 2017. Snow pit numbers and locations are shown in the photo by C.W. Queen, July 24th, 2017.

Meltwater samples (a through c) taken from areas of notable rill and sheet flow from the downslope margins of the three snowbanks in late-July 2018 helped to characterize sediment fluxes (Table 9). The transported material ranged from dissolved solids to gravels (maximum gravel diameter was 38 mm). The majority of mass in transit consisted of coarse silt to medium sands. Over extended periods, weathered materials are transported off the treads of these incipient terraces, contributing to denudation and terrace formation.

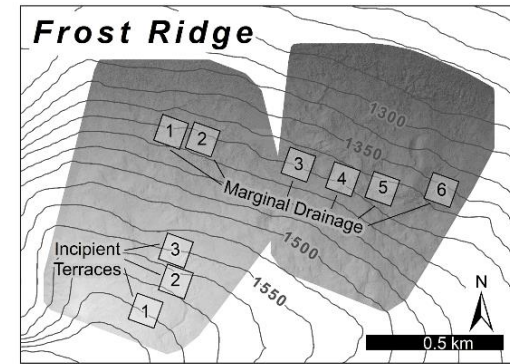
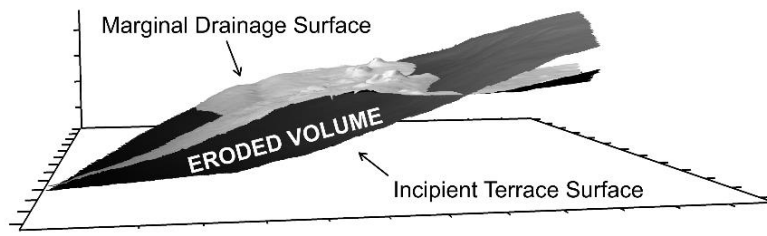
Table 9. Meltwater Discharge Rate and Transported Material Characterization. Data on discharge and sediment being transported away from the margins of the three late-lying snowbanks observed in incipient terraces (IT- 1 through 3) on Frost Ridge.

Incipient Terrace	Sample	Total Dissolved Solids (mg/L)	Gravel (g)	Fines (g)	% Clay	% Silt	% Sand	Discharge Rate (m³h⁻¹)	Average Discharge Rate (m³h⁻¹)
	a	7.77	13.98	38.24	18.3	64.6	17.0	3.15 x 10 ⁻³	
1	b	6.84	31.46	128.6	13.6	39.2	47.1	1.48 x 10 ⁻³	1.88 x 10 ⁻³
	c	3.27	0.5400	8.860	8.7	33.8	57.5	9.97 x 10 ⁻⁴	
	a	15.0	20.04	89.57	15.3	38.4	46.3	7.48 x 10 ⁻⁴	
2	b	5.12	9.560	30.71	13.7	30.9	55.4	1.87 x 10 ⁻³	7.11 x 10 ⁻³
	c	3.83	6.330	18.95	9.2	43.3	47.5	1.87 x 10 ⁻²	
	a	5.82	123.4	132.0	3.0	16.6	80.4	19.7 x 10 ⁻²	
3	b	11.5	51.54	126.3	5.6	25.9	68.5	12.1 x 10 ⁻²	13.5 x 10 ⁻²
	c	7.85	21.03	87.34	7.7	29.5	62.8	8.55 x 10 ⁻²	

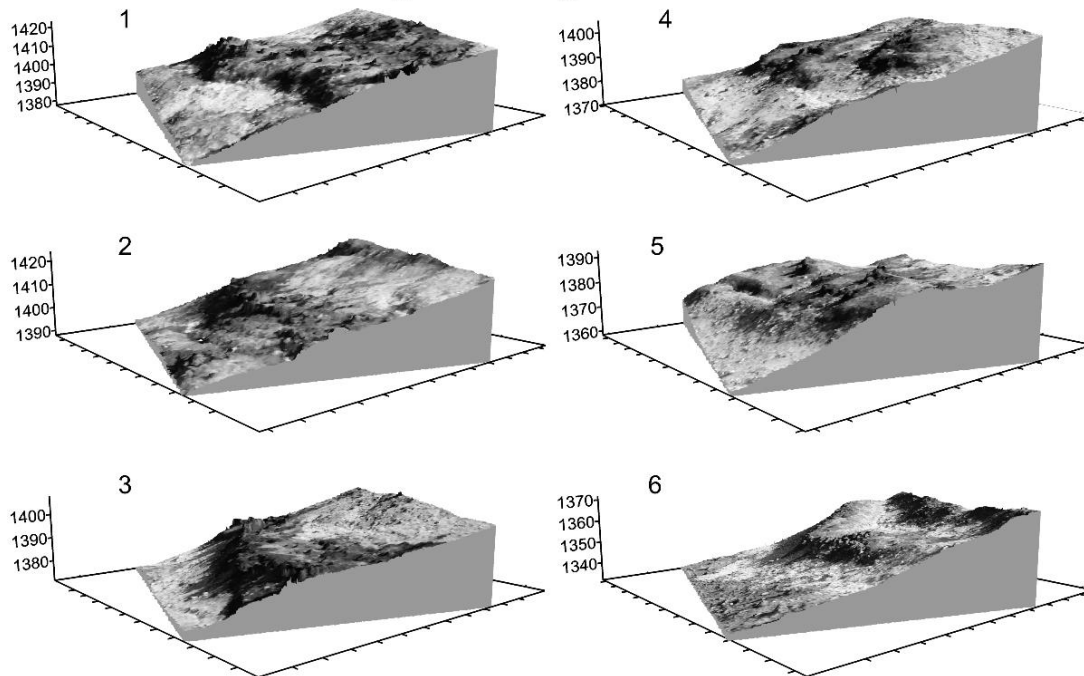
Volumetric Comparison of Landforms

Three-dimensional representations of the marginal drainage (MD) features and incipient terraces (IT) are shown in Figure 27. The incipient terrace scarps are from 9 to 25 m high, with slopes from 20 to 35°. Treads are from 30 to 75 m in length with slopes of less than 20°. The marginal drainage features have distinct reverse slopes (Figure 24C), and the typical V-shaped profiles associated with fluvial erosion.

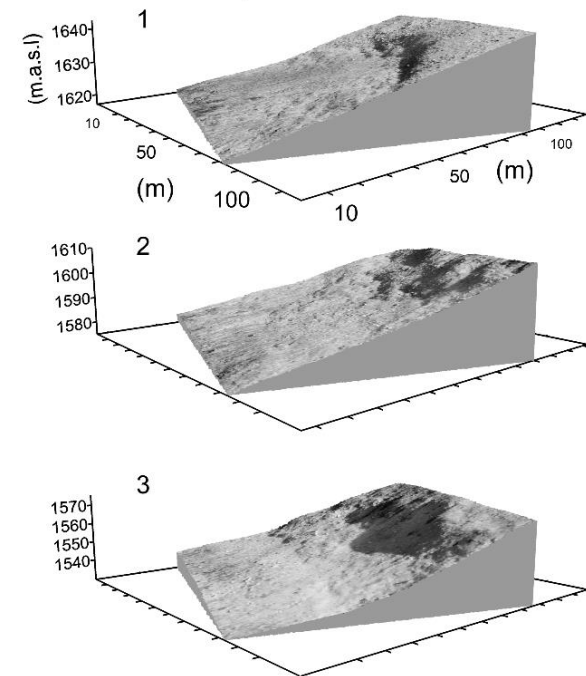
Figure 27. 3D Representations of Marginal Drainage and Incipient Terrace Features. Volume comparison of marginal drainage and incipient terraces to estimate erosion, map showing extent covered by UAV survey (average 5.84 cm² spatial resolution), and hectare plots (25 cm² resolution).



Marginal Drainage Features



Incipient Terraces



Assuming the marginal drainage features at lower elevations represent the approximate shape and size of original landforms immediately after deglaciation, differences between these and the modified features upslope will provide estimates of the volume of material eroded by nivation processes since deglaciation. Comparisons were performed for all combinations of the six marginal drainage features and three incipient terraces, and eroded volumes and areas are reported in Table 10. The reverse slopes were completely eroded in these manipulations and infilling occurs largely at the toes of the incipient terrace treads as these surfaces assume shallower slopes over time.

Table 10. Volume Differences between Marginal Drainage and Incipient Terraces.

		Incipient Terrace			
		1	2	3	
Marginal Drainage Feature	1	Volume Eroded (m ³)	36658.9	26373.6	11600.7
		Area Eroded (m ²)	9896.2	9897.9	8360.2
	2	Volume	15096.9	5484.2	779.8
		Area	9758.9	7922.4	1839.3
	3	Volume	17497.8	7859.2	2688.1
		Area	9752.1	8021.7	2919.7
	4	Volume	19676.2	9435.4	2504.2
		Area	9868.8	9494.3	4034.5
	5	Volume	22461.8	13466.9	6585.6
		Area	9882.2	7664.3	5632.8
	6	Volume	15341.9	6047.0	1093.5
		Area	9205.9	7174.0	2129.1

Nivation-Driven Denudation Rates

Denudation rate estimates based on eroded volume, area eroded, and published temporal deglaciation “envelopes” for Frost Ridge, are shown in Table 11. Several authors have reported mid- to late-Wisconsin deglaciation chronologies for the Edgar Lake valley (Jones, 1975, p. 35; Miller, 1975, p. 131-132; Slupetzky & Krisai, 2009, p. 207). We therefore used bounds of 25 ka

and 11 ka to generate minimum and maximum possible denudation rates for these features. Denudation rates range from 1.6 to 33.6 cm ka⁻¹. The average rate is 9.4 cm ka⁻¹ (8.9 cm ka⁻¹ if the extreme value of 33.6 is omitted).

Table 11. Frost Ridge Minimum and Maximum Nivation-Driven Denudation Rates. Rates based on the middle- (25 ka) to late-Wisconsin (11 ka) envelope for the deglaciation of Frost Ridge.

min. - max. (cm ka ⁻¹)		Incipient Terraces		
		1	2	3
Marginal Drainage Feature	1	14.8 – 33.6	10.8 – 24.6	5.6 – 12.7
	2	6.0 – 13.6	2.8 – 6.4	1.6 – 3.6
	3	7.2 – 16.4	4.0 – 9.1	3.6 – 8.2
	4	8.0 – 18.2	4.0 – 9.1	2.4 – 5.5
	5	9.2 – 20.9	7.2 – 16.4	4.8 – 10.9
	6	6.4 – 14.6	3.2 – 7.3	2.0 – 4.6

Discussion

The size and morphology of the incipient terraces observed on Frost Ridge, and particularly of IT2 and IT3, approach those of what have been described as “well-developed” CTs in eastern Beringia and elsewhere (e.g., Demek, 1969; Reger, 1975). CTs have been summarized as typically having treads from tens to hundreds of meters in length with gradients < 10° and scarps 15 to 40° rising tens of meters high (Ballantyne, 2018, p. 200).

Calculated denudation rate estimates (Table 11) are comparable with other works published for nivation in unconsolidated material. For example, Thorn (1976) reported a nivation erosion rate of 7.5 mm ka⁻¹ (0.75 cm ka⁻¹); Rączkowska reported (1995), 0.004 to 0.64 cm yr⁻¹ (4 to 640 cm ka⁻¹); and Kňazková et al. (2018) estimated 0.77 ± 0.12 mm yr⁻¹ (77 ± 12 cm ka⁻¹).

Although the denudation estimates reported here are similar to other published nivation rates (Thorn, 1976; Rączkowska, 1995; Kňažková et al., 2018), the variability in results and differences in local geology of these study areas suggests that more research is needed before deterministic modeling of these processes can be attempted.

Conclusions

The circumstances of deglaciation in the Edgar Lake valley constitutes a relatively well-controlled natural field experiment on Frost Ridge. This work establishes that Frost Ridge is an active nivation environment in which large, late-lying snowbanks are present at high elevations typically through the month of July. The snowbanks were observed actively eroding the underlying unconsolidated materials. Nivation acting over long periods on this slope has likely produced denudation rates ranging from 1.6 to 33.6 cm ka⁻¹ based on the volumetric comparisons of marginal drainage and incipient terraces.

Future work at this site might include installation of sediment traps, thermal sensors, and hydrological instruments across incipient terrace treads. We also anticipate repeated UAV surveying using differential GPS for establishment of ground control points. Frost Ridge constitutes a highly unusual situation that makes for an exemplary study area for future monitoring of nivation processes.

The proximity of the ridge to local alpine glaciers means it shares the hypothetical climate space defined by mean annual temperature and precipitation required by both cirques and CTs (Nelson, 1989, p. 39). The conditions defining the climate space are similar to those during Pleistocene cold intervals, when CTs are thought to have been actively forming across Beringia (Nelson & Nyland, 2017). We interpret Frost Ridge as being in an area of active CT development,

and a location at which the repeated calls for long-term process monitoring can be addressed (e.g., Demek, 1969; Prieznitz, 1988; Thorn & Hall, 2002; Nelson & Nyland, 2017).

Improving our understanding of nivation has significant implications not only for periglacial geomorphology, but also for the emerging field of glacial archaeology, which focuses on perennial snow and ice patches in southwestern Yukon Territory (e.g., Hare et al., 2012; Dixon et al., 2014). Annual air temperature anomalies have increased on average 2° C over the last 50 years in the Yukon (Streicker, 2016, p. 2). During the 1970s, the late-lying snowbanks observed in this study on Frost Ridge were perennial and contained thick basal accumulations of very cold ice (Nelson, 1975, unpublished data). Embedded within the basal ice were inclined sediment bands representing snow-patch surfaces in multiple prior years. The snow patches on Frost Ridge during that era were similar to the ice patches currently under study by Yukon archaeologists (Andrews & MacKay, 2012). The transition from perennial to late-lying snowbanks is also likely to be experienced at the Yukon sites, at which point a thorough understanding of the deposition patterns and rates will be crucial for continuing artifact retrieval.

CHAPTER 6. CONCLUSIONS

Summary of Results

The previous four chapters present several new findings in support of climatic influences on the origins and development of cryoplanation terraces (CTs). Chapter 2 highlights the ubiquity of CTs globally and tracks the evolution of formation hypotheses for these features, and particularly, the two hypotheses still supported and debated in modern works. The co-citation analysis from Chapter 2 indicates that neither individual works nor authors have performed “gatekeeping” roles, contributing to the notable lack of explicit field testing of any particular formation hypothesis over the last 50 years. Findings from Chapters 3, 4, and 5 address some arguments posed by supporters of the geologic structure hypothesis (e.g., Padalka, 1928; Hall & André, 2010; French, 2016) and lend new support to the hypothesis that CT formation is controlled by climate via nivation processes (e.g., Cairnes, 1912a; Demek, 1969; Reger & Péwé, 1976; Nelson & Nyland, 2017).

Spatial statistical analyses of a variety of relative weathering indices measured across terrace treads at three different locations spanning eastern Beringia indicate these are likely to be time-transgressive (forming through scarp retreat). This finding is in agreement with the observations and interpretations made by others that these are erosional features, including H.M. French, a leader for those considering that CTs are the result of geologic structural coincidence (e.g., French & Harry, 1992, p. 145; French, 2016, p. 224-225).

Several works have also concluded that current conditions and processes are not actively eroding scarps of well-developed terraces (e.g., French & Harry, 1992; Lauriol et al., 2006; French, 2016). Boulder exposure ages from terraces near Eagle Summit and on Mt. Fairplay presented in Chapter 4 support these conclusions. However, exposure ages generated are synchronous with

cold-climate intervals including the most recent localized glaciations in the Yukon-Tanana Upland. Increased frost action and other processes associated with the nivation process suite would have been intensified during these colder periods.

Lastly, H.M. French stated that the, "... problem of initiation is compounded by the fact that quantitative field studies have yet to demonstrate the active formation of these terraces (French, 2016, p. 226)." Chapter 5 addresses this issue on Frost Ridge of the Cathedral Massif, in British Columbia. Frost Ridge is a documented active nivation environment where the particular deglaciation history has preserved marginal drainage features and incipient terraces development since deglaciation. The long-term nivation denudation rates that produced these landforms approaching the morphology and scale of CTs are comparable not only with previously published nivation rates, but also those from the exposure ages in Chapter 4.

This dissertation offers a multidisciplinary, field-based assessment of the nivation formation hypothesis for CTs using cutting-edge field and lab techniques, the results from which indicate that nivation plays an important role in the development of CTs, a group of climatic and geomorphological processes characteristic of upland periglacial landscapes. Suggestions for future research outlined in the next section could solidify this connection and better quantify nivation processes, providing a new path by which periglacial research contributes more effectively to Quaternary science.

Recommendations for Future Research

More terrestrial cosmogenic nuclide (TCN) age determinations are required to fully understand the geochronology of scarp retreat on both Eagle Summit and Mt. Fairplay. TCN ages from Frost Ridge may also help to resolve the significant differences in estimated erosion rates between the Yukon-Tanana Upland and the Cathedral Massif (Tables 8 and 11) generated in this

work. A geochronology study on Frost Ridge would be well complemented by monitoring active nivation processes. Process monitoring could include repeat drone-based surveys using ground control points maintained with differential global positioning systems measurements. Incipient terraces on Frost Ridge should also be outfitted with sediment traps, Rudberg pillars, and mass-movement survey markers to more accurately measure sediment fluxes and displacement. With nivation process data, deterministic modeling of CT development will be needed before it is likely to be widely accepted within the geomorphic community.

Broader Impacts

High-latitude environments are changing rapidly, largely due to climate change (e.g., ACIA, 2004; IPCC, 2013). Understanding past landscape evolution is therefore crucial for good land-management practices today. Efforts to preserve periglacial landscapes are underway in other countries, including the Czech Republic and Canada. Cryoplanation landforms are protected in the Czech Republic under Government Act No. 114/1992: Gazette on Nature and Landscape Protection (Demek et al., 2010). Also, in the Yukon Territory of Canada, ice patches have been added to the UNESCO world heritage sites tentative list (UNESCO, 2018).

Preservation of significant landscapes for societal benefit and public education is also a core element of the U.S. National Park Service's mission. CTs are found in many of Alaska's national parks, monuments, and preserves, including Denali National Park, Cape Krusenstern National Monument, and Yukon-Charley Rivers and Bering Land Bridge Preserves. The superintendent of the Bering Land Bridge National Preserve and Chief of Interpretation has expressed interest in developing this topic to enhance visitor understanding of Beringian landscape evolution and associated features (Superintendent Jeanette Koelsch and Chief of Interpretation

Katie Cullen, personal communications, 2016 and 2017). Outreach materials have been prepared in collaboration with the Nome National Park Service office to this end.

APPENDICES

APPENDIX A

Chapter 2 Supplementary Materials

Appendix A.1. Co-citation analysis articles and “stance” assigned.

First Author	Year	Journal	Title	Stance
Barsch, D.	1971	Geographica Helvetica	Periglaziale Formung am Kendrick Peak in Nord-Arizona während der letzten Kaltzeit	skeptical
Tufnell, L.	1971	Weather	Erosion by Snow Patches in the North Pennines	neutral
Dury, G.H.	1972	Earth Science Reviews	Some Current Trends in Geomorphology	neutral
Williams, R.B.G.	1973	Antiquity	Frost and the Works of Man	neutral
Reger, R.D.	1976	Quaternary Research	Cryoplanation Terraces: Indicators of a Permafrost Environment	climatic
Pekala, K.	1977	Annales, Universitatis Mariae Curie-Sklodowska Sectio B	Cryoplanation Terraces in the Area of the Southern Khangai, Mongolia	climatic
Thorn, C.E.	1978	Annals of the Association of American Geographers	The Geomorphic Role of Snow	climatic
Washburn, A.L.	1980	Earth Science Reviews	Permafrost Features as Evidence of Climatic Change	climatic
Castleden, R.	1980	Catena	Fluvioperiglacial Pedimentation. A General Theory of Fluvial Valley Development in Cool Temperate Lands, Illustrated from Western and Central Europe	climatic
Guilcher, A.	1981	Geographie Physique et Quaternaire	Coastal Cryoplanation and Boulder Barricades in the Rimouski Area, South Shore of the St. Lawrence Estuary, Quebec	climatic
Washburn, A.L.	1981	Geologische Rundschau	Periglaziale Forschung in Revue	neutral
Péwé, T.L.	1982	Norsk Polarinstitut Skrifter	Glacial and Periglacial Geology of Northwest Blomesletta Peninsula, Spitsbergen, Svalbard	climatic
Karte, J.	1982	Polar Geography and Geology	Development and Present Status of German Periglacial Research in the Polar and Subpolar Regions	climatic
Péwé, T.L.	1983	Late-Quaternary environments of the United States. Vol. 1	The Periglacial Environment in North America during Wisconsin Time	climatic
Czudek, T.	1983	Foldrajzi Ertesito	Some Problems of the Valley Cryopediments in Eastern Siberia	climatic
Demek, J.	1983	Foldrajzi Kozlomenyek	Fossil Periglacial Phenomena in Czechoslovakia and their Paleoclimatic Evaluation.	climatic

Ballantyne, C.K.	1984	Quaternary Science Reviews	The Late Devensian Periglaciation of Upland Scotland	neutral
Dohrenwend, J.C.	1984	Quaternary Research	Nivation Landforms in the Western Great Basin and their Paleoclimatic Significance	climatic
Vryuein, B.I.	1985	Geomorfologiya	Cryogenic Landforms at the King George Island, Southern Shetland Islands.	neutral
Jones, P.F.	1985	Proceedings of the Geologists' Association	A Re-Appraisal of the Denudation Chronology of South Derbyshire, England	climatic
Vtyurin, B.I.	1985	Polar Geography and Geology	Cryogenic Landforms on King George Island, South Shetland Islands	climatic
Ballantyne, C.K.	1985	Scottish Geographical Magazine	Nivation Landforms and Snowpatch Erosion on Two Massifs in the Northern Highlands of Scotland	climatic
Tuckfield, C.G.	1986	Earth Surface Processes and Landforms	A Study of Dells in the New Forest, Hampshire, England	climatic
Youyu, X.	1986	Scientia Geographica Sinica	A Preliminary Study on Periglacial Landforms of the Taibaishan.	climatic
Rapp, A.	1986	Progress in Physical Geography	Slope Processes in High Latitude Mountains	climatic
Jaśkowski, B.	1986	Przegląd Geograficzny	Lithological and Structural Conditioning of the Cryoplanation Terraces on the Slopes of the Lysa Gora Massif in the Swietokrzyskie Mountains	neutral
French, H.M.	1987	Progress in Physical Geography	Periglacial Geomorphology in North America: Current Research and Future Trends	skeptical
Székely, A.	1987	Loess and periglacial phenomena. INQUA and IGU symposium, 1986	Nature and Extent of Periglacial Sculpturing of Relief in the Hungarian Mountains	climatic
Csorba, P.	1988	Studia Geomorphologica Carpatho-Balcanica	Problems of Cryoplanational Slope Evolution in the NW Part of the Tokaj Mountains	neutral
Gerrard, J.	1988	Physical Geography	Periglacial Modification of the Cox Tor—Staple Tors Area of Western Dartmoor, England	climatic
Coxon, P.	1988	Zeitschrift fur Geomorphologie, Supplementband	Remnant Periglacial Features on the Summit of Truskmore, Counties Sligo and Leitrim, Ireland	neutral

Yoshikawa, T.	1988	New Zealand Journal of Geology and Geophysics	Origin and Age of Erosion Surfaces in the Upper Drainage Basin of Waiapu River, Northeastern North Island, New Zealand	climatic
Clark, G.M.	1988	Geomorphology	Periglacial Geomorphology of the Appalachian Highlands and Interior Highlands South of the Glacial Border - A Review	climatic
Nelson, F.E.	1989	Geografiska Annaler, Series A	Cryoplanation Terraces: Periglacial Cirque Analogs	climatic
Czudek, T.	1989	Acta Scientiarum Naturalium - Academiae Scientiarum Bohemoslovacae Brno	Cryoplanation Terraces in Recent Permafrost	climatic
Göbel, P.	1989	Frankfurter Geowissenschaftliche Arbeiten, Serie D; Physische Geographie	Investigations of Cryoplanation Terraces in the Mountain-Tundra of Northern Norway and Finnish Lapland	neutral
Raczkowska, Z.	1990	Pirineos	Observations on Nivation and its Geomorphological Effects in Mountains at High Latitude (with Mt. Njulla Massif in Northern Sweden as Example)	climatic
Lauriol, B.	1990	Canadian Geographer	Cryoplanation Terraces, Northern Yukon	climatic
Karlstrom, E.T.	1990	Permafrost and Periglacial Processes	Relict Periglacial Features East of Waterton-Glacier Parks, Alberta and Montana, and their Palaeoclimatic Significance	climatic
Boardman, J.	1990	Progress in Physical Geography	Periglacial Geomorphology	neutral
Johnson, R.H.	1990	Journal of Quaternary Science	The Seal Edge Coombes, North Derbyshire — A Study of their Erosional and Depositional History	climatic
Grosso, S.A.	1991	Permafrost and Periglacial Processes	Cryoplanation Surfaces in the Central Andes at Latitude 35° S	climatic
Middlekauff, B.D.	1991	Physical Geography	Probable Paleoperiglacial Morphosequences in the Northern Blue Ridge	neutral
Wright, M.D.	1991	Geological Society Engineering Geology Special Publication	Pleistocene Deposits of the South Wales Coalfield and their Engineering Significance	climatic
Uredea, P.	1992	Permafrost and Periglacial Processes	Rock Glaciers and Periglacial Phenomena in the Southern Carpathians	climatic

Hall, K.	1992	South African Geographical Journal	A Discussion of the Need for Greater Rigour in Southern African Cryogenic Studies	skeptical
Clark, G.M.	1992	Periglacial geomorphology. Proc. 22nd annual symposium in geomorphology, Binghamton, 1991	Origin of Certain High-Elevation Local Broad Uplands in the Central Appalachians South of the Glacial Border, USA - A Paleoperiglacial Hypothesis	climatic
Lynch, A.J.J.	1992	Australian Journal of Botany	Pattern and Process in Alpine Vegetation and Landforms at Hill One, Southern Range, Tasmania	climatic
Czudek, T.	1993	Permafrost and Periglacial Processes	Pleistocene Periglacial Structures and Landforms in Western Czechoslovakia	climatic
Barsch, D.	1993	Geomorphology	Periglacial Geomorphology in the 21st Century	neutral
Bockheim, J.G.	1995	Permafrost and Periglacial Processes	Permafrost Distribution in the Southern Circumpolar Region and its Relation to the Environment: A Review and Recommendations for Further Research	climatic
Czudek, T.	1995	Geografiska Annaler, Series A	Cryoplanation Terraces - A Brief Review and Some Remarks	climatic
Lynch, A.J.J.	1995	Australian Journal of Botany	Pattern and Process in Alpine Vegetation and Landforms at Hill One, Southern Range, Tasmania	climatic
Hall, K.	1997	Permafrost and Periglacial Processes	Rock Temperatures and Implications for Cold Region Weathering. I: New Data from Viking Valley, Alexander Island, Antarctica	skeptical
Lauriol, B.M.	1997	Permafrost and Periglacial Processes	Weathering of Quartzite on a Cryoplanation Terrace in Northern Yukon, Canada	climatic
Hall, K.	1997	Antarctic Science	Observations on 'Cryoplanation' Benches in Antarctica	skeptical
Seppälä, M.	1997	Geomorphology	Piping Causing Thermokarst in Permafrost, Ungava Peninsula, Quebec, Canada	neutral
Zoltán, P.	1997	Foldrajzi Ertesito	Evolution and Types of Cryoplanation Surfaces in Tokaj Mountains	climatic
Hall, K.	1998	Polar Geography	Nivation or Cryoplanation: Different terms, Same Features?	climatic
Humlum, O.	1998	Permafrost and Periglacial Processes	Mountain Climate and Periglacial Phenomena in the Faeroe Islands	skeptical

Nelson, F.E.	1998	Geografiska Annaler, Series A: Physical Geography	Cryoplanation Terrace Orientation in Alaska	climatic
Lomborinchen, R.	1998	Permafrost and Periglacial Processes	Periglacial Processes and Physical (Frost) Weathering in Northern Mongolia	climatic
Lamirande, I.	1999	Canadian Journal of Earth Sciences	The Production of Silt on the Cryoplanation Terraces of the Richardson Mountains, Canada	climatic
French, H.M.	2000	Permafrost and Periglacial Processes	Does Lozinski's Periglacial Realm Exist Today? A Discussion Relevant to Modern Usage of the Term 'Periglacial'	neutral
Kunitsky, V.	2000	Polarforschung	Snow Patches in Nival Landscapes and their Role for the Ice Complex Formation in the Laptev Sea Coastal Lowlands	climatic
Traczyk, A.	2000	Acta Universitatis Carolinae, Geographica	Cold-Climate Landform Patterns in the Sudetes. Effects of Lithology, Relief and Glacial History	skeptical
Křížek, M.	2000	Acta Universitatis Carolinae, Geographica	Frost-Riven Cliffs and Cryoplanation Terraces in the Hostýnské Vrchy Hills (East Moravia, Czech Republic)	climatic
Schroder, H.	2000	Pirineos	Periglacial Morphology of Mt. Llullaillaco (Chile/Argentina)	climatic
Gualtieri, L.	2001	Arctic	The Age and Origin of the Little Diomedé Island Upland Surface	climatic
Migon, P.	2001	Zeitschrift für Geomorphologie	Inherited Landscapes of Britain-Possible Reasons for Survival	skeptical
Křížek, M.	2001	Acta Universitatis Carolinae, Geographica	The Quaternary Sculpturing of Sandstones in the Rusavská Hornatina Mountains	climatic
Oguchi, T.	2001	Chikei/Transactions, Japanese Geomorphological Union	Large-Scale Landforms and Hillslope Processes in Japan and Korea	neutral
Hall, K.	2002	South African Journal of Science	Review of Present and Quaternary Periglacial Processes and Landforms of the Maritime and Sub-Antarctic Region	neutral
Boelhouwers, J.C.	2002	South African Journal of Science	Quaternary Periglacial and Glacial Geomorphology of Southern Africa: Review and Synthesis	skeptical
Thorn, C.E.	2002	Progress in Physical Geography	Nivation and Cryoplanation: The Case for Scrutiny and Integration	climatic

French, H.	2003	Permafrost and Periglacial Processes	The Development of Periglacial Geomorphology: 1- up to 1965	skeptical
Thorn, C.E.	2003	Permafrost and Periglacial Processes	Making the Most of New Instrumentation	neutral
Křížek, M.	2003	Geografie-Sbornik CGS	Characteristic Features of Frost-Riven Cliffs: Comparison of Active Frost-Riven Cliffs in the World and (Non-Active) Frost-Riven Cliffs in the Rusavská Hornatina (Mountains)	climatic
Bernatchez, P.	2004	Geographie Physique et Quaternaire	A Review of Coastal Erosion Dynamics on Laurentian Maritime Quebec Coasts	climatic
Grab, S.	2005	Geomorphology	Controls on Basalt Terrace Formation in the Eastern Lesotho Highlands	skeptical
Worsley, P.	2005	Proceedings of the Geologists' Association	Martin Theodore Te Punga (1921-1989) and the Periglacial Legacy of Southern England	climatic
Munroe, J.S.	2006	Geomorphology	Investigating the Spatial Distribution of Summit Flats in the Uinta Mountains of Northeastern Utah, USA	climatic
Kuzmina, S.	2006	Quaternary Science Reviews	Some Features of the Holocene Insect Faunas of Northeastern Siberia	skeptical
Lauriol, B.	2006	Permafrost and Periglacial Processes	The Giant Steps of Bug Creek, Richardson Mountains, N.W.T., Canada	skeptical
Goodfellow, B.W.	2007	Earth-Science Reviews	Relict Non-Glacial Surfaces in Formerly Glaciated Landscapes	skeptical
Nelson, K.J.P.	2007	Permafrost and Periglacial Processes	Periglacial Appalachia: Palaeoclimatic Significance of Blockfield Elevation Gradients, Eastern USA	climatic
Bajgier-Kowalska, M.	2008	Catena	Lichenometric Dating of Landslide Episodes in the Western Part of the Polish Flysch Carpathians	neutral
Liaudat, D.T.	2008	Developments in Quaternary Science	Geocryology of Southern South America	climatic
Štěpančíková, P.	2008	Acta Geodynamica et Geomaterialia	Rock Landforms that Reflect Differential Relief Development in the North-Eastern Sector of the Rychlebské Hory and the Adjacent Area of Žulovská Pahorkatina (se Sudeten Mountains, Czech Republic)	climatic

Grab, S.W.	2009	Geografiska Annaler, Series A: Physical Geography	Spatial Associations Between Longest-Lasting Winter Snow Cover and Cold Region Landforms in the High Drakensberg, Southern Africa	neutral
Vočadlova, K.	2009	Moravian Geographical Reports	Comparison of Glacial Relief Landforms and the Factors which Determine Glaciation in the Surroundings of Černé Jezero Lake and Čertovo Jezero Lake (Šumava Mountains, Czech Republic)	climatic
Vočadlova, K.	2010	Antarctic Science	Some Further Observations Regarding "Cryoplanation Terraces" on Alexander Island	skeptical
Miller, S.R.	2010	Tectonics	Cenozoic Range-Front Faulting and Development of the Transantarctic Mountains near Cape Surprise, Antarctica: Thermochronologic and Geomorphologic Constraints	climatic
Demek, J.	2010	Moravian Geographical Reports	Relict Cryoplanation and Nivation Landforms in the Czech Republic: A Case Study of the Sýkorská Hornatina Mountains	climatic
Křížek, M.	2010	Czasopismo Geograficzne	Are the Highest Parts of the Sudetes Above the Upper Timber Line a Periglacial Domain?	neutral
Francelino, M.R.	2011	Catena	Geomorphology and Soils Distribution Under Paraglacial Conditions in an Ice-Free Area of Admiralty Bay, King George Island, Antarctica	neutral
Margold, M.	2011	Geografiska Annaler, Series A: Physical Geography	Snowpatch Hollows and Pronival Ramparts in the Krkonoše Mountains, Czech Republic: Distribution, Morphology and Chronology of Formation	climatic
Bronguleyev, V.V.	2011	Geomorfologiya	3-D Cinematic Model of Slope Evolution	neutral
Pawelec, H.	2011	Geomorphology	Periglacial Evolution of Slopes - Rock Control Versus Climate Factors (Cracow Upland, S. Poland)	skeptical
Schirrmeister, L.	2011	Quaternary International	Sedimentary Characteristics and Origin of the Late Pleistocene Ice Complex on North-East Siberian Arctic Coastal Lowlands and Islands - A Review	climatic

Starkel, L.	2011	Geografia Fisica e Dinamica Quaternaria	Shifting of Climatic-Vegetation Belts in Eurasian Mountains and their Expression in Slope Evolution	climatic
Obu, J.	2011	Dela	Periglacial and Glacial Landforms in Western Part of Pohorje Mountains	climatic
Gillespie, A.R.	2011	Encyclopedia of Earth Sciences Series	Glacial Geomorphology and Landforms Evolution	climatic
Guglielmin, M.	2012	Geomorphology	Advances in Permafrost and Periglacial Research in Antarctica: A Review	skeptical
Evans, D.J.A.	2012	Quaternary Science Reviews	The Glaciation of Dartmoor: The Southernmost Independent Pleistocene Ice Cap in the British Isles	climatic
Rączkowska, Z.	2012	Recent Landform Evolution: The Carpatho-Balkan-Dinaric Region	Recent Landform Evolution in the Polish Carpathians	neutral
Hall, K.	2013	Geological Society Special Publication	Periglacial Processes and Landforms of the Antarctic: A Review of Recent Studies and Directions	neutral
Goodfellow, B.W.	2013	Treatise on Geomorphology	Hillslope Processes in Cold Environments: An Illustration of High-Latitude Mountain and Hillslope Processes and Forms	skeptical
Rixhon, G.	2013	Treatise on Geomorphology	Evolution of Slopes in a Cold Climate	neutral
Hall, K.	2013	Treatise on Geomorphology	Mechanical Weathering in Cold Regions	skeptical
Orme, A.R.	2013	Treatise on Geomorphology	Denudation, Planation, and Cyclicity: Myths, Models, and Reality	climatic
Łajczak, A.	2014	Quaestiones Geographicae	Relief Development of the Babia Góra Massif, Western Carpathian Mountains	climatic
Pánek, T.	2014	Landslides	Large Late Pleistocene Landslides from the Marginal Slope of the Fylsch Carpathians	climatic
Calvet, M.	2015	Geomorphology	Flat-Topped Mountain Ranges: Their Global Distribution and Value for Understanding the Evolution of Mountain Topography	skeptical

Harrison, S.	2015	Journal of Quaternary Science	The Southernmost Quaternary Niche Glacier System in Great Britain	climatic
French, H.M.	2016	Permafrost and Periglacial Processes	Do Periglacial Landscapes Exist? A Discussion of the Upland Landscapes of Northern Interior Yukon, Canada	skeptical
Nešić, D.	2017	Carpathian Journal of Earth and Environmental Sciences	Relict Cryoplanation Terraces of Central Kopaonik (Serbia)	neutral
Nelson, F.E.	2017	Geomorphology	Periglacial Cirque Analogs: Elevation Trends of Cryoplanation Terraces in Eastern Beringia	climatic
Giles, D.P.	2017	Geological Society Engineering Geology Special Publication	Geomorphological Framework: Glacial and Periglacial Sediments, Structures and Landforms	neutral
Evans, D.J.A.	2017	Journal of Maps	Periglacial Geomorphology of Summit Tors on Bodmin Moor, Cornwall, SW England	climatic
Astakhov, V.I.	2018	Boreas	Late Quaternary Glaciation of the Northern Urals: A Review and New Observations	neutral
Mather, A.E.	2018	Progress in Physical Geography	Automated Mapping of Relict Patterned Ground: An Approach to Evaluate Morphologically Subdued Landforms Using Unmanned-Aerial-Vehicle and Structure-from-Motion Technologies	neutral

APPENDIX B

Chapter 3 Supplementary Materials

Appendix B.1. Fracture count data.

	Surface Fracture	< 30% Mass Lost	No Fracture	Total Count
Skookum Pass				
T1 A	43	2	35	80
T1 B	28	3	31	62
T1 C	21	1	14	36
T2 A	89	5	28	122
T2 B	52	5	27	84
T2 C	4	0	9	13
Control A	40	1	23	64
Control B	50	1	11	62
Control C	64	0	20	84
Eagle Summit				
T6 A	69	12	79	160
T6 B	3	0	10	13
T6 C	11	0	12	23
T9 A	86	6	6	98
T9 B	72	2	13	87
T9 C	51	0	38	89
T10 A	89	4	35	128
T10 B	69	4	56	129
T10 C	15	1	25	41
Control A	26	3	13	42
Control B	29	0	20	49
Control C	21	2	10	33
Mt. Fairplay				
T25 A	29	4	19	52
T25 B	24	0	43	67
T25 C	7	0	16	23
T23 A	40	3	18	61
T23 B	42	0	9	51
T23 C	5	0	17	22
T20 A	23	6	17	46
T20 B	15	0	40	55
T20 C	19	1	29	49
Control A	9	0	72	81
Control B	2	1	51	54
Control C	5	1	46	52

Appendix B.2. Summary and ANOVA statistics for roundness.

	\bar{X}	Median	σ	Range	Shapiro-Wilk ¹	Levene's ²	ANOVA F-Ratio	Tukey's HSD Q Statistic	
								A	B
<i>Skookum Pass</i>									
T1 A	91.75	81.67	56.64	233.05				X	X
T1 B	157.88	151.92	63.37	319.19	0.96***	5.03**	18.30***	6.42**	X
T1 C	175.29	162.28	91.53	414.77				8.11**	1.69
T2 A	87.78	73.62	51.32	233.05				X	X
T2 B	93.76	85.14	45.17	195.63	0.93***	1.53	11.67***	0.80	X
T2 C	134.63	120.00	59.28	292.86				6.28**	5.48**
Control A	75.00	71.43	36.66	159.87				X	X
Control B	82.61	65.94	49.56	265.51	0.84***	5.91**	8.20***	0.90	X
Control C	120.10	100.00	81.52	457.32				5.35**	4.45**
<i>Eagle Summit</i>									
T6 A	112.86	93.07	64.11	253.48				X	X
T6 B	127.10	111.71	60.90	251.97	0.95***	7.55*	19.158***	1.26	X
T6 C	204.98	195.24	105.11	436.46				8.13**	6.87**
T9 A	51.75	40.41	34.64	157.89				X	X
T9 B	61.65	53.34	35.67	136.25	0.93***	23.49***	22.88***	1.37	X
T9 C	115.90	90.91	72.05	269.98				8.88**	7.51**
T10 A	113.63	99.18	57.12	251.19				X	X
T10 B	143.60	127.05	84.68	354.31	0.96***	3.37*	23.71***	2.64	X
T10 C	220.61	216.69	91.92	466.10				9.44**	6.79**
Control A	78.70	73.40	44.18	212.53				X	X
Control B	85.36	79.71	49.37	274.40	0.91***	0.06	2.37	0.99	X
Control C	65.02	50.86	47.88	215.08				2.03	3.02
<i>Mt. Fairplay</i>									
T25 A	148.56	128.97	92.81	397.44				X	X
T25 B	156.66	160.00	77.89	313.34	0.93***	0.94	0.58	0.08	X
T25 C	229.46	210.41	90.82	408.99				1.28	1.35
T23 A	67.98	61.55	33.82	142.77				X	X
T23 B	91.32	88.24	38.51	182.80	0.98*	0.53	14.07***	4.41**	X
T23 C	107.51	103.57	38.70	165.52				7.46**	3.06
T20 A	194.84	187.67	104.12	420.88				X	X
T20 B	193.56	163.85	131.07	556.84	0.93***	0.54	12.73***	0.65	X
T20 C	216.28	212.32	115.54	686.50				6.48**	5.83**
Control A	144.39	108.19	114.91	461.29				X	X
Control B	169.66	116.52	172.32	1120.51	0.70***	1.99	2.06	1.38	X
Control C	117.19	82.21	79.12	300.00				1.49	2.87

¹Asterisks indicate p -values <0.05 (*), <0.01 (**), and <0.001 (***)

²Levene's Test based on the mean reported.

Appendix B.3. Summary and ANOVA statistics for flatness.

	\bar{X}	Median	σ	Range	Shapiro-Wilk ¹	Levene's ²	ANOVA F-Ratio	A	B
<i>Skookum Pass</i>									
T1 A	364.40	350.00	165.37	750.71				X	X
T1 B	286.98	287.50	88.13	311.87	0.94***	4.59*	6.08**	4.22**	X
T1 C	285.04	269.54	120.26	513.00				4.32**	0.12
T2 A	376.09	336.06	152.08	608.97				X	X
T2 B	469.82	417.76	221.11	855.00	0.94***	3.90**	4.73**	3.25	X
T2 C	495.05	452.98	223.87	900.00				4.13*	0.88
Control A	395.58	316.59	244.85	1265.63				X	X
Control B	480.88	396.88	262.38	1097.62	0.884***	0.406	1.55	2.40	X
Control C	418.41	374.18	238.17	1121.21				0.64	1.76
<i>Eagle Summit</i>									
T6 A	441.87	374.10	194.04	994.81				X	X
T6 B	518.31	471.78	219.85	908.89	0.93***	5.36**	13.81***	2.89	X
T6 C	323.15	286.67	130.26	497.56				4.49**	7.37**
T9 A	482.10	369.17	348.11	2019.44				X	X
T9 B	390.89	304.91	217.47	1190.71	0.69***	5.74**	10.11***	2.59	X
T9 C	259.53	220.94	116.48	482.14				6.32**	3.73*
T10 A	519.69	424.17	302.19	1365.54				X	X
T10 B	363.83	327.70	149.09	722.07	0.84***	5.97**	9.64***	4.75**	X
T10 C	328.03	247.50	211.72	1005.36				5.84**	1.09
Control A	714.62	603.77	361.83	1597.44				X	X
Control B	725.31	589.69	465.78	2544.29	0.88***	4.66*	1.83	0.16	X
Control C	879.88	760.71	582.56	3087.50				2.42	2.26
<i>Mt. Fairplay</i>									
T25 A	279.76	244.74	141.41	587.50				X	X
T25 B	294.97	267.71	117.30	496.22	0.80***	0.82	1.79	2.67	X
T25 C	230.33	220.10	64.52	279.72				1.37	1.30
T23 A	280.88	258.71	109.98	497.37				X	X
T23 B	318.20	313.25	99.82	394.69	0.95***	1.64	12.42***	2.32	X
T23 C	392.24	366.67	126.30	555.95				6.93**	4.60**
T20 A	210.15	186.10	95.98	394.27				X	X
T20 B	248.80	208.12	119.60	715.63	0.89***	5.94**	4.43*	0.95	X
T20 C	229.95	209.57	85.09	412.75				3.08	4.02*
Control A	356.42	303.75	204.29	1192.92				X	X
Control B	282.61	256.35	144.47	969.32	0.75***	2.75	2.44	2.93	X
Control C	343.05	288.19	175.29	1008.70				0.53	2.40

¹Asterisks indicate p -values <0.05 (*), <0.01 (**), and <0.001 (***).

²Levene's Test based on the mean reported.

Appendix B.4. Summary and ANOVA statistics for sphericity.

	\bar{X}	Median	σ	Range	Shapiro -Wilk ¹	Levene's ²	ANOVA F-Ratio	A	B
<i>Skookum Pass</i>									
T1 A	0.54	0.54	0.11	0.52				X	X
T1 B	0.54	0.54	0.09	0.49	0.99	0.54	1.23	0.38	X
T1 C	0.57	0.56	0.10	0.49				2.09	1.70
T2 A	0.48	0.47	0.07	0.35				X	X
T2 B	0.47	0.47	0.10	0.49	0.99	3.36*	10.67***	0.45	X
T2 C	0.55	0.55	0.10	0.48				5.42**	5.87**
Control A	0.52	0.55	0.12	0.45				X	X
Control B	0.48	0.46	0.11	0.49	0.98	1.69	1.91	2.76	X
Control C	0.50	0.51	0.10	0.39				1.31	1.46
<i>Eagle Summit</i>									
T6 A	0.44	0.43	0.09	0.35				X	X
T6 B	0.42	0.43	0.10	0.49	0.97**	2.23	11.53***	1.17	X
T6 C	0.52	0.48	0.12	0.58				5.21**	6.38**
T9 A	0.42	0.45	0.10	0.50				X	X
T9 B	0.43	0.43	0.09	0.36	0.99	2.8	28.99***	0.87	X
T9 C	0.56	0.57	0.13	0.54				9.73**	8.86**
T10 A	0.41	0.41	0.08	0.38				X	X
T10 B	0.46	0.46	0.08	0.41	0.99	4.31*	31.94***	3.05	X
T10 C	0.57	0.57	0.12	0.51				10.95**	7.90**
Control A	0.43	0.43	0.10	0.43				X	X
Control B	0.42	0.41	0.08	0.42	0.92***	2.28	1.10	1.16	X
Control C	0.40	0.38	0.13	0.76				2.09	0.93
<i>Mt. Fairplay</i>									
T25 A	0.59	0.58	0.12	0.57				X	X
T25 B	0.53	0.53	0.07	0.36	0.99	2.41	2.62	2.60	X
T25 C	0.62	0.61	0.09	0.39				2.97	0.38
T23 A	0.55	0.55	0.09	0.39				X	X
T23 B	0.52	0.50	0.09	0.35	0.98	0.92	5.34**	2.84	X
T23 C	0.50	0.48	0.08	0.31				4.58**	1.74
T20 A	0.67	0.69	0.14	0.55				X	X
T20 B	0.62	0.61	0.12	0.54	0.99	4.20*	11.11***	4.27**	X
T20 C	0.62	0.61	0.11	0.45				2.30	6.57**
Control A	0.52	0.52	0.10	0.51				X	X
Control B	0.55	0.55	0.07	0.37	0.99	4.09*	1.90	2.13	X
Control C	0.51	0.53	0.10	0.43				0.44	2.58

¹Asterisks indicate p -values <0.05 (*), <0.01 (**), and <0.001 (***).

²Levene's Test based on the mean reported.

Appendix B.5. Summary and ANOVA statistics for Schmidt hammer rebound.

	\bar{X}	Median	σ	Range	Shapiro -Wilk ¹	Levene's	ANOVA F-Ratio	A	B
<i>Skookum Pass</i>									
T1 A	38.09	39.00	8.60	44.60				X	X
T1 B	34.35	33.60	10.09	37.80	0.99	1.97	7.03**	2.96	X
T1 C	31.40	29.90	7.68	33.60				5.29**	2.34
T2 A	27.52	27.20	8.29	39.20				X	X
T2 B	24.58	25.60	9.64	37.60	0.95***	2.75	3.69*	2.03	X
T2 C	21.97	19.50	12.05	45.20				3.84*	1.81
Control A	30.09	31.90	11.15	38.40				X	X
Control B	24.15	24.50	10.51	37.20	0.96***	1.37	3.24*	3.60*	X
Control C	26.91	27.20	12.90	45.40				1.93	1.67
<i>Eagle Summit</i>									
T6 A	34.77	32.80	11.06	45.40				X	X
T6 B	35.10	37.00	9.81	44.00	0.99	1.77	19.70***	0.23	X
T6 C	45.88	45.70	8.93	41.40				7.80**	7.57**
T9 A	25.89	26.00	9.34	37.60				X	X
T9 B	27.10	27.30	9.43	34.20	0.99	0.93	50.26***	0.85	X
T9 C	43.94	42.60	11.02	52.00				12.68**	11.83**
T10 A	47.36	47.20	9.13	36.20				X	X
T10 B	44.16	44.60	7.27	31.40	0.93***	1.95	6.80**	2.28	X
T10 C	51.46	52.60	12.35	68.37				2.92	5.20**
Control A	23.92	22.50	9.16	37.60				X	X
Control B	25.96	24.70	8.78	39.00	0.96***	0.43	0.77	1.58	X
Control C	24.08	23.70	9.18	53.60				0.12	1.46
<i>Mt. Fairplay</i>									
T25 A	48.35	47.20	9.04	36.20				X	X
T25 B	34.30	33.70	9.57	41.00	0.99	3.15*	50.79***	14.09**	X
T25 C	40.47	40.10	9.92	45.20				8.89**	5.21**
T23 A	36.78	36.00	8.57	32.00				X	X
T23 B	35.68	36.00	9.34	49.80	0.99	0.92	14.88***	0.82	X
T23 C	27.32	27.60	10.17	37.20				7.05**	6.23**
T20 A	48.70	48.50	6.87	28.00				X	X
T20 B	31.09	31.30	10.18	47.60	0.98	1.42	26.85***	10.34**	X
T20 C	37.60	37.30	8.85	33.20				5.79**	4.54**
Control A	34.51	34.10	15.68	54.20				X	X
Control B	33.99	32.90	13.12	50.80	0.96**	2.40	1.30	0.25	X
Control C	30.22	28.80	14.17	47.60				2.09	1.83

¹Asterisks indicate p -values <0.05 (*), <0.01 (**), and <0.001 (***).

²Levene's Test based on the mean reported.

Appendix B.6. Summary and ANOVA statistics for maximum weathering rind thickness.

	\bar{X}	Median	σ	Range	Shapiro -Wilk ¹	Levene's ²	ANOVA F-Ratio	A	B
<i>Skookum Pass</i>									
T1 A	5.93	6.25	3.37	12.50				X	X
T1 B	11.97	12.00	5.83	24.00	0.96***	8.82***	16.84***	7.08**	X
T1 C	12.02	10.00	7.86	33.00				7.14**	0.06
T2 A	1.33	0.00	2.41	14.00				X	X
T2 B	2.27	2.00	2.03	8.50	0.81***	4.07*	2.49	2.63	X
T2 C	2.34	1.00	2.96	10.00				2.83	0.20
Control A	6.00	5.00	6.11	26.50				X	X
Control B	2.19	0.00	3.02	14.00	0.87***	8.53***	9.52***	5.81**	X
Control C	2.92	0.00	4.09	13.00				4.70**	1.11
<i>Eagle Summit</i>									
T6 A	4.07	2.25	4.92	20.00				X	X
T6 B	4.64	2.75	6.75	32.00	0.79***	0.11	5.33**	0.68	X
T6 C	7.65	6.25	5.68	28.00				4.30**	3.61*
T9 A	2.94	2.00	4.34	25.00				X	X
T9 B	4.12	3.00	3.15	15.00	0.82***	8.79***	10.67***	1.74	X
T9 C	7.24	4.50	6.26	30.00				6.32**	4.59**
T10 A	5.60	1.50	9.69	34.00				X	X
T10 B	6.52	3.75	7.16	24.00	0.82***	1.18	0.73	0.82	X
T10 C	7.51	7.25	6.21	23.00				1.71	0.89
Control A	3.36	2.00	4.04	17.00				X	X
Control B	3.06	2.00	3.58	18.00	0.84***	4.60*	2.82	0.63	X
Control C	1.84	1.00	2.15	8.00				3.17	2.55
<i>Mt. Fairplay</i>									
T25 A	1.45	0.25	1.83	6.00				X	X
T25 B	2.78	2.00	3.14	13.00	0.86***	9.43***	22.60***	2.86	X
T25 C	5.57	4.00	4.31	21.00				8.86**	6.00**
T23 A	2.04	2.00	1.40	7.00				X	X
T23 B	2.34	2.00	1.87	12.00	0.87***	1.17	0.96	1.26	X
T23 C	2.50	2.00	1.70	8.00				1.93	0.67
T20 A	1.27	0.00	1.64	6.00				X	X
T20 B	3.23	2.75	2.53	13.50	0.81***	5.31**	20.46***	4.99**	X
T20 C	5.00	4.00	3.68	16.00				9.50**	4.51**
Control A	2.96	2.00	2.42	10.00				X	X
Control B	2.90	3.00	1.77	7.00	0.93***	1.14	0.12	0.20	X
Control C	2.76	2.00	2.08	9.00				0.66	0.46

¹Asterisks indicate *p*-values <0.05 (*), <0.01 (**), and <0.001 (***).

²Levene's Test based on the mean reported.

APPENDIX C

Chapter 4 Supplementary Materials

Appendix C.1. Field sampling documentation for TCN geochronology.

Sample No.: T6-A

Collection Date: June 27th, 2017

Time: 17:00 (Alaska Standard Time)

Coordinates: 65.4674° N, 145.3783° W (± 10 m)

Elevation: 1244 m.a.s.l. (± 10 m)

Context: Scarp tread junction of terrace

Physical Characteristics:

Size: 40 x 37 x 26 cm

Shape: angular equant

Lithology: Quartzite

Color: (Munsell)

Exposed: 10YR 8/1

Buried: 7.5 YR 5/4

Grain Size: coarse

Lichen Cover: ~40% cover

Visible Cracks: none

Emergent Veins: none

Weathering Pits: none

Other:

Topographic Shielding:

N: -1°

NE: 8°

E: 15°

SE: 11°

S: 0°

SW: -1°

W: 0°

NW: 0°

Sample/Fragments Thickness:

4 fragments

4 – 5 cm thickness from surface



Sample No.: T6-B

Collection Date: June 27th, 2017

Time: 16:40 (Alaska Standard Time)

Coordinates: 65.4652° N, 145.3635° W (± 5 m)

Elevation: 1243 m.a.s.l. (± 5 m)

Context: Edge of felsenmeer or talus from scarp

Physical Characteristics:

Size: ~1.5 x 0.5 x 0.5 m

Shape: subangular ellipsoidal

Lithology: Quartzite

Color: (Munsell)

Exposed: 10YR 8/1

Buried: 7.5YR 4/4

Grain Size: coarse

Lichen Cover: ~70% cover

Visible Cracks: none

Emergent Veins: none

Weathering Pits: none

Other:

Topographic Shielding:

N: -1°

NE: 5°

E: 7°

SE: 4°

S: 0°

SW: -1°

W: 1°

NW: 0°

Sample/Fragments Thickness:

3 fragments

2.5 – 4.5 cm thickness from surface



Sample No.: T6-C

Collection Date: June 27th, 2017

Time: 16:15 (Alaska Standard Time)

Coordinates: 65.4665° N, 145.3688° W (± 5 m)

Elevation: 1221 m.a.s.l. (± 5 m)

Context: Outer edge of terrace

Physical Characteristics:

Size: 45 x 21 x 16 cm

Shape: subrounded tabular

Lithology: Quartzite

Color: (Munsell)

Exposed: 10YR 8/1

Buried: 10YR 4/2

Grain Size: coarse

Lichen Cover: ~40%

Visible Cracks: few 1 - 2 cm depth

Emergent Veins: none

Weathering Pits: none

Other:

Topographic Shielding: N: 0°

NE: 1°

E: 2°

SE: 1°

S: 1°

SW: 0°

W: 1°

NW: 1°

Sample/Fragments Thickness:

2 fragments

5 cm thickness from surface



**Photo taken after breaking the rock*

Sample No.: T10-A

Collection Date: June 28th, 2017

Time: 14:00 (Alaska Standard Time)

Coordinates: 65.4652° N, 145.363° W (± 5 m)

Elevation: 1141 m.a.s.l. (± 5 m)

Context: Scarp tread junction of terrace

Physical Characteristics:

Size: 35 x 29 x 24 cm

Shape: subangular equant

Lithology: Quartzite

Color: (Munsell)

Exposed: 7.5YR 8/0

Buried: 10YR 6/4

Grain Size: coarse

Lichen Cover: ~50% cover

Visible Cracks: none

Emergent Veins: none

Weathering Pits: none

Other:

Topographic Shielding:

N: 4°

NE: 21°

E: 25°

SE: 12°

S: 2°

SW: -1°

W: 2°

NW: 2°

Sample/Fragments Thickness:

3 fragments

3 – 5 cm thickness from surface



**Photos taken after breaking the rock*

Sample No.: T10-B

Collection Date: June 28th, 2017

Time: 14:20 (Alaska Standard Time)

Coordinates: 65.4675°N, 145.3789°W (± 5 m)

Elevation: 1137 m.a.s.l. (± 5 m)

Context: Edge of felsenmeer or talus from scarp

Physical Characteristics:

Size: 47 x 23 x 22 cm

Shape: subangular ellipsoidal

Lithology: Quartzite

Color: (Munsell)

Exposed: 7.5YR 8/0

Buried: 10 YR 7/6

Grain Size: coarse

Lichen Cover: ~50% cover

Visible Cracks: none

Emergent Veins: none

Weathering Pits: none

Other:

Topographic Shielding:

N: 3°

NE: 6°

E: 20°

SE: 11°

S: 1°

SW: -1°

W: 1°

NW: 1°

Sample/Fragments Thickness:

4 fragments and several chips

<1 – 4 cm thickness from surface



**Photo taken after breaking the rock*

Sample No.: T10-C

Collection Date: June 28th, 2017

Time: 14:55 (Alaska Standard Time)

Coordinates: 65.4681° N, 145.3825° W (± 5 m)

Elevation: 1113 m.a.s.l. (± 5 m)

Context: Outer edge of terrace

Physical Characteristics:

Size: 54 x 49 x 40 cm

Shape: Angular Equant

Lithology: Quartzite

Color: (Munsell)

Exposed: 7.5YR 8/0

Buried: 10YR 6/6

Grain Size: coarse

Lichen Cover: ~50% cover

Visible Cracks: none

Emergent Veins: none

Weathering Pits: none

Other:

Topographic Shielding:

N: -1°

NE: 3°

E: 9°

SE: 3°

S: 2°

SW: -1°

W: 1°

NW: 1°

Sample/Fragments Thickness:

4 fragments

1 - 5 cm thickness from surface



Sample No.: T25-A

Collection Date: July 13th, 2017

Time: 16:49 (Alaska Standard Time)

Coordinates: 63.6785°N, 142.2125°W (± 5 m)

Elevation: 1571 m.a.s.l. (± 5 m)

Context: Bedrock scarp tread junction of terrace

Physical Characteristics:

Size: bedrock

Shape: angular bedrock

Lithology: intermediate/mafic volcanic rock

Color:

Exposed: 10YR 6/3

Interior: 7.5YR 4/0

Grain Size: 0.5 – 4 mm crystals in fine matrix

Lichen Cover: ~50%

Visible Cracks:

Numerous, ~2–30 cm deep, ~15–100 cm long

Emergent Veins: none

Weathering Pits: none

Other:

Topographic Shielding:

N: 0°

NE: 1°

E: 1°

SE: 27°

S: 30°

SW: 29°

W: 11°

NW: -1°

Sample/Fragments Thickness:

1 fragment

17.5 cm thickness from surface



Sample No.: T25-B

Collection Date: July 13th, 2017

Time: 17:40 (Alaska Standard Time)

Coordinates: 63.6794°N, 142.2117°W (±5 m)

Elevation: 1564 m.a.s.l. (±5 m)

Context: Edge of or talus from scarp

Physical Characteristics:

Size: 1 x 0.5 x 0.5 m

Shape: Subrounded equant

Lithology: intermediate/mafic volcanic rock

Color: (Munsell)

Exposed: 7.5YR 7/0

Interior: 7.5RY 5/0

Grain Size: 0.5 – 3 mm crystals

Lichen Cover: ~40%

Visible Cracks:

Several, ~1-3 cm deep, ~20-30 cm long

Emergent Veins: none

Weathering Pits: none

Other:

Topographic Shielding:

N: -1°

NE: -1°

E: -1°

SE: 1°

S: 6°

SW: 16°

W: 1°

NW: -1°

Sample/Fragments Thickness:

2 fragments

9 cm, and 3.5 cm thickness from surface



Sample No.: T25-C

Collection Date: July 13th, 2017

Time: 17:10 (Alaska Standard Time)

Coordinates: 63.6810°N, 142.2108°W (± 10 m)

Elevation: 1532 m.a.s.l. (± 10 m)

Context: outer edge of terrace

Physical Characteristics:

Size: ~ 1 x 1 x 0.5 m

Shape: Subangular equant

Lithology: intermediate/mafic volcanic rock

Color: (Munsell)

Exposed: 7.5YR 6/2

Interior: 7.5YR 4/0

Grain Size: 0.5 – 4 mm crystals

Lichen Cover: ~30%

Visible Cracks: None

Emergent Veins: None

Weathering Pits: None

Other:

Topographic Shielding:

N: 0°

NE: -1°

E: -1°

SE: -1°

S: 4°

SW: 12°

W: 8°

NW: 6°

Sample/Fragments Thickness:

1 fragment

6.5 cm thickness from surface



Sample No.: T20-A

Collection Date: July 14th, 2017

Time: 15:57 (Alaska Standard Time)

Coordinates: 63.6884° N, 142.2103° W (± 5 m)

Elevation: 1389 m.a.s.l. (± 5 m)

Context: Bedrock scarp tread junction of terrace



Physical Characteristics:

Size: bedrock

Shape: angular bedrock

Lithology: Rhyolite (felsic volcanic rock)

Color: (Munsell)

Exposed: 7.5YR 8/0

Interior: 7.5YR4/2

Grain Size: crystals from 1 – 3 cm

Lichen Cover: ~30%

Visible Cracks: many, 10 – 35 cm depth

Emergent Veins: none

Weathering Pits: none

Other:

Topographic Shielding:

N: -1°

NE: -1°

E: -1°

SE: 9°

S: 21°

SW: 22°

W: 3°

NW: -1°

Sample/Fragments Thickness:

1 fragment

10 cm thickness from surface

Sample No.: T20-B

Collection Date: Just 14th, 2017

Time: 16:25 (Alaska Standard Time)

Coordinates: 63.6888°N, 142.2098°W (± 5 m)

Elevation: 1385 m.a.s.l. (± 5 m)

Context: Edge of felsenmeer or talus from scarp

Physical Characteristics:

Size: 51 x 48 x 28 cm

Shape: rounded ellipsoidal

Lithology: intermediate/felsic

Color: (Munsell)

Exposed: 10YR 8/1

Interior: 7.5YR 4/0

Grain Size: 2 – 12 mm crystals

Lichen Cover: ~60%

Visible Cracks: one, ~3 cm depth

Emergent Veins: none

Weathering Pits: none

Other: lithic fragments of potassium feldspar



Topographic Shielding:

N: -1°

NE: -1°

E: -1°

SE: 0°

S: 5°

SW: 9°

W: 4°

NW: -1°

Sample/Fragments Thickness:

1 fragment

12 cm thickness from surface

Sample No.: T20-C

Collection Date: July 15th, 2017

Time: 11:19 (Alaska Standard Time)

Coordinates: 63.6895°N, 142.2086°W (± 5 m)

Elevation: 1376 m.a.s.l. (± 5 m)

Context: Outer edge of terrace,
boulder at the top of a stone stripe

Physical Characteristics:

Size: 80 x 80 x 65 cm

Shape: Subangular irregular shape

Lithology: intermediate/mafic volcanic rock

Color: (Munsell)

Exposed: 7.5YR 4/0

Interior: 7.5YR 5/0

Grain Size: 1-4 mm crystals

Lichen Cover: ~ 40%

Visible Cracks: none

Emergent Veins: none

Weathering Pits: none

Other:

Topographic Shielding:

N: -1°

NE: -1°

E: -1°

SE: 6°

S: 7°

SW: 11°

W: 6°

NW: 0°

Sample/Fragments Thickness:

1 fragment

16.5 cm thickness from surface



Appendix C.2. Lab protocol for ^{10}Be target preparation.

Target preparation was performed at the University of Cincinnati ^{10}Be geochronology labs. Samples were crushed, pulverized, and sieved into $> 500\ \mu\text{m}$, $250 - 500\ \mu\text{m}$, and $< 250\ \mu\text{m}$ particle size fractions (fraction weights for each sample are reported in Appendix C.4). The $250 - 500\ \mu\text{m}$ fraction was used for subsequent chemical preparation and the $> 500\ \mu\text{m}$ fraction was retained for further pulverizing if more sample was required. Samples were leached with aqua regia (HCl/HNO_3) for 12 to 24 hours to remove carbonates, phosphates, and organics. Samples were run through a Franz Magnetic Barrier Separator, despite their relatively few magnetic grains. After, in order to etch the quartz surface to remove meteoric ^{10}Be and to dissolve other silicates, samples were leached in a 5% followed by 1% solution of HF/HNO_3 for approximately 24 hours on hot-rollers. Quartz was separated from feldspars and other heavy minerals in the remaining sample using lithium polytungstate ($\sim 2.67\ \text{g}/\text{cm}^3$ LST) in gravity separation funnels. The quality of the quartz was tested and confirmed. About ~ 15 to 20 grams of quartz were then weighed and ^9Be carrier was added (amounts reported in Table 6) to the quartz sample and then dissolved in concentrated HF and HNO_3 . After the sample was dissolved and volume reduced, NaOH was added to precipitate out Fe and Ti in solution. Al and Be were precipitated as hydroxide gels with HNO_3 and NH_4OH . The hydroxide gels were dissolved with Oxalic acid and beryllium was then separated from the sample using cation exchange columns. The resulting beryllium gel was ignited at $750\ ^\circ\text{C}$ for 20 minutes yielding beryllium oxide. Niobium binder was mixed with the beryllium oxide and loaded into steel cathodes for accelerator mass spectrometry at the Purdue University PRIME lab. Measured ratios of $^{10}\text{Be}/^9\text{Be}$ and subsequent ages reported were corrected based on a chemical blank prepared alongside the samples.

Appendix C.3. Lab protocol for ^{36}Cl target preparation.

Whole rock target preparation was performed at the University of Cincinnati ^{36}Cl geochronology labs. A sledge hammer and rock saw were used to break samples and then only the uppermost 5 cm from exposed surfaces of the boulders were considered. Samples were crushed, pulverized, and sieved into $> 500 \mu\text{m}$, $250 - 500 \mu\text{m}$, and $< 250 \mu\text{m}$ particle size fractions (fraction weights for each sample reported in Appendix C.4). The $250 - 500 \mu\text{m}$ fraction was used for subsequent chemical preparation and the $> 500 \mu\text{m}$ fraction was retained for further pulverizing if more $250-500 \mu\text{m}$ sample was required. Approximately 100 g of the $250-500 \mu\text{m}$ fraction of the sample was leached using 10% trace metal grade (TMG) nitric acid for 12 to 24 hours three times and then decanted, rinsed with deionized water, and dried. Aliquots of approximately 10 g of the leached sample as well of the pre-leached sample were isolated and sent to Activation Laboratories Limited in Ancaster, Ontario, for geochemical analysis of major elements, uranium, thorium, and gamma emission spectrometry of boron and gadolinium. Chloride dilution spike carrier was added (amounts reported in Table 7) to approximately 30 g of the leached sample and dissolved in hydrofluoric and nitric acid TMG solution. Fluorites and sulfates were removed, and Cl was isolated from the solution through precipitation of silver chloride via the addition of silver nitrate. The Cl was finally extracted by passing the sample through anion columns, and drying for approximately eight hours at 65°C . The isolated chlorine was loaded into copper cathodes for accelerator mass spectrometry at the Purdue University PRIME lab. Measured $^{36}\text{Cl}/^{35}\text{Cl}$ ratios and subsequent ages reported were corrected based on a blank and direct measurement of the chemical blank with ^{35}Cl carrier prepared alongside the samples.

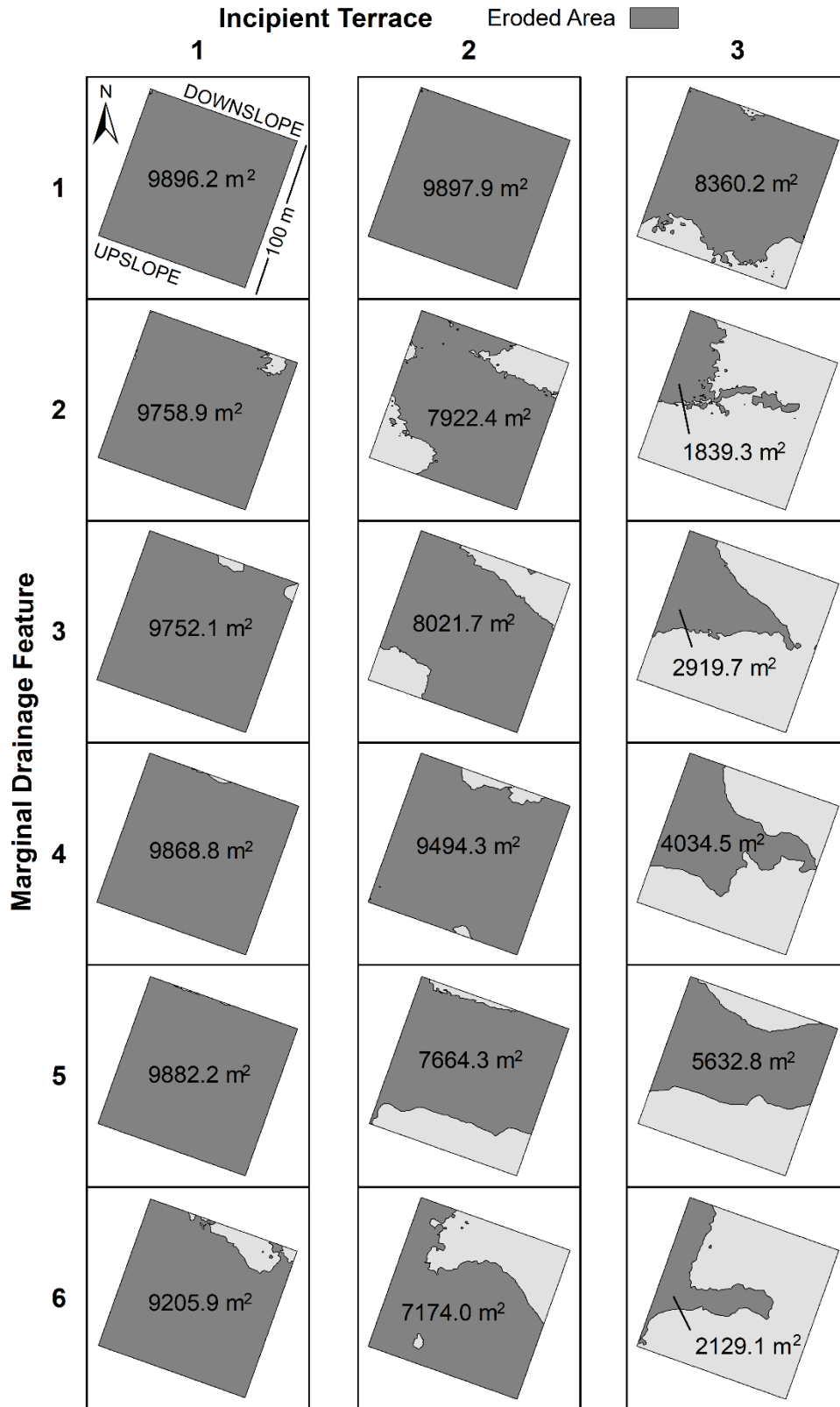
Appendix C.4. Sample particle size fractions after pulverization and weights.

Sample	Fragment Thickness (mm from surface)	Weight (g)	>500μm (g)	250-500μm (g)	<250μm (g)
T10-A	35	386			
	37	292	291	129	355
T10-B	50	376	236	66	79
T10-C	28	443	194	107	134
T6-A	50	555			
	48	227	395	152	215
T6-B	72	391			
	39	211	262	158	156
T6-C	80	959	565	220	260
T20-A	87	1999	1345	201	318
	69	488			
	66	388			
	43	185			
	36	138			
	17	73			
T20-B	24	138	1254	270	416
	23	108			
	18	23			
	46	192			
	≤ 69 (chips)	258			
	61	286			
T20-C	39	163			
	56	517			
	54	86			
	34	35	932	132	219
	35	58			
	51	82			
T25-A	≤ 3 (chips)	86			
	48	271			
T25-B	58	482	859	97	143
	≤ 58 (chips)	386			
T25-C	48	2045	1444	184	292
	66	722			
	71	263			
T25-C	54	327	1150	115	155
	48	153			

APPENDIX D

Chapter 5 Supplementary Materials

Appendix D.1. Erosion and accumulation maps.



BIBLIOGRAPHY

BIBLIOGRAPHY

- ACIA. 2004. Arctic Climate Impact Assessment—Policy Document. Arctic Climate Impact Assessment issued by the Fourth Arctic Council Ministerial Meeting Reykjavík, 24 November 2004.
- Aleschkow, A.M. 1936. Über Hochterrassen des Ural. *Zeitschrift für Geomorphologie*, 9, 143-149.
- Andersson, J.G. 1906. Solifluction, a Component of Subaerial Denudation. *The Journal of Geology*, 14, 91-112.
- André, M.F. 2003. Do Periglacial Landscapes Evolve Under Periglacial Conditions? *Geomorphology*, 52, 149-164.
- Andrews, H.P., Snee, R.D., Sarner, M.H. 1980. Graphical Display of Means. *The American Statistician*, 34: 195-199.
- Andrews, T.D., MacKay, G. (eds.) 2012. The Archaeology and Paleoecology of Alpine Ice Patches. *Arctic*, 65, 202 pp.
- Balco, G., Stone, J.O., Lifton, N.A., Dunai, T.J. 2008. A Complete and Easily Accessible Means of Calculating Surface Exposure Ages or Erosion Rates from ^{10}Be and ^{26}Al Measurements. *Quaternary Geochronology*, 3, 174-195.
- Ballantyne, C.K. 1978. The Hydrologic Significance of Nivation Features in Permafrost Areas. *Geografiska Annaler: Series A, Physical Geography*, 60, 51-54.
- Ballantyne, C.K. 1984. The Late Devensian Periglaciation of Upland Scotland. *Quaternary Science Reviews*, 3, 311-343.
- Ballantyne, C.K. 1985. Nivation Landforms and Snowpatch Erosion on Two Massifs in the Northern Highlands of Scotland. *The Scottish Geographical Magazine*, 101, 40-49.
- Ballantyne, C.K. 2018. *Periglacial Geomorphology*. John Wiley & Sons, New York.
- Ballantyne, C.K., Black, N.M., Finlay, D.P. 1989. Enhanced Boulder Weathering Under Late-Lying Snowpatches. *Earth Surface Processes and Landforms*, 14, 745-750.
- Barrett, P.J. 1980. The Shape of Rock Particles, a Critical Review. *Sedimentology*, 27, 291-303.
- Bass, P. 2007. *Nunataks and Island Biogeography in the Alaska-Canada Boundary Range*. Ph.D. Thesis. University of Georgia 191 p. (Athens, Georgia).
- Bastian, M., Heymann, S., Jacomy, M. 2009. Gephi: An Open Source Software for Exploring and Manipulating Networks. In: *International AAAI Conference on Weblogs and Social Media. Association for the Advancement of Artificial Intelligence*.

- Benn, D.I., Ballantyne, C.K. 1993. The Description and Representation of Particle Shape. *Earth Surface Processes and Landforms*, 18, 665-672.
- Benn, D.I., Ballantyne, C.K. 1994. Reconstructing the Transport History of Glacigenic Sediments: A New Approach Based on the Co-Variance of Clast Form Indices. *Sedimentary Geology*, 91, 215-227.
- Benn, D.I., Evans, D.J.A. 2004. *A Practical Guide to the Study of Glacial Sediments*. Routledge, London.
- Berrisford, M.S. 1991. Evidence for Enhanced Mechanical Weathering Associated with Seasonally Late-Lying and Perennial Snow Patches, Jotunheimen, Norway. *Permafrost and Periglacial Processes*, 2, 331-40.
- Biot, P. 1968. *The Cycle of Erosion in Different Climates*. University of California Press, Los Angeles, 144 pp.
- Bloom, A.L. 2004. *Geomorphology: A Systematic Analysis of Late Cenozoic Landforms*. Third Edition, Long Grove, IL: Waveland Press, 482 pp.
- Boch, S.G., Krasnov, I.I. 1943. O Nagornykh Terraskh i Drevnikh Poverkhnostyakh Yravnivaniya na Urale Isvyazannykh s Nimi Problemakh. *Vsesoyuznogo Geograficheskogo obshchestva, Izvestiya*, 75, 14-25 (English Translation by Gladunova, A. 1994. On Altiplanation Terraces and Ancient Surfaces of Leveling in the Urals and Associated Problems. In Evans, D.J.A. (ed.), *Cold Climate Landforms*, John Wiley & Sons, Chichester, 1994, 177-186.)
- Boch, S.G., Krasnov, I.I. 1951. Proces Golcovogo Yravnivaniya i Obrazovanie Nagornykh Teras. *Priroda*, 5, 25-35 (English Translation 1974. Process of Altiplanation and the Formation of Mountain Terraces. No. *CRREL-TL-410*, Cold Regions Research and Engineering Lab, Hanover, NH.)
- Boelhouwers, J., Jonsson, M. 2013. Critical Assessment of the 2°C Min-1 Threshold for Thermal Stress Weathering. *Geografiska Annaler, Series A, Physical Geography*, 95, 285-293.
- Boggs, S., 2006, *Principles of Sedimentology and Stratigraphy*. Princeton Prentice Hall.
- Borromei, A.M., Coronato, A., Franzén, L.G., Ponce, J.F., Sáez, J.A.L., Maidana, N., Rabassa, J., Candel, M.S. 2010. Multiproxy Record of Holocene Paleoenvironmental Change, Tierra del Fuego, Argentina. *Palaeogeography, Palaeoclimatology, Palaeoecology*, 286, 1-16.
- Briner, J.P., Kaufman, D.S., Manley, W.F., Finkel, R.C., Caffee, M.W. 2005. Cosmogenic Exposure Dating of Late Pleistocene Moraine Stabilization in Alaska. *Geological Society of America Bulletin*, 117, 1108-1120.
- Brozović, N., Burbank, D.W., Meigs, A.J. 1997. Climatic Limits on Landscape Development in the Northwestern Himalaya. *Science*, 276, 571-574.

- Brunnschweiler, D.H. 1965. *The Morphology of Altiplanation in Interior Alaska*. Unpublished Report to the U.S. Army Cold Regions Research and Engineering Laboratory, Hanover, NH, 48 pp.
- Bryan, K. 1940. The retreat of slopes. *Annals of the Association of American Geographers*, 30, 254-267.
- Bryan, K. 1946. Cryopedology, the Study of Frozen Ground and Intensive Frost-Action, with Suggestions on Nomenclature. *American Journal of Science*, 244, 622-642.
- Büdel, J. 1982. *Climatic Geomorphology*. Princeton University Press.
- Cailleux, A., 1946. Distinction des Sables Marins et Fluviatiles. *Bulletin de la Société Géologique de France*, 125–138.
- Cairnes, D.D. 1912a. Differential Erosion and Equiplanation in Portions of Yukon and Alaska. *Bulletin of the Geological Society of America*, 23, 333-348.
- Cairnes, D.D. 1912b. Some Suggested New Physiographic Terms. *American Journal of Science*, 34: 75-87.
- Cialek, C.J. 1977. The Cathedral Massif, Atlin Provincial Park, British Columbia. Foundation for Glacier and Environmental Research, Pacific Science Center, Seattle, WA, map scale 1:20,000.
- Cockburn, H.A., Summerfield, M.A. 2004. Geomorphological Applications of Cosmogenic Isotope Analysis. *Progress in Physical Geography*, 28, 1-42.
- Collier, A.J. 1902. A Reconnaissance of the Northwestern Portion of Seward Peninsula, Alaska. *U.S. Geological Survey Professional Paper 2*, 70 pp.
- Collier, A.J. 1906. Geology and Coal Resources of the Cape Lisburne Area, Alaska. *U.S. Geological Survey Bulletin*, 18, 79-85.
- Coronato, A. M., Coronato, F., Mazzoni, E., Vázquez, M. 2008. The Physical Geography of Patagonia and Tierra del Fuego. *Developments in Quaternary Sciences*, 11: 13-55.
- Corte, A.E. 1983. Geocryogenic Morphology at Seymour Island (Marambio) Antarctica: A Progress Report. In *Proceedings of the Fourth International Conference on Permafrost*. National Academy Press, Washington, DC, 192-197.
- Czudek, T. 1995. Cryoplanation Terraces—a Brief Review and Some Remarks. *Geografiska Annaler: Series A, Physical Geography*, 77, 95-105.
- Czudek, T., Demek, J., 1973. The Valley Cryopediments in Eastern Siberia. *Biuletyn Peryglacjalny*, 22, 117–130.

- Darvill, C.M. 2013. Cosmogenic Nuclide Analysis. In: Clark, L.E., Nield, J.M. (Eds.), *Geomorphological Techniques*, London, UK: British Society for Geomorphology, pp. 1-25.
- Davies, J.L. 1958. The Cryoplanation of Mount Wellington. In *Papers and Proceedings of the Royal Society of Tasmania*, 92: 151-154.
- Davis, W.M. 1909. *Geographical Essays*. Boston: Ginn and Company.
- Davis, W.M. 1932. Piedmont benchlands and Primärrumpfe. *Bulletin of the Geological Society of America*, 43,399-440.
- Dawson, G.M. 1896. Report on the Area of the Kamloops Map-Sheet, British Columbia. *Canada Geological Survey Annual Report*, 7B, p. 11.
- Day, M.H., Goudie, A.S. 1977. Field Assessment of Rock Hardness Using the Schmidt Test Hammer. *BGRG Technical Bulletin*, 18, 19-29.
- Delucchi, K.L. 1983. The Use and Misuse of Chi-Square: Lewis and Burke Revisited. *Psychological Bulletin*, 94, 166 - 176.
- Demek, J. 1969. Cryoplanation Terraces, Their Geographical Distribution, Genesis and Development. *Rozprawy CAeskoslovenské Akademie veÆd, RÆada matematickych a pírodních veÆd*, 79, 80 pp.
- Demek, J., 1968. Cryoplanation Terraces in Yakutia. *Biuletyn Peryglacjalny*, 17, 91–116.
- Demek, J., Havlíček, M., Mackovčín, P. 2010. Relict Cryoplanation and Nivation Landforms in the Czech Republic: A Case Study of the Sýřská Hornatina Mtns. *Moravian Geographical Reports*, 18, 14 – 25.
- Derbyshire, E., Evans, I.S. 1976. The Climatic Factor in Cirque Variation. In: Derbyshire, E. (ed.), *Geomorphology and Climate*, John Wiley & Sons, New York, 447-494.
- Dixon, E.J., Callanan, M.E., Hafner, A., Hare, P.G. 2014. The Emergence of Glacial Archaeology. *Journal of Glacial Archaeology*, 1, 1-9.
- Dorn, R.I. 2002. Analysis of Geomorphology Citations in the Last Quarter of the 20th Century. *Earth Surface Processes and Landforms*, 27, 667-672.
- Eakin, H.M. 1916. The Yukon-Koyukuk Region, Alaska. *U.S. Geological Survey Bulletin*, 631, 88 pp.
- Egholm, D.L., Nielsen, S.B., Pedersen, V.K., Lesemann, J.E. 2009. Glacial effects limiting mountain height. *Nature*, 460.7257, 884-887.
- Embleton, C., King, C.A.M. 1968. *Glacial and Periglacial Geomorphology*. New York, St. Martin's Press, 608 pp.

- Embleton, C., King, C.A.M. 1975. *Periglacial Geomorphology* (2nd ed.). John Wiley & Sons, New York, 2, 142-143.
- Evans, D.J., Harrison, S., Vieli, A., Anderson, E. 2012. The Glaciation of Dartmoor: the Southernmost Independent Pleistocene Ice Cap in the British Isles. *Quaternary Science Reviews*, 45, 31-53.
- Evans, D.J., Kalyan, R., Orton, C. 2017. Periglacial Geomorphology of Summit Tors on Bodmin Moor, Cornwall, SW England. *Journal of Maps*, 13, 342-349.
- Evans, I.S. 1994. *Lithological and Structural Effects on Forms of Glacial Erosion: Cirques and Lake Basins*. John Wiley & Sons, London.
- Evans, I.S. 2006. Allometric Development of Glacial Cirque Form: Geological, Relief and Regional Effects on the Cirques of Wales. *Geomorphology*, 80, 245-266.
- Flint, R.F. 1971. *Glacial and Quaternary Geology*. John Wiley & Sons, New York, 892 p.
- Font, M., Lagarde, J.L., Amorese, D., Coutard, J.P., Dubois, A., Guillemet, G., Ozuf, J.C., Védie, E. 2006. Physical Modelling of Fault Scarp Degradation Under Freeze-Thaw Cycles. *Earth Surface Processes and Landforms*, 31, 1731-1745.
- Foster, H.L. 1967. Geology of the Mount Fairplay Area, Alaska. *U.S. Geological Survey Bulletin* 1241-B, 18 pp.
- Foster, H.L. 1992. Geologic Map of the Eastern Yukon-Tanana Region, Alaska. U.S. Geological Survey, Open-File Report No. 92-313, 26 pp. map scale 1:250,000.
- Foster, H.L., Weber, F.R., Forbes, R.B., Brabb, E.E. 1973. Regional Geology of the Yukon-Tanana Upland, Alaska. *Arctic Geology: American Association of Petroleum Geologists, Memoir*, 19, 388-395.
- French, H.M. 2000. Does Lozinski's Periglacial Realm Exist Today? A Discussion Relevant to Modern Usage of the Term 'Periglacial'. *Permafrost and Periglacial Processes*, 11, 35-42.
- French, H.M. 2011. Frozen Sediments and Previously-Frozen Sediments. In: Martini, I.P., French, H.M., Perez Alberti, A. (Eds.), *Ice-Marginal and Periglacial Processes and Sediments*. Geological Society, London, Special Publication 354, 153-166.
- French, H.M. 2016. Do Periglacial Landscapes Exist? A Discussion of the Upland Landscapes of Northern Interior Yukon, Canada. *Permafrost and Periglacial Processes*, 27, 219-228.
- French, H.M. 2017. *The Periglacial Environment* (4th ed.). John Wiley & Sons, Hoboken, NJ.
- French, H.M. Harry, D.G. 1992. Pediments and Cold-Climate Conditions, Barn Mountains, Unglaciated Northern Yukon, Canada. *Geografiska Annaler: Series A, Physical Geography*, 74, 145-157.

- French, H.M., Nelson, F.E. 2008. The Permafrost Legacy of Siemon W. Muller. In: Kane, D.L., Hinkel, K.M. (eds.), *Proceedings of the Ninth International Conference on Permafrost*. University of Alaska Press: Fairbanks, 475-480.
- Galán de Mera, A., Méndez, E., Linares Perea, E., Campos de la Cruz, J., Orellana, J.A.V. 2014. Plant Communities Linked with Cryogenic Processes in the Peruvian Andes. *Phytocoenologia*, 44, 121-161.
- Gehrels, G., Rusmore, M., Woodsworth, G., Crawford, M., Andronicos, C., Hollister, L., Patchett, J., Ducea, M., Butler, R., Klepeis, K., Davidson, C., Friedman, R., Haggart, J., Mahoney, B., Crawford, W., Pearson, D., Girardi, J. 2009. U-Th-Pb Geochronology of the Coast Mountains Batholith in North-Coastal British Columbia: Constraints on age and Tectonic Evolution. *Geological Society of America Bulletin*, 121, 1342-1361.
- Gerrard, J. 1988. Periglacial Modification of the Cox Tor—Staple Tors Area of Western Dartmoor, England. *Physical Geography*, 9, 280-300.
- Golden Software. 2014. *Surfer User's Guide*, v. 12. Golden Software Inc., Golden, CO, 1089 pp.
- Goldich, S.S. 1938. A Study in Rock-Weathering. *The Journal of Geology*, 46, 17-58.
- Goodfellow, B.W., Boelhouwers, J. 2013. Hillslope Processes in Cold Environments: An Illustration of High Latitude Mountain and Hillslope Processes and Forms. *Treatise in Geomorphology*, 117-71.
- Gosse, J.C., Phillips, P.M. 2001. Terrestrial In Situ Cosmogenic Nuclides: Theory and Application. *Quaternary Science Reviews*, 20: 1475-1560.
- Goudie, A.S. 2006. The Schmidt Hammer in Geomorphological Research. *Progress in Physical Geography*, 30, 703-718.
- Grab, S., Boelhouwers, J., Hall, K., Meiklejohn, K.I., Sumner, P. 1999. *Quaternary Periglacial Phenomena in the Sani Pass Area, Southern Africa*. XV INQUA International Conference Field Guide, Durban, South Africa.
- Grab, S., van Zyl, C., Mulder, N. 2005. Controls on Basalt Terrace Formation in the Eastern Lesotho Highlands. *Geomorphology*, 67, 473-485.
- Gravis, G.F. 1964. Stadiynost v razvitií nagornykh terras (na primere khrebta Udokan). *Voprosy geografii Zabaykalskogo Severa*, 1964: 133-142.
- Gregory, K.J. 1966. Aspect and Landforms in Northeast Yorkshire. *Biuletyn Peryglacjalny*, 15, 115-120.
- Grosso, S.A., Corte, A.E. 1991. Cryoplanation Surfaces in the Central Andes at Latitude 35° S. *Permafrost and Periglacial Processes*, 2, 49-58.
- Guoqing, Q., Guodong, C. 1995. Permafrost in China: Past and Present. *Permafrost and Periglacial Processes*, 6, 3-14.

- Hagberg, A.A., Schult, D.A., Swart, P.J. 2008. Exploring Network Structure, Dynamics, and Function Using Networkx. In: Varoquaux, G., Vaught, T., Millman, J. (Eds.), *Proceedings of the 7th Python in Science Conference (SciPy2008)*. pp. 11–15.
- Hagedorn, J. 1984. Pleistozäne Periglacial-Formen in Gebirgen des Südlichen Kaplandes (Süd-Afrika) und ihre Bedeutung als Paläoklima-Indikatoren. *Palaeoecology of Africa and the Surrounding Islands*, 16, 405-410.
- Hales, T., Roering, J. 2009. A Frost “Buzzsaw” Mechanism for Erosion of the Eastern Southern Alps, New Zealand. *Geomorphology*, 107, 241 – 253.
- Hall, A.M., Kleman, J. 2014. Glacial and Periglacial Buzzsaws: Fitting Mechanisms to Metaphors. *Quaternary Research*, 81, 189-192.
- Hall, K. 1987. The Physical Properties of Quartz-Micaschist and Their Application to Freeze-Thaw Weathering Studies in the Maritime Antarctic. *Earth Surface Processes and Landforms*, 12, 137-149.
- Hall, K. 1993. Rock moisture data from Livingston Island (Maritime Antarctic) and implications for weathering processes. *Permafrost and Periglacial Processes*, 4, 245-253.
- Hall, K. 1997a. Observations on “Cryoplanation” Benches in Antarctica. *Antarctic Science*, 9, 181-187.
- Hall, K. 1997b. Rock Temperatures and Implications for Cold Region Weathering. I: New Data from Viking Valley, Alexander Island, Antarctica. *Permafrost and Periglacial Processes*, 8, 69-90.
- Hall, K. 1998. Nivation or Cryoplanation: Different Terms, Same Features? *Polar Geography*, 22, 1-16.
- Hall, K. 1999. The Role of Thermal Stress Fracture in the Breakdown of Rock in Cold Regions. *Geomorphology*, 31, 47-63.
- Hall, K. 2013. Periglacial Processes and Landforms of the Antarctic: A Review of Recent Studies and Directions. *Geological Society, London, Special Publications*, 381, SP381-16.
- Hall, K., André, M. F. 2010. Some Further Observations Regarding "Cryoplanation Terraces" on Alexander Island. *Antarctic Science*, 22, 175.
- Hall, K., Thorn, C.E. 2011. The Historical Legacy of Spatal Scales in Freeze-Thaw Weathering: Misrepresentation and Resultant Misdirection. *Geomorphology*, 130, 83-90.
- Hall, K., Thorn, C.E. 2014. Thermal Fatigue and Thermal Shock in Bedrock: An Attempt to Unravel the Geomorphic Process and Products. *Geomorphology*, 206, 1-13.

- Hallet, B., Walder, J.S., Stubbs, C.W. 1991. Weathering by segregation ice growth in microcracks at sustained subzero temperatures: verification from an experimental study using acoustic emissions. *Permafrost and Periglacial Processes*, 2, 283-300.
- Hansen, V.L., Dusel-Bacon, C. 1998. Structural and Kinematic Evolution of the Yukon-Tanana Upland Tectonites, East-Central Alaska: A Record of Late Paleozoic to Mesozoic Crustal Assembly. *Geological Society of America Bulletin*, 110, 211-230.
- Hare, P.G., Thomas, C.D., Topper, T.N., Gotthardt, R.M. 2012. The Archaeology of Yukon Ice Patches: New Artifacts, Observations, and Insights. *Arctic*, 65, 118-135.
- Harrison, S., Knight, J., Rowan, A.V. 2015. The Southernmost Quaternary Niche Glacier System in Great Britain. *Journal of Quaternary Science*, 30, 325-334.
- Heyman, J., Stroeven, A.P., Harbor, J.M., Caffee, M.W. 2011. Too Young or Too Old: Evaluating Cosmogenic Exposure Dating Based on an Analysis of Compiled Boulder Exposure Ages. *Earth and Planetary Science Letters*, 302, 71-80.
- Hopkins, D.M., Sigafos, R.S. 1951. Frost Action and Vegetation Patterns on Seward Peninsula, Alaska. *U.S. Geological Survey Bulletin*, 974, 51-100.
- Hughes, O.L. 1990. Surficial Geology and Geomorphology, Aishihik Lake, Yukon Territory. *Geological Survey of Canada, Paper*, 87-29, 23 pp.
- Humlum, O., Christiansen, H.H. 1998. Mountain Climate and Periglacial Phenomena in the Faeroe Islands. *Permafrost and Periglacial Processes*, 9, 189-211.
- IPCC. 2013. *Climate Change 2013: The Physical Science Basis, Contribution of Working Group I to the Fifth Assessment Report of the Intergovernmental Panel on Climate Change*. Stocker, T.F., Qin, D., Plattner, G.K., Tignor, M., Allen, S.K., Boschung, J., Nauels, A., Xia, Y., Bex, V, Midgley, P.M. (Eds.) Cambridge University Press, Cambridge.
- Ivy-Ochs, S., Kerschner, H., Schlüchter, C. 2007. Cosmogenic Nuclides and the Dating of Lateglacial and Early Holocene Glacier Variations: The Alpine Perspective. *Quaternary International*, 164, 53-63.
- Jahn, A. 1975. *Problems of the Periglacial Zone (Zagadnienia strefy peryglacjalnej)*. Warsaw: Polish Scientific Publishers, 223 pp.
- Jahn, A. 1979. The Varanger Peninsula (Norway) and the Problem of the Fossilisation of Periglacial Phenomena in Europe. *Geografiska Annaler. Series A. Physical Geography*, 61, 1-10.
- Jones, V.K. 1975. *Contributions to the Geomorphology and Neoglacial Chronology of the Cathedral Glacier System, Atlin Wilderness Park, British Columbia*. M.S. Thesis, Michigan State University, 183 p. (East Lansing, Michigan).

- Karrasch H. 1972. Flächenbildung unter periglazialen Klimabedingungen? In: Hövermann, J. and Oberbeck, G. (eds.) Hans-Poser-Festschrift. *Göttinger Geographische Abhandlungen* 60: 155-168.
- Kaufman, D.S., Hopkins, D.M. 1986. Glacial History of the Seward Peninsula. In: Hamilton, T.D., Reed, K.M., Thorson, R.M. (eds.) *Glaciation in Alaska—The Geologic Record*, Anchorage, Alaska Geological Society, p. 51–77.
- Kaufman, D.S., Manley, W.F. 2004. Pleistocene Maximum and Late Wisconsin Glacier Extents Across Alaska, USA. In: Ehlers, J., Gibbard, P.L. (eds.) *Quaternary Glaciations – Extent and Chronology, Part II, North America*, Amsterdam, Elsevier, *Developments in Quaternary Science*, 2B, 9-27.
- Kaufman, D.S., Young, N.E., Briner, J.P., Manley, W.F. 2011. Alaska Paleo-Glacier Atlas (Version 2). In: Ehlers, J., Gibbard, P.L., Hughes, P.D. (Eds.), *Quaternary Glaciations—Extent and Chronology. A Closer Look*. Elsevier, Amsterdam, pp. 427-445 (*Developments in Quaternary Science* 15).
- King, C.A.M. 1966. *Techniques in Geomorphology*. St. Martin's Press, New York.
- King, L. 1962. *Morphology of the Earth*. New York: Hafner Publishing, 699 pp.
- Kirk, R.E. 1982. *Experimental Design: Procedures for the Behavioral Sciences*, Wadsworth, Inc., Belmont, CA, 911 pp.
- Kňažková, M., Nývlt, D., Hrbáček, F. 2018. Quantification of Holocene Nivation Rates on Deglaciation Surfaces of James Ross Island, Antarctica. In: 5th European Conference on Permafrost, June 23rd – July 1st, 2018, Chamonix, France, pp. 519-520.
- Kohl, C.P., Nishiizumi, K. 1992. Chemical Isolation of Quartz for Measurement of In-Situ-Produced Cosmogenic Nuclides. *Geochimica et Cosmochimica Acta*, 56, 3583-3587.
- Kozmin, N.M. 1890. O Lednikovykh Yavleniyakh v Olekminsko-Vitimskoy Gornoy Strane i o Svyazi ikh s Obrazovaniyem Zolotnoshykh Rossyepy. *Izvestiia Vostochno-Sibirskogo otdela Geograficheskogo obshchestva*, 21.
- Krivolutskiy, A.Ye. 1965. Processes of Bald Mountain Planation. *Doklady Akademii Nauk SSSR*, 161, 60-61.
- Krumbein, W.C. 1941. Measurement and Geologic Significance of Shape and Roundness of Sedimentary Particles. *Journal of Sedimentary Petrology*, 11, 64-72.
- Lal, D. 1991. Cosmic Ray Labeling of Erosion Surfaces: In Situ Nuclide Production Rates and Erosion Models. *Earth and Planetary Science Letters*, 104, 424-439.
- Lauriol, B. 1990. Cryoplanation Terraces, Northern Yukon. *Canadian Geographer/Le Géographe Canadien*, 34, 347-351.

- Lauriol, B.M., Lalonde, A.E., Dewez, V. 1997. Weathering of Quartzite on a Cryoplanation Terrace in Northern Yukon, Canada. *Permafrost and Periglacial Processes*, 8, 147-153.
- Lauriol, B.M., Lamirande, I., Lalonde, A.E. 2006. The Giant Steps of Bug Creek, Richardson Mountains, NWT, Canada. *Permafrost and Periglacial Processes*, 17, 267-275.
- Leslie, D.M. 1973. Definition of the Portobello Soil Set in Relation to Regolith Stratigraphy and Landscape Periodicity. *New Zealand Journal of Science*, 16, 259-285.
- Levene, H. 1960. Robust Tests for Equality of Variances. In Olkins, I. (ed.), *Contributions to Probability and Statistics*, Stanford, CA, pp. 278-292.
- Lewis, W.V. 1939. Snow-patch erosion in Iceland. *Geographical Journal*. 94, 153-161.
- Lifton, N., Sato, T., Dunai, T.J. 2014. Scaling In Situ Cosmogenic Nuclide Production Rates Using Analytical Approximations to Atmospheric Cosmic-Ray Fluxes. *Earth and Planetary Science Letters*, 386, 149-160.
- Lisiecki, L.E., Raymo, M.E. 2005. A Pliocene-Pleistocene Stack of 57 Globally Distributed Benthic $\delta^{18}\text{O}$ Records. *Paleoceanography*, 20, doi:10.1029/2004PA001071.
- Lomborinchen, R. 1998. Periglacial Processes and Physical (Frost) Weathering in Northern Mongolia. *Permafrost and Periglacial Processes*, 9, 185-188.
- Maag, H.U. 1969. Ice-dammed lakes and marginal drainage on Axel Heiberg Island, Canadian Arctic Archipelago. *Axel Heiberg Island Research Reports*, McGill University, 147 pp.
- Mackay, J.R. 1990. Some Observations on the Growth and Deformation of Epigenetic, Syngenetic and Anti-Syngenetic Ice Wedges. *Permafrost and Periglacial Processes*. 1, 15-29.
- Marrero, S.M., Phillips, F.M., Borchers, B., Lifton, N., Aumer, R., Balco, G. 2016. Cosmogenic Nuclide Systematics and the CRONUScalc Program. *Quaternary Geochronology*, 31, 160-187.
- Martini, I.P., French, H.M., Perez Alberti, A. 2011. Ice-Marginal and Periglacial Processes and Sediments: An Introduction. In Martini, I.P., French, H.M., Perez Alberti, A. (Eds.), *Ice-Marginal and Periglacial Processes and Sediments*. Geological Society, London, Special Publication 354: 1-13.
- Matsuoka, N., Murton, J. 2008. Frost Weathering: Recent Advances and Future Directions. *Permafrost and Periglacial Processes*, 19, 195-210.
- Matthes, F.E. 1900. Glacial Sculpture of the Bighorn Mountains. Wyoming. *U.S. Geological Survey Twenty-first Annual Report Part II*, 167-190.

- Matthews, J.A., Dawson, A.G., Shakesby, R.A. 1986. Lake Shoreline Development, Frost Weathering and Rock Platform Erosion in an Alpine Periglacial Environment, Jotunheimen, Southern Norway. *Boreas*, 15, 33-50.
- May, J.H. 2008. A Geomorphological Map of the Quebrada de Purmamarca, Jujuy, NW Argentina. *Journal of Maps*, 4, 211-224.
- McCarroll, D. 1989. Potential and Limitations of the Schmidt Hammer for Relative-Age Dating: Field Tests on Neoglacial Moraines, Jotunheimen, Southern Norway. *Arctic and Alpine Research*, 21, 268-275.
- McKinney, W. 2010. Data Structures for Statistical Computing in Python. In *Proceedings of the 9th Python in Science Conference*, 445, 51-56.
- Mertie, J.B., Jr. 1937. The Yukon-Tanana Region, Alaska. *U.S. Geological Survey Bulletin*, 872, 276 pp.
- Migon, P. 2006. Büdel, J. 1982. Climatic Geomorphology (Translation of Klima-Geomorphologie, Berlin-Stuttgart: Gebrüder Borntraeger, 1977). *Progress in Physical Geography*, 30, 99-103.
- Migon, P., Goudie, A.S. 2001. Inherited Landscapes of Britain-Possible Reasons for Survival. *Zeitschrift für Geomorphologie*, 45, 417-441.
- Miller, M.M. 1975. Mountain and Glacier Terrain Study and Related Investigations in the Juneau Icefield Region, Alaska-Canada. *Foundation for Glacier and Environmental Research, Monograph Series*, 136 p. (Seattle, Washington).
- Mitchell, S.G., Montgomery, D.R. 2006. Influence of a Glacial Buzzsaw on the Height and Morphology of the Cascade Range in Central Washington State, USA. *Quaternary Research*, 65, 96-107.
- Moffit, F.H. 1905. *The Fairhaven Gold Placers, Seward Peninsula, Alaska*. U.S. Geological Survey Bulletin, 247, 85pp.
- Mongeon, P., Paul-Hus, A. 2016. The Journal Coverage of Web of Science and Scopus: A Comparative Analysis. *Scientometrics*, 106, 213-228.
- Mortensen, J.K. 1992. Pre-Mid-Mesozoic Tectonic Evolution of the Yukon-Tanana Terrane, Yukon and Alaska. *Tectonics*, 11, 836-853.
- Murton, J.B., Peterson, R., Ozouf, J.C. 2006. Bedrock Fracture by Ice Segregation in Cold Regions. *Science*, 324, 1127-1129.
- Nelson, F.E. 1975. Periglacial features on the Cathedral Massif, northwestern British Columbia: a preliminary investigation. Open File Report 75, *Juneau Icefield Research Program and Foundation for Glacier and Environmental Research*, Seattle, WA, 36 pp.

- Nelson, F.E. 1979. *Patterned Ground in the Juneau Icefield Region, Alaska – British Columbia*. M.S. Thesis. Michigan State University 136 p. (East Lansing, Michigan).
- Nelson, F.E. 1989. Cryoplanation Terraces: Periglacial Cirque Analogs. *Geografiska Annaler. Series A. Physical Geography* 71, 31-41.
- Nelson, F.E. 1998. Cryoplanation Terrace Orientation in Alaska. *Geografiska Annaler: Series A, Physical Geography*, 80, 135-151.
- Nelson, F.E., Nyland, K.E. 2017. Periglacial Cirque Analogs: Elevation Trends of Cryoplanation Terraces in Eastern Beringia. *Geomorphology*, 293, 305-317.
- Nelson, F.E., Schimek, M.A. 2015. Topoclimatic Controls on Active-Layer Thickness, Alaskan Coastal Plain. In: Burn, C.R. (ed.) *Proceedings of a Symposium to Commemorate the Contributions of Professor J. Ross Mackay (1915-2014) to Permafrost Science in Canada*, Seventh Canadian Permafrost Conference, Quebec City, QC, 20-23 September 2016, 119-126. <http://carelton.ca/permafrost/symposium-honour-professor-j-r-mackay-1915-2014/>.
- Nešić, D., Milinčić, M.A., Lukić, B. 2017. Relict Cryoplanation Terraces of Central Kopaonik (Siberia). *Carpathian Journal of Earth and Environmental Sciences*, 12, 61-68.
- Nielsen, S.B., Gallagher, K., Leighton, C., Balling, N., Svenningsen, L., Jacobsen, B.H., Thomsen, E., Nielsen, O.B., Heilmann-Clausen, C., Egholm, Summerfield, M.A., Clausen, O.R., Piotrowski, J.A., Thorsen, M.R., Huuse, M., Abrahamsen, N., King, C., Lykke-Andersen, H. 2009. The Evolution of Western Scandinavian Topography: A Review of Neogene Uplift Versus the ICE (Isostasy–Climate–Erosion) Hypothesis. *Journal of Geodynamics*, 47, 72-95.
- Nyberg, R. 1991. Geomorphic Processes at Snow Patch Sites in the Abisko Mountains, Northern Sweden. *Zeitschrift für Geomorphologie*, 35, 321-343.
- Obruchev, S.A., 1937. Soliflukcionnye (Nagornyye) Terrasy i Yikh Genezis no Osnovanii Rabot v Chukotsom Kraye. *Problemy Arktiki I Antarktiki*, 3, 57-83. Leningrad. (In Russian)
- Ollier, C. 1981. *Tectonics and Landforms*. Longman, London. pp. 324.
- Osareh, F. 1996. Bibliometrics, Citation Analysis and Co-Citation Analysis: A Review of Literature I. *Libri*, 46, 149-158.
- Padalka, G.L. 1928. High Terraces in the Northern Ural Mountains. *Geologicheskogo Komiteta Vestnik*, 3, 9-15. (In Russian)
- Paquette, M., Fortier, D. and Vincent, W.F. 2017. Water Tracks in the High Arctic: A Hydrological Network Dominated by Rapid Subsurface Flow Through Patterned Ground. *Arctic Science*, 334-353, DOI: 10.1139/as-2016-0014.

- Peltier, L.C. 1950. The Geographic Cycle in Periglacial Regions as it is Related to Climatic Geomorphology. *Annals of the Association of American Geographers*. 40, 214-236.
- Penck, W. 1924. *Die morphologische Analyse. Ein Kapitel der physikalische Geologie*. Stuttgart: J. Engelmann's Nachfolger, 283 pp. English translation by H. Czech and K.C. Boswell (1953) as *Morphological Analysis of Land Forms: A Contribution to Physical Geology*. New York: St. Martin's Press, 429 pp.
- Perucca, L., Angillieri, Y.E. 2008. A Preliminary Inventory of Periglacial Landforms in the Andes of La Rioja and San Juan, Argentina, at about 28 S. *Quaternary International*, 190, 171-179.
- Péwé, T.L. 1973. Ancient Altiplanation Terraces Near Fairbanks, Alaska. *Biuletyn Peryglacjalny*, 23, 99-100.
- Péwé, T.L. 1975. Quaternary Geology of Alaska. *U.S. Geological Survey Professional Paper*, 853.
- Péwé, T.L. and Reger, R.D. 1968. *Investigation of the Origin, Distribution, and Environmental Significance of Altiplanation Terraces*. Unpublished report to the U.S. Army Cold Regions Research and Engineering Laboratory, Hanover, New Hampshire, 184 pp.
- Péwé, T.L., Burbank, L., Mayo, L.R. 1967. Multiple Glaciation of the Yukon-Tanana Upland, Alaska. US Geological Survey Miscellaneous Geological Investigations Map, I-105, scale 1:500,000.
- Péwé, T.L., Reger, R.D. 1972. Modern and Wisconsinan Snowlines in Alaska. Proceedings of the 24th International Geological Congress, 12, 187-197.
- Péwé, T.L., Reger, R.D. 1983. *Guidebook to Permafrost and Quaternary Geology Along the Richardson and Glenn Highways Between Fairbanks and Anchorage, Alaska*. Alaska Division of Geological & Geophysical Surveys Guidebook 1, 263 pp.
- Popov, A.I., 1960. Periglacial Formations under Conditions of Predominant Denudation. In Markov, K.K., Popov, A.I. (Eds.), *Periglacial phenomena on the territory of the U.S.S.R.*, Moscow: Moscow State University, pp. 28-36.
- Porter, C., Morin, P., Howat, I., Noh, M., Bates, B., Peterman, K., Keeseey, S., Schlenk, M., Gardiner, J., Tomko, K., Willis, M., Kelleher, C., Cloutier, M., Husby, E., Foga, S., Nakamura, H., Platson, M., Wethington, M., Williamson, C., Bauer, G., Enos, J., Arnold, G., Kramer, W., Becker, P., Doshi, A., D'Souza, C., Cummins, P., Laurier, F., Bojesen, M. 2018, "ArcticDEM", <https://doi.org/10.7910/DVN/OHHUKH>, Harvard Dataverse, V2.0, [December 15th, 2018].
- Prieznitz, K. 1988. Cryoplanation. In: Clark, M.J. (ed.), *Advances in Periglacial Geomorphology*, John Wiley & Sons Ltd: Chichester; 1988, 49-67.

- Prindle, L.M. 1905. *The Gold Placers of the Fortymile, Birch Creek, and Fairbanks Regions, Alaska*. U.S. Geological Survey Bulletin, 251, 89 pp.
- Prindle, L.M. 1913. *A Geologic Reconnaissance of the Circle Quadrangle, Alaska*. U.S. Geological Survey Bulletin, 538, 82 pp.
- Queen, C.W. 2018. *Large-Scale Mapping and Geomorphometry of Upland Periglacial Landscapes in Eastern Beringia*. M.S. Thesis. Michigan State University 164 pp. (East Lansing, Michigan).
- Quinn, I.M. 2011. The Significance of Periglacial Features on Knocknadober, South West Ireland. In Boardman, J. (Ed.), *Periglacial Processes and Landforms in Britain and Ireland*. Cambridge University Press, Cambridge, pp. 287–294.
- Rączkowska, Z. 1995. Nivation in the High Tatras, Poland. *Geografiska Annaler: Series A, Physical Geography*, 77, 251-258.
- Rapp, A. 1986. Comparative Studies of Actual and Fossil Nivation in North and South Sweden. *Zeitschrift für Geomorphologie*, 60, 251-263.
- Raup, H.M. 1951. Vegetation and Cryoplanation. *Ohio Journal of Science*, 51, 105-116.
- Rea, L.M., Parker, R.A. 2014. *Designing and Conducting Survey Research: A Comprehensive Guide*. John Wiley and Sons.
- Reger, R.D. 1975. *Cryoplanation Terraces of Interior and Western Alaska*. Ph.D. Thesis. Arizona State University 326 p. (Tempe, Arizona).
- Reger, R.D., Péwé, T.L. 1976. Cryoplanation Terraces: Indicators of a Permafrost Environment. *Quaternary Research*, 6, 99-109.
- Richter, H., Hasse, G., Berthell, H., 1963. Die Goleztterrassen. *Petermanns Geographische Mitteilungen*, 107, 183–192.
- Rixhon, G., Demoulin, A. 2013. Evolution of Slopes in a Cold Climate. In: Shroder, J. (ed.) *Treatise on Geomorphology (Glacial and Periglacial Geomorphology)*, 8, 392-415.
- Sainsbury, C.L. 1965. *Geology and Ore Deposits of the Central York Mountains, Western Seward Peninsula, Alaska*. U.S. Geological Survey Open File Report, 146 pp.
- Sanders, J.W., Cuffey, K.M., Moore, J.R., MacGregor, K.R., Kavanaugh, J.L. 2012. Periglacial Weathering and Headwall Erosion in Cirque Glacier Bergschrunds. *Geology*, 40, 779-782.
- Schaetzl, R.J., Thompson, M.L. 2015. *Soils: Genesis and Geomorphology*. New York: Cambridge University Press.

- Schrott, L. 1991. Global Solar Radiation, Soil Temperature and Permafrost in the Central Andes, Argentina: A Progress Report. *Permafrost and Periglacial Processes*, 2, 59-66.
- Schunke, E. 1974. Formungsvorgänge an Schneeflecken im Isländischen Hochland. *Abhandlungen der Akademie Wissenschaften in Göttingen*, Mathematisch-Physikalische Klasse, Dritte Folge, 29, 274-286.
- Schunke, E. 1975. Die Periglazialerscheinungen Islands in Abhängigkeit von Klima und Substrat. *Abhandlungen der Akademie Wissenschaften in Göttingen*, Mathematisch-Physikalische Klasse, Dritte Folge, 30, 273 pp.
- Schunke, E., Heckendorf, W.D. 1976. Resistenzstufen und Kryoplanation—Beobachtungen aus dem periglazialen Milieu Islands. *Zeitschrift für Geomorphologie Supplementband*, 24, 88-98.
- Sekyra, J. 1969. Periglacial Phenomena in the Oases and Mountains of the Enderby Land and the Dronning Maud Land (East Antarctica). Preliminary report. *Biuletyn Peryglacjalny*, 19, 277-289.
- Seong, Y.B., Kim, J.W. 2003. Application of In-Situ Produced Cosmogenic ^{10}Be and ^{26}Al for Estimating Erosion Rate and Exposure Age of Tor and Block Stream Detritus: Case Study from Mt. Maneo, South Korea. *Journal of the Korean Geographical Society*, 38, 389-399.
- Shapiro, S.S., Wilk, M.B. 1965. An analysis of variance test for normality (complete samples). *Biometrika*, 52, 591-611.
- Shear, J.A. 1964. The Polar Marine Climate. *Annals of the Association of American Geographers*, 54, 310-317.
- Sherman, D.I. 1996. Fashion in Geomorphology. In: Rhoads, B.L. and Thorn, C.E. (eds.), *The Scientific Nature of Geomorphology*. Chichester: Wiley, 481 pp.
- Simons, M. The Morphological Analysis of Landforms: A New Review of the Work of Walther Penck (1888-1923). *Transactions of the Institute of British Geographers*, 31, 1-14.
- Skyles, E., Vanching, G. 2007. Palso Fields and Cryoplanation Terraces, Hangay Nuruu, Central Mongolia. In: *Proceedings of the 20th Annual Keck Symposium*, 49-53.
- Slupetzky, H., Krisai, R. 2009. Indications of Late Glacial to Holocene Fluctuations of Cathedral Massif Glacier, Coast Range (Northern British Columbia, Canada). *Zeitschrift für Gletscherkunde und Glazialgeologie*, 43/44, 187-212.
- Smith, H.T.U. 1968. 'Piping' in relation to periglacial boulder concentrations. *Biuletyn Peryglacjalny*, 17, 195-204.
- Smith, P.S., Mertie, J.B. 1930. Geology and Mineral Resources of Northwestern Alaska. *U.S. Geological Survey Bulletin*, 815, 351 pp.

- St-Onge, D.A. 1969. Nivation Landforms. *Geological Survey of Canada Paper*, 69-30, 12 pp.
- Stone, J.O. 2000. Air Pressure and Cosmogenic Isotope Production. *Journal of Geophysical Research: Solid Earth*, 105, 23753-23759.
- Stone, J.O., Allan, G.L., Fifield, L.K., Cresswell, R.G. 1996. Cosmogenic Chlorine-36 from Calcium Spallation. *Geochimica et Cosmochimica Acta*, 60, 679-692.
- Streicker, J. 2016. Yukon Climate Change Indicators and Key Findings 2015. *Northern Climate ExChange, Yukon Research Centre, Yukon College*, 84 pp.
- Sumner, P., Nel, W. 2002. The Effect of Rock Moisture on Schmidt Hammer Rebound: Tests on Rock Samples from Marion Island and South Africa. *Earth Surface Processes and Landforms*, 27, 1137-1142.
- Syverson, K.M., Mickelson, D.M. 2009. Origin and significance of lateral meltwater channels formed along a temperate glacier margin, Glacier Bay, Alaska. *Boreas*, 38, 132-145.
- Taber, S. 1943. Perennially Frozen Ground in Alaska: Its Origin and History. *Geological Society of America Bulletin*, 54, 1433-1548.
- Te Punga, M.T. 1956. Altiplanation Terraces in Southern England. *Biuletyn Peryglacjalny*, 4, 331-338.
- Thorn, C.E. 1976. Quantitative Evaluation of Nivation in the Colorado Front Range. *Geological Society of America Bulletin*, 87: 1169-1178.
- Thorn, C.E. 1983. Seasonal Snowpack Variability and Alpine Periglacial Geomorphology. *Polarforschung*, 53, 31-35.
- Thorn, C.E. 2003. Making the Most of New Instrumentation. *Permafrost and Periglacial Processes*, 14, 411-419.
- Thorn, C.E., Hall, K. 1980. Nivation: An Arctic-Alpine Comparison and Reappraisal. *Journal of Glaciology*, 25, 109-124.
- Thorn, C.E., Hall, K. 2002. Nivation and Cryoplanation: The Case for Scrutiny and Integration. *Progress in Physical Geography*, 26, 533-550.
- Thornbury, W.D. 1969. *Principles of Geomorphology*, 2nd Edition. John Wiley & Sons, New York.
- Tricart, J., Cailleux, A. 1972. *Introduction to Climatic Geomorphology*. New York: St. Martin's Press.

- Trombotto, D., Buk, E., Hernández, J. 1997. Short Communication Monitoring of Mountain Permafrost in the Central Andes, Cordon del Plata, Mendoza, Argentina. *Permafrost and Periglacial Processes*, 8, 123-129.
- Tufnell, L. 1971. Erosion by Snow Patches in the North Pennines. *Weather*, 26, 492-498.
- Tukey, J.W. 1949. Comparing Individual Means in the Analysis of Variance. *Biometrics*, 5, 99-114.
- UNESCO. 2018. Yukon Ice Patches. United Nations Educational, Scientific and Cultural Organization Reference No. 6343. Accessed on March 26th, 2018 at <https://whc.unesco.org/en/tentativelists/6343/>.
- von Lozinski, W. 1909. Uber die Mechanische Verwitterung der Sandsteine im Gemassigten Klima. *Acad. Sci. Cracovie Bull. Internat. cl. sci. math et naturelles*. 1, 1-25 (English translation: On the Mechanical Weathering of Sandstones in Temperate Climates. In Evans, D.J. (ed.) *Cold Climate Landforms*, John Wiley & Sons: Chichester; 119-134.)
- von Lozinski, W. 1912. Die Periglaziales Fazies der Mechanischen Verwitterung. In *Comptes Rendus, XI Congres Internationale Geologie*. Stockholm, 1910, 1039-1053.
- Vtyurin, B.I. 1986. A Geocryological Account of the Schirmacher Oasis. *Polar Geography and Geology*, 10, 293-317.
- Wahrhaftig, C. 1965. Physiographic Divisions of Alaska. *U.S. Geological Survey Professional Paper*, 482, 52 pp.
- Walder, J.S., Hallet, B. 1985. A Theoretical Model of the Fracture of Rock During Freezing. *Geological Society of America Bulletin*, 96, 336-346.
- Walder, J.S., Hallet, B. 1986. The Physical Basis of Frost Weathering: Toward a More Fundamental and Unified Perspective. *Arctic and Alpine Research*, 18, 27-32.
- Wang, J. Veugelers, R., Stephan, P. 2017. Bias against novelty in science: A cautionary tale for users of bibliometric indicators. *Research Policy*, 46, 1416-1436.
- Washburn, A.L. 1973. *Periglacial Processes and Environments*. New York: St. Martin's Press, 320 pp.
- Washburn, A.L. 1979. *Geocryology: A Survey of Periglacial Proceses and Environments*. London: Edward Arnold, 406 pp.
- Waters, R.S. 1962. Altiplanation Terraces and Slope Development in Vest-Spitsbergen and Southwest England. *Biuletyn Peryglacjalny*, 11, 89-101.

- Weber, F.R., 1986, Glacial Geology of the Yukon-Tanana Upland. In: Hamilton, T.D., Reed, K.M., Thorson, R.M. (eds.) *Glaciation in Alaska—The Geologic Record*, Anchorage, Alaska Geological Society, p. 79–98.
- Weldon, M.B., Stevens, D.S.P., Newberry, R.J., Szumigala, D.J., Athey, J.E., Hicks, S.A. 2005. Geologic Map of the Big Hurrah Area, Northern Half of the Solomon C-5 Quadrangle, Seward Peninsula, Alaska. Alaska Division of Geological and Geophysical Surveys Report of Investigation 2005-1A, map scale 1:50,000.
- Wilkinson, T.J., Bunting, B.T. 1975. Overland Transport of Sediment by Rill Water in a Periglacial Environment in the Canadian High Arctic. *Geografiska Annaler*, 57A, 105-116.
- Wiltse, M.A., Reger, R.D., Newberry, R.J., Pessel, G.H., Pinney, D.S., Robinson, M.S., Solie, D.N. 1995a. Geologic Map of the Circle Mining District, Alaska. Alaska Division of Geological and Geophysical Surveys Report of Investigations 95-2a, map scale 1:63,360.
- Wiltse, M.A., Reger, R.D., Newberry, R.J., Pessel, G.H., Pinney, D.S., Robinson, M.S., Solie, D.N. 1995b. Bedrock Geologic Map of the Circle Mining District, Alaska. Alaska Division of Geological and Geophysical Surveys Report of Investigation 95-2b, map scale 1:63,360.
- Wood, B.L. 1969. Periglacial Tor Topography in Southern New Zealand. *New Zealand Journal of Geology and Geophysics*, 12, 361-375.
- Wright, W.B. 1914. *The Quaternary Ice Age*. Mcmillian & Co., London, p. 6.
- Yangxing, D., Xiaofeng, D. 1983. Characteristics of Periglacial Landforms in Bogda Area, Tian Shan. *Journal of Glaciology and Geocryology*, 3, 1983-19.
- Yoshikawa, T., Ikeda, Y., Iso, N., Moriya, I., Hull, A.G., Ota, Y. 1988. Origin and Age of Erosion Surfaces in the Upper Drainage Basin of Waiapu River, Northeastern North Island, New Zealand. *New Zealand Journal of Geology and Geophysics*, 31, 101-109.
- Zhigarev, L.A., Kaplina, T.N., 1960. Soliflukcionnye Formy Relyefa na Severo-Vostoke SSSR. *Trudy Instituta Merzlotovedeniya im. V.A. Obrucheva*, 16, Moskva.